Illinois U. Library

The American Mineralogist

Journal of the Mineralogical Society of America

Vol. 41 SEPTEMBER-OCTOBER, 1956 Nos. 9 and 10

Contents

Coffinite, a uranous silicate with hydroxyl substitution: a new mineral. L. R. Stieff, T. W. Stern, and A. M. Sherwood 675
A restudy of bakerite, priceite, and veatchite. Henry Kramer and Robert D. Allen 689
Thermal studies of ammonium fixation and release in certain clay minerals. A. D. Scott, J. J. Hanway, and G. Stanford 701
The chemical formula of empressite. Gabrielle Donnay, F. C. Kracek, and W. R. Rowland, Jr. 722
Clinopyroxenes of alkali olivine-basalt magma. J. F. G. Wilkinson 724
Experimental determination of calcite-aragonite equilibrium relations at elevated temperatures and pressures. Gordon J. F. MacDonald 744
Application of the rule of Gladstone and Dale to minerals. Howard W. Jaffe 757
Twinning in diamond-type structures: High-order twinning in silicon. J. A. Kohn 778
Notes and news: Niocalite—a new calcium niobium silicate mineral. E. H. Nickel 785
A new technique for micrometric analysis of thin-sections. Joseph A. Mandarino 786
Anomalous fluorescence in torbernite from Rum Jungle, N. T., Australia. R. J. P. Lyon 789
Note on twinning and pseudo-twinning in detrital quartz grains. Iris Borg 792
Note on large cordierite porphyroblasts, Fremont County, Colorado. Russell B. Travis 796
Hydrothermal alteration of muscovite in steam gage-glasses. William T. Holser 799
Confirmation of the crystal structure of pentlandite. A. David Pearson and M. J. Buerger 804
A note on the calcite-wollastonite equilibrium. A. J. Ellis and W. S. Fyfe 805
Book reviews. 808
New mineral names. 814



EDITOR: WALTER F. HUNT
ASSISTANT EDITOR: LEWIS S. RAMSDELL
BOARD OF ASSOCIATE EDITORS:
IAN CAMPBELL
WILLIAM F. BRADLEY
E. WM. HEINRICH
BRIAN MASON (1956)
FRANCIS J. TURNER (1956–57)
CHARLES L. CHRIST (1956–58)

Published bi-monthly by the Society

Mineralogical Society of America

ASSOCIATED WITH THE GEOLOGICAL SOCIETY OF AMERICA

President: Clifford Frondel, Harvard University, Cambridge, Mass.
Vice-President: D. Jerome Fisher, University of Chicago, Chicago, Illinois.
Secretary: C. S. Hurlbut, Jr., Harvard University, Cambridge 38, Massachusetts.
Treasurer: Earl Ingerson, U. S. Geological Survey, Washington 25, D. C.
Editor: Walter F. Hunt, University of Michigan, Ann Arbor, Michigan.
Councillors: C. Osborne Hutton, Stanford University, Palo Alto, California.
Felix Chayes, Geophysical Laboratory, Washington, D. C.
Leonard G. Berry, Queen's University, Kingston, Ontario, Canada.
Chester B. Slawson, University of Michigan, Ann Arbor, Mich.
Alfred O. Woodford, Pomona College, Claremont, California.
Harry H. Hess, Princeton University, Princeton, New Jersey.

The enlarged issues of this journal for 1956 are made possible by a grant from the Penrose Fund of the Geological Society of America.

The American Mineralogist—Journal of the Mineralogical Society of America

A journal containing articles on mineralogy, crystallography, petrography, and allied sciences, is issued every two months. Contributions are invited from everyone. Office of Publication, Mineralogical Laboratory, Ann Arbor, Michigan.

The general conduct of the journal is in the hands of the editor, **Walter F. Hunt**, Ann Arbor, Michigan, to whom all manuscripts should be submitted. To assist the editor the council of the Mineralogical Society has appointed **Lewis S. Ramsdell**, Ann Arbor, Michigan, assistant editor, and the following board of associate editors:

William F. Bradley, Illinois State Geological Survey, Urbana, Illinois.
Ian Campbell, California Institute of Technology, Pasadena 4, California.
Charles L. Christ, U. S. Geological Survey, Washington 25, D. C.
E. Wm. Heinrich, Dept. of Mineralogy, Univ. of Michigan, Ann Arbor, Mich.
Brian H. Mason, American Museum of Natural History, New York, N. Y.
Francis J. Turner, University of California, Berkeley 4, California.

It will expedite publication if two copies of each manuscript are submitted to the editor.

REPRINT PRICE SCALE

Pages	*1–4*	*5–8*	*9–12*	*13–16*	*17–20*	*21–24*	*25–28*	*29–32*	*Covers*
Copies									
25	$6.60	$ 8.80	$ 9.70	$12.00	$14.20	$17.20	$18.80	$19.60	$ 7.60
50	7.00	9.60	11.00	13.40	15.90	19.10	21.00	21.90	8.40
75	7.40	10.40	12.20	14.80	17.60	21.00	23.10	24.20	9.20
100	7.80	11.20	13.50	16.20	19.30	22.90	25.30	26.50	10.00
Add. 100s to 500	3.00	5.00	7.00	8.00	10.00	12.00	13.00	14.00	3.20

Extra charges: Refolioing—$.60 per page; Remaking—$1.25 per page; Cover composition—$3.50 per page; Title page composition—$3.50 per page; Reimposition—$1.00 per page.

Reprint prices for inserts available subject to special quotation. Copies in excess of 500 are subject to special quotations.

Postage is additional in all reprint orders.

Sent to all members and fellows of the Mineralogical Society of America. Membership dues $4.00 annually, fellowship dues $5.00 annually. Subscriptions for libraries, colleges, institutions, companies and similar organizations $6.00 annually.

Entered as second class matter at the post office at Menasha, Wis., under Act of March 3, 1879. Acceptance for mailing at the special rate of postage provided for in section 1103, Act of Oct. 3, 1917, paragraph 4 section 429 P. L. & R. authorized March 13, 1922.

Notice of change of address, orders, and remittances should be sent to Dr. Earl Ingerson, U. S. Geological Survey, Washington 25, D. C.

Printed by the George Banta Company, Inc., Menasha, Wisconsin
Printed in the United States of America

THE AMERICAN MINERALOGIST

JOURNAL OF THE MINERALOGICAL SOCIETY OF AMERICA

Vol. 41 SEPTEMBER–OCTOBER, 1956 Nos. 9 and 10

COFFINITE, A URANOUS SILICATE WITH HYDROXYL SUBSTITUTION: A NEW MINERAL*

L. R. STIEFF, T. W. STERN, AND A. M. SHERWOOD, *U. S. Geological Survey, Washington 25, D.C.*

ABSTRACT

A uranous silicate that shows substitution of $(OH)_4^{-4}$ for $(SiO_4)^{-4}$ has been identified as a new mineral. This new mineral, coffinite, named for Reuben Clare Coffin, has been found in more than 25 uranium deposits in the sedimentary rocks of the Colorado Plateaus province, in several localities peripheral to this province, and in association with uraninite in vein deposits in the Copper King mine, Larimer County, Colorado. It is also associated with asphaltic pellets from sediments in Texas and Oklahoma.

In many Colorado Plateau mines coffinite and uraninite are the main uranium minerals in the unoxidized ore. In hand specimen coffinite is black; many of the samples have an adamantine luster resembling that of a high-rank coal. On the Plateau, coffinite occurs as replacements of organic material, as disseminations in sandstone, and in association with low-valence vanadium minerals, uraninite, clay, quartz, and organic material. In transmitted light the smaller particles of coffinite-bearing material are pale brown to very dark brown on thin edges; they contain numerous opaque inclusions. The optical properties of coffinite could not be determined. The mineral is very fine grained, as evidenced by its apparent isotropy and by the broadened lines of its *x*-ray diffraction powder pattern.

X-ray diffraction powder studies indicate that coffinite is tetragonal and isostructural with zircon; material from the Arrowhead mine in Mesa County, Colorado, has $a_0=6.94$ Å, $c_0=6.31$ Å, $a_0:c_0=1:0.909$. Coffinite is best identified by its *x*-ray diffraction powder pattern.

Owing to its fine-grained nature and its association with uraninite and low-valence vanadium minerals, coffinite could not be completely purified. The specific gravity of coffinite-bearing material is variable, with a measured maximum of 5.1. Chemical analyses on carefully selected and concentrated but impure material indicated 46.37 to 68.29 per cent uranium (UO_2) and 5.20 to 8.50 per cent silica. Heating, leaching, and alpha-plate studies have demonstrated that vanadium, aluminum, and arsenic, which are present in many samples and could substitute for silicon, are not essential constituents of coffinite. Oxidation-potential measurements on a suspension of coffinite in 1 *N* H_2SO_4 indicate that most of the uranium is in the quadrivalent state. Infrared studies on coffinite show that there are hydroxyl as well as silicon-oxygen bonds in the tetrahedral groups, and in this respect its infrared absorption spectrum resembles that of thorogummite, $Th(SiO_4)_{1-x}(OH)_{4x}$. The proposed chemical formula for coffinite is $U(SiO_4)_{1-x}(OH)_{4x}$.

* Publication authorized by the Director, U. S. Geological Survey.

Introduction and Acknowledgments

Goldschmidt (1954, p. 563) wrote, "The entrance of quadrivalent uranium into minerals of the thorite group (e.g., uranium entering into $ThSiO_4$ in replacement of thorium ions) suggests the possibility of an unknown compound $USiO_4$. . . ." This prediction was fulfilled with the discovery of a black highly radioactive ore from the La Sal No. 2 mine, Mesa County, Colorado, which gave a zircon-type *x*-ray diffraction powder pattern. This ore contained a new mineral, coffinite, named in honor of Reuben Clare Coffin for his outstanding geologic studies in southwestern Colorado. His report on the uranium-vanadium deposits (1921, p. 1) is a major contribution. Mr. Coffin has been with the Stanolind Oil and Gas Company for many years and is also a consultant to the U. S. Geological Survey on its regional geophysical studies on the Colorado Plateaus province.

In the summer of 1951 a shipment of about five tons of high-grade uranium ore from the La Sal No. 2 mine was received at the U. S. Vanadium Company processing mill at Uravan, Colorado. The chemical assay on the ore shipment showed more than 20 per cent uranium and about 10 per cent vanadium. In August 1951 L. B. Riley, L. R. Stieff, and T. W. Stern examined the mine from which the high-grade black ore had come. Since August 1951 the new mineral first identified at the La Sal No. 2 mine has been found in more than 25 mines on the Colorado Plateau and in several other localities in the United States. Associated with coffinite is a new low-valence vanadium mineral which will be described later.

The authors, in 1953, wrote a preliminary description of coffinite which has been abstracted (Stern and Stieff, 1954). Weeks and Thompson (1954, p. 31), using data from the preliminary description, listed this mineral as "new black uranium mineral." Fleischer (1954) refers to this mineral as coffinite. Rosenzweig, Gruner, and Gardiner (1954, p. 356) made reference to "coffinite." A preliminary description of coffinite was published recently (Steiff, Stern, and Sherwood, 1955, p. 608). Gruner and Smith (1955, p. 16) in their annual report to the Atomic Energy Commission covering the period April 1, 1954, to March 31, 1955, discuss their work on coffinite. Many of their conclusions are similar to ours.

We gratefully acknowledge the assistance of many colleagues of the U. S. Geological Survey. Besides those credited directly in this paper, they include A. D. Weeks, who identified and submitted samples of coffinite; R. G. Coleman, who made polished section studies; J. M. Schopf, who made a study of associated organic material; and F. S. Grimaldi, who gave advice on chemical leaching studies. H. R. Hoekstra, of the Argonne National Laboratory, discussed with us the chemical aspects of the problem and suggested the application of infrared analysis.

Professor Clifford Frondel, of Harvard University, furnished specimens of thorite and thorogummite that he had previously studied and gave advice on many aspects of the problem. Professor J. W. Gruner, of the University of Minnesota, discussed the coffinite problem on several occasions.

This report concerns work done on behalf of the Divisions of Research and Raw Materials of the U. S. Atomic Energy Commission.

Occurrence of Coffinite

In hand specimen, coffinite is black, and many of the samples have an adamantine luster resembling that of a high-rank coal. On the Colorado Plateau coffinite occurs chiefly as replacements of organic material and to a lesser extent as disseminations in sandstone or as masses in which the original texture of the host material is no longer evident. In many localities on the Colorado Plateau the mineral is closely associated with fine-grained black low-valence vanadium minerals, with uraninite, and with finely disseminated black organic material. It is often impossible to distinguish between coffinite and uraninite in hand specimen, but in the laboratory coffinite can be identified by its *x*-ray diffraction powder pattern and by its infrared absorption spectrum. This mineral is tetragonal and gives a zircon-type *x*-ray pattern similar to that of thorite ($ThSiO_4$), and its infrared absorption spectra show hydroxyl bonds as well as silicon-oxygen bonds in the tetrahedral groups.

Up to the present time most of the coffinite studied is from the black vanadium-rich ores of the Salt Wash sandstone member of the Morrison formation (Jurassic) in the Uravan mineral belt (Fischer and Hilpert, 1952, p. 1) on the Colorado Plateau. In this belt coffinite and uraninite seem to be the most abundant uranium minerals in the black ores. Only one sample of coffinite has been identified from the Shinarump conglomerate in the Denise No. 1 mine, Green River district, Emery County, Utah. The major uranium minerals in the Mi Vida, Cal Uranium, and Homestake mines, Monticello district, San Juan, County, Utah, in the Chinle formation (Triassic) are uraninite and coffinite.

Although coffinite was first found in the uranium deposits in the sedimentary rocks of the Colorado Plateau, it has been found more recently with uraninite and pitchblende in the vein deposits of the Copper King mine, Prairie Divide, Larimer County, Colorado. The environment of deposition of the Pleateau ores is not known; however, the Copper King vein occurrence might be used to support the hypothesis that the source of the metals in the Plateau ores is at depth. The presence of low-valence vanadium minerals suggests that, in the sediments at least, reducing conditions were necessary for the deposition of coffinite.

Physical Properties

The physical properties of coffinite-bearing material are variable; even the best concentrates consist of intimate mixtures in varying amounts of very fine-grained carbonaceous substances, low-valence black vanadium minerals, clay or roscoelite, and uraninite. In general, coffinite is brittle, and the hardness of these coffinite-bearing specimens ranges from about 5 to 6. The typical hard massive variety shows no regular cleavage and has an irregular to subconchoidal fracture. The specific gravity of the most highly purified specimen is 5.1; however, we have obtained *x*-ray diffraction powder patterns of coffinite on material with a specific gravity of only 2.2. Coffinite does not fluoresce in either long or short wavelength ultraviolet radiation.

Coffinite has been identified from the formations and localities shown in Table 1.

Optical Properties

The optical properties of coffinite cannot be determined because of the very fine grained nature and opacity of the material. Although *x*-ray studies indicate that coffinite is a tetragonal mineral, in balsam mounts of mineral separates the most abundant material is so fine grained that it appears isotropic. The broadening of the lines in its *x*-ray diffraction powder pattern suggests that the individual crystallites are approximately 10^{-5} to 10^{-6} cm. in diameter (H. T. Evans, Jr., oral communication). At high magnifications the smallest grains of the purest separates containing coffinite are pale brown to very dark brown and contain many minute opaque inclusions. The larger grains are usually opaque except on thin edges, which are dark brown. Examination of the balsam mounts of the purest coffinite separates showed the presence of at least four phases. Only the use of nuclear-track plates (alpha plates), sensitive to alpha particles (Stieff and Stern, 1952, p. 184), made possible the positive recognition of the radioactive coffinite.

The alpha plates of the mineral separates contained an opaque and a pale-brown birefringent nonradioactive phase. They also contained two radioactive components: (1) small pale-brown to dark-brown isotropic grains with opaque inclusions, and (2) grains that are opaque except on thin edges, where they are dark brown. The opaque nonradioactive grains and some of the opaque inclusions in the radioactive grains are believed to be low-valence vanadium minerals or organic material. The very fine grained birefringent material resembles a clay. The remaining isotropic pale-brown to opaque radioactive material is coffinite.

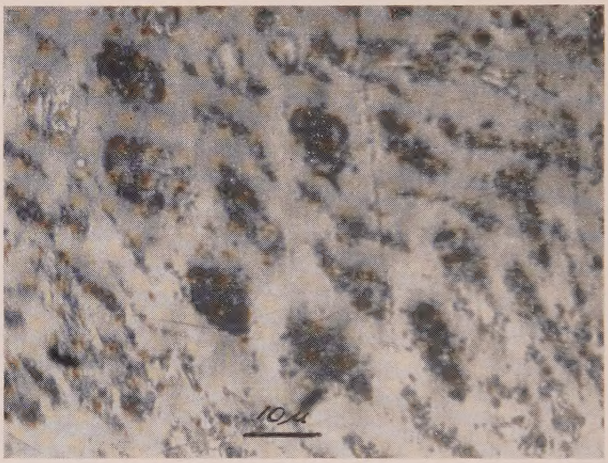
Coffinite in polished section presents even greater difficulties than in balsam mounts. Polished sections were made of the most intensely radio-

TABLE 1. COFFINITE LOCALITIES LISTED BY MINE OR PROPERTY NAME AND GEOLOGIC FORMATION

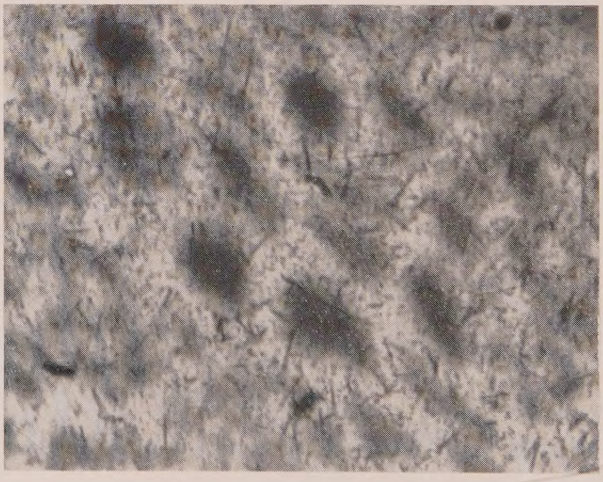
Formation	Mine or district	County	State
Browns Park formation (Miocene)	Poison Basin claims[1]	Carbon	Wyo.
Wind River formation (Eocene)	Vitro Uranium mine	Fremont	Wyo.
	Lucky Mc mine	Fremont	Wyo.
Fort Union formation (Eocene)	Kell Roy No. 3 mine[1]	Johnson	Wyo.
Vein deposit (Tertiary)	Copper King mine	Larimer	Colo.
Laramie formation (Cretaceous)	Old Leyden mine[2]	Jefferson	Colo.
Mesaverde formation (Cretaceous)	La Ventana	San Doval	N. Mex.
Morrison formation (Jurassic)	Arrowhead mine	Mesa	Colo.
	Black Mama mine	Mesa	Colo.
	La Sal No. 2 mine	Mesa	Colo.
	Matchless mine	Mesa	Colo.
	Small Spot mine[1]	Mesa	Colo.
	Shattuck Denn shaft	Montrose	Colo.
	Virgin No. 2 mine	Montrose	Colo.
	Wild Steer mine	Montrose	Colo.
	Oversight mine	Montrose	Colo.
	J. J. mine[3]	Montrose	Colo.
	Peanut mine[3]	Montrose	Colo.
	Little Muriel mine	San Miguel	Colo.
	Corvusite mine	Grand	Utah
	Grey Dawn mine	San Juan	Utah
	Jack Pile mine	Valencia	N. Mex.
	Woodrow Pipe mine	Valencia	N. Mex.
	Wind Whip mine[1]	Valencia	N. Mex.
	Poison Canyon mine[1]	Valencia	N. Mex.
	Mesa Top mine[1]	Valencia	N. Mex.
Chinle formation (Triassic)	Mi Vida mine	San Juan	Utah
	Cal Uranium mine	San Juan	Utah
	Homestake mine	San Juan	Utah
	Ruth group mine[1]	Navajo	Ariz.
	Stinking Spring Mountain[1]	Navajo	Ariz.
Shinarump conglomerate (Triassic)	Denise No. 1 mine	Emery	Utah
Dolores formation (Triassic)	Robinson property, near Placerville[2]	San Miguel	Colo.
Cutler formation (Permian)	Weatherly property, near Placerville[2]	San Miguel	Colo.
Garber formation (Permian)	J. B. Smith farm, sec unit 1, Saddle Mountain[2]	Kiowa	Okla.
San Andres formation (Permian)	Sec. 63, block 47, H. and T. C. Survey[2]	Potter	Texas
Dripping Spring quartzite (Precambrian)	Workman No. 1 mine	Gila	Ariz.
Vein (unknown age)	Little Mo mine (Arrowhead No. 1)[1]	Fremont	Wyo.

[1] Identified by J. W. Gruner and D. K. Smith, Jr., University of Minnesota.
[2] Identified by A. J. Gude, 3d., U. S. Geological Survey.
[3] Identified by M. E. Thompson, U. S. Geological Survey.

active fragments of mineralized wood. This wood shows cellular structure, and coffinite fills the cell cavities (pl. 1). The most easily recognizable minerals in the polished sections are montroseite, paramontroseite, new low-valence vanadium minerals, and uraninite. The organic material



(*A*) Cell cavities, some showing deformation, are replaced by coffinite. The light-colored areas of high reflectance are carbonaceous materials.



(*B*) Alpha-particle tracks (short dark lines) in nuclear-track film overlying the polished section shown in (*A*). Note radial arrangement of alpha tracks around cells filled with radioactive coffinite.

PLATE 1

Photomicrographs of polished section of radioactive ore from La Sal No. 2 mine, Mesa County, Colorado. Magnification approximately 900×.

in stringers and in the cell walls is anisotropic and has a moderately high yellowish reflectance. The use of high-resolution autoradiographic stripping-film techniques made it possible to localize the most radioactive phase—coffinite. Even under the highest magnifications (1000×) the mineral appears as grayish-black to brown aggregates of very fine particles. The reflectance of coffinite from the La Sal No. 2 mine, west Gateway district, Mesa County, Colorado, is low, and the mineral appears to be isotropic.

In the polished sections of La Sal No. 2 ore, coffinite is found both in the cell cavities and as veinlets. The veinlets of coffinite appear as thin elongated masses, oriented more or less perpendicularly to the walls of the vein. The coffinite masses are completely surrounded by carbonaceous material. Some deformation of the veinlets evidently occurred after emplacement, as can be seen by the dispersal and rearrangement of elongated fragments of coffinite. In many other mines uraninite and coffinite are intimately associated. The reflective characteristics of uraninite are somewhat higher than those of coffinite but are otherwise similar.

X-ray Diffraction

Coffinite was first recognized as a new mineral by *x*-ray diffraction powder patterns. Its structure is of the zircon type. In Table 2 the interplanar spacings of coffinite from the Arrowhead mine, Gateway mining district, Mesa County, Colorado, are compared with the calculated *d*-spacings, assuming the same reflections and orientation as for zircon. The $c:a$ ratio for this specimen of coffinite is 0.909. The $c:a$ ratio varies slightly from sample to sample. The similarity in *x*-ray diffraction powder patterns of thorite and coffinite originally suggested that this new mineral probably had the formula $USiO_4$.

As has been mentioned, the *x*-ray diffraction powder lines show a broadening, indicating that the coffinite crystallites are extremely small, probably on the order of 10^{-5} to 10^{-6} cm. in diameter. The very small size of the coffinite crystallites and the association of coffinite with black very fine grained vanadium and uranium minerals and with black organic material made it impossible to obtain pure separates of coffinite.

Chemical Analyses

The highest grade coffinite ores were hand picked to obtain a preliminary concentrate as low as possible in vanadium minerals, uraninite, and organic material. This preliminary concentrate was crushed, sieved, and a methylene iodide heavy-liquid separation was made. The separates that

TABLE 2. *X*-RAY DIFFRACTION POWDER DATA FOR COFFINITE FROM THE ARROWHEAD MINE, GATEWAY MINING DISTRICT, MESA COUNTY, COLORADO

Indexed assuming tetragonal zircon-type cell with $a_0=6.94$ Å, $c_0=6.31$ Å. Calculations by E. A. Cisney, U. S. Geological Survey (Cu/Ni radiation).

I	*d* meas., (Å)	*d* calc., (Å)	*hkl*
S	4.66	4.66	011
S	3.47	3.47	200
W	2.78	2.78	121
M	2.64	2.65	112
F	2.46	2.45	220
W	2.18	2.17	031
F	2.01	2.01	013
W	1.841	1.841	321
M	1.801	1.801	312
W	1.737	1.740	123
		1.735	400
F	1.629	1.626	411
F	1.556	1.552	420
F	1.451	1.452	332
F	1.435	1.435	024

F=faint. W=weak. M=medium. S=strong.

were heavier than methylene iodide (density 3.3) were used for the various chemical analyses. A series of separations with the Frantz isodynamic separator did not make any significant improvement in the concentration of the coffinite. The results of chemical analyses of three samples are given in Table 3.

As can be seen from the analyses in Table 3, there is no simple relation between uranium, silicon, vanadium, arsenic, and aluminum. The low silica content of the samples reduced the possibility that coffinite had the simple formula $USiO_4$. The presence of amorphous uranium or the substitution of hydroxyl, arsenic, vanadium, and aluminum for silicon was a distinct possibility. On the basis of the chemical analyses alone, however, coffinite could not be adequately characterized.

Oxidation-potential measurements by A. M. Pommer and J. C. Chandler on a suspension of coffinite in 1 *N* H_2SO_4 indicated that most of the uranium was in the quadrivalent state. These *Eh* measurements also ruled out the possibility of the presence of sexivalent amorphous uranium.

SYNTHESIS

The impurity of the natural coffinite-bearing concentrates immediately suggested that the uncertainties concerning the chemical composition could be overcome if coffinite could be synthesized. The problem of synthesis was undertaken at the Geological Survey laboratories, by Dr.

TABLE 3. CHEMICAL ANALYSES OF COFFINITE-BEARING SAMPLES[1]

	$USiO_4$	La Sal No. 2 mine	Arrowhead mine	Arrowhead mine[2]
UO_2	81.80	68.29	46.37	58.60
SiO_2	18.20	5.20	7.40	8.50
As_2O_5		4.35	1.44	1.22
Al_2O_3		3.87	6.80	10.12
V_2O_5		2.85	18.90	3.25
Fe_2O_3		1.24	1.57	4.44
P_2O_5			2.69	
S			0.80	
Pb		0.12	0.52	0.15
CaO				2.00
Loss on ignition[3] at				
110° C.		1.68	0.44	
110–450° C.		6.81	9.60	
450–800° C.		0	0	
250° C.				6.00
250–500° C.				6.80
500–850° C.				1.20
	100.00	94.41	96.53	102.28

[1] Analyses by A. M. Sherwood, U. S. Geological Survey.

[2] Sample prepared by M. E. Thompson, U. S. Geological Survey.

[3] Results of loss on ignition are not a direct indication of water content because of the presence of carbonaceous material.

George W. Morey at the Geophysical Laboratory of the Carnegie Institution of Washington, and by Prof. Clifford Frondel at Harvard University. Previously Dr. S. M. Lang of the National Bureau of Standards had attempted to obtain $USiO_4$ from melts at high temperatures without success. At the present time, July 1955, in spite of repeated attempts, $USiO_4$ has not been prepared by any of the workers mentioned above. Attempts to prepare coffinite from aqueous solution are being continued by the authors.

ALPHA-PLATE AND LEACHING STUDIES

The complete failure of the synthesis studies and the ambiguous results of the chemical analyses made it necessary to use several indirect techniques to arrive at the composition of coffinite. In addition, the minute opaque inclusions had not been identified. It also remained to determine if the vanadium, aluminum, and arsenic were essential. The presence of bonded hydroxyl groups in the structure of coffinite could not be established by chemical analyses of the natural material, and the relatively low silica content of the samples raised legitimate doubts as to whether the silicon was essential, present in quartz, or present in amorphous silica.

Representative samples of the coffinite-bearing material, some heavier and some lighter than methylene iodide, were heated in closed tubes, and heated under controlled atmospheres. The sample highest in arsenic, on heating in a closed tube, produced an arsenic mirror. The *x*-ray diffraction powder pattern of the heated material showed that coffinite was still the only major crystalline material present. This experiment suggests that arsenic is not essential to coffinite.

When the heated coffinite was dispersed on alpha plates it was seen that the material had changed in several aspects. The transparent moderately radioactive grains had changed from brown to a gray color. The edges of the opaque highly radioactive grains appeared to be more granular, and only a few showed a reddish-brown color on thin edges. Hence, heating the coffinite separates had also visibly reduced the amount of organic material in the samples.

Chemical analyses for soluble silica and total silica were made on four samples of coffinite and two samples of thorogummite. The soluble silica was determined on the solutions obtained by treating the mineral concentrates with (1+3) HNO_3. The total silica content of the two purest separates of coffinite was 6.0 to 7.0 per cent. The HNO_3 leach solutions of coffinite separates contained 4.50 and 1.25 per cent silica. The HNO_3 leach solutions from two thorogummite specimens contained 5.25 and 7.50 per cent silica. Originally these two thorogummite samples contained 19.00 and 37.50 per cent total silica. The coffinite residue did not give an *x*-ray diffraction pattern, and the uranium content of the residue dropped from that of a major constituent (>10 per cent) to less than 0.0001 per cent.

Following these preliminary leaching studies a more detailed series of experiments were undertaken on coffinite from the La Sal No. 2 mine to establish, if possible, the relation of the soluble silica to the uranium content, the form of the insoluble silica, and the role of vanadium. The results of these experiments are summarized in Table 4.

The Si/U ratios of the filtrates, F_1 and F_2 (Table 4), are 0.0536 and 0.0537, respectively. The theoretical Si/U ratio for $USiO_4$ is 0.1176. From these data, it would appear that this specimen of coffinite contains slightly less than half as much silica as the theoretical maximum. The similarities in the Si/U ratios of F_1 and F_2 support the oxidation-potential measurements in suggesting that amorphous uranium, readily soluble in H_2SO_4, was not present and that the U and Si are combined in a single phase. In contrast, the V/U ratios of the filtrates F_1 and F_2 are 0.214 and 0.463, respectively. The large difference suggests that the V was not an essential constituent of the uranium mineral. This interpretation was strengthened by the study of the polished sections of La Sal ore, which

TABLE 4. RESULTS OF LEACHING EXPERIMENTS ON COFFINITE SAMPLE FROM LA SAL NO. 2 MINE, GATEWAY DISTRICT, MESA COUNTY, COLORADO

	Original sample (per cent)	Treated with 1 N H_2SO_4 for 1 hr.		R_1 treated with 1 N HNO_3 for 16 hr.	
		Filtrate, F_1 (per cent)	Residue, R_1 (per cent)	Filtrate, F_2 (per cent)	Residue, R_2 (per cent)
U	39.50	30.78	8.72[1]	7.82	<0.0001[2]
Si	4.80	1.65	3.15[1]	0.42	2.73[1]
V	10.38	6.59	3.79[1]	3.62	0.17[1]
Al	1–10[2]		1–10[2]		1–10[2]
As	4.08	~4.08	0.1–1[2]		<0.0001[2]
Fe	1.83		0.1–1[2]		
H_2O-	2.87				
H_2O+	6.13				
H	0.63–0.73[3]				
C	5.89–5.94[3]				
Specific gravity	4.64		3.23		2.75
X-ray	coffinite		coffinite		no pattern

[1] By difference.

[2] Semiquantitative spectrographic analysis by C. S. Annell, U. S. Geological Survey.

[3] Analyses by R. T. Moore, U. S. Geological Survey.

showed numerous intergrowths of montroseite VO(OH), and other low-valence vanadium oxides with coffinite.

Comparative alpha-plate studies of the original La Sal ore and residue from the H_2SO_4 and HNO_3 leaches show a number of marked changes. R_1, the residue of the H_2SO_4 leach, contains relatively few pale- to dark-brown isotropic radioactive grains compared with the original sample. The number of brown birefringent nonradioactive grains appeared greater. Most opaque radioactive grains were not transparent on thin edges, and the grain boundaries were irregular. The alpha activity of the opaque grains appeared somewhat reduced. Radiocolloids were abundant.

The alpha plate of the residue from the HNO_3 leach, R_2, contained only pale-brown birefringent nonradioactive grains, weakly radioactive opaque grains, and scattered radiocolloids. The opaque grains were lacy in appearance showing abundant evidence of the removal of material by the nitric acid leach. This evidence suggested that many of the opaque inclusions noted in the radioactive brown isotropic grains were carbonaceous, and that the opacity of many of the radioactive particles was due to carbonaceous material. The fine-grained birefringent phase most

resembled a clay. The presence of a clay mineral would account for the silicon and aluminum reported in the analyses of the residues, R_1 and R_2 (Table 4).

Infrared Analyses

Although the experiments described above suggested that arsenic and vanadium are not essential and that coffinite does contain some silica, the total silica content of the coffinite concentrates was not sufficient to allow a formula of the type $USiO_4$. McConnell (1950, p. 166) proposed the substitution of $(OH)_4^{-4}$ for $(SiO_4)^{-4}$ in montmorillonite. Frondel (1953, p. 1007) has shown that hydroxyl substitution exists in thorogummite. During the authors' visit at the Argonne National Laboratory, Dr. H. R. Hoekstra suggested that the presence of bonded hydroxyl groups in the coffinite structure might be established by infrared analyses. Following his suggestion, specimens of coffinite, thorogummite furnished by Professor Frondel of Harvard University, zircon, and uraninite were ground to pass through a 400-mesh sieve, vacuum dried in an Abderhalden drying pistol, and analyzed in an infrared spectrometer for hydroxyl and silicon-oxygen bonds by R. G. Milkey of the Geological Survey.

Figure 1 shows the results of infrared absorption studies on zircon, thorogummite, coffinite, and uraninite. The silicon-oxygen bonds in the tetrahedral groups in zircon, $ZrSiO_4$, show absorption from wavelengths of about 10.2 to 11.2 microns. This is the region where Launer (1952, p. 770) has shown that silicates with isolated tetrahedra, such as zircon, will absorb strongly. He has also shown that zircon has an absorption at a shorter wavelength band, approximately 9.7 microns. The thorogummite from Iisaka, Japan, and Baringer Hill, Llano County, Texas, showed absorption in the 9.7 and 11.2 micron region. In addition, these samples showed strong absorption in the region between 2.8 and 3.1 microns. The latter absorption is characteristic of bonded OH groups with some unbonded OH present.

Coffinite from three localities on the Colorado Plateau showed absorption spectra closely resembling either the Iisaka or the Baringer Hill specimen of thorogummite. In general, the absorption band in the OH region was not as sharp as that obtained for thorogummite. In contrast, the infrared absorption pattern for very pure uraninite, essentially UO_2, from the Happy Jack mine, San Juan County, Utah, did not show any significant absorption throughout the region from 2 to 14 microns. The infrared analyses strongly suggest that coffinite, like thorogummite, does contain bonded OH.

Conclusions

Difficulties in obtaining pure coffinite concentrates and the complete failure of repeated attempts to synthesize $USiO_4$ made it necessary to use

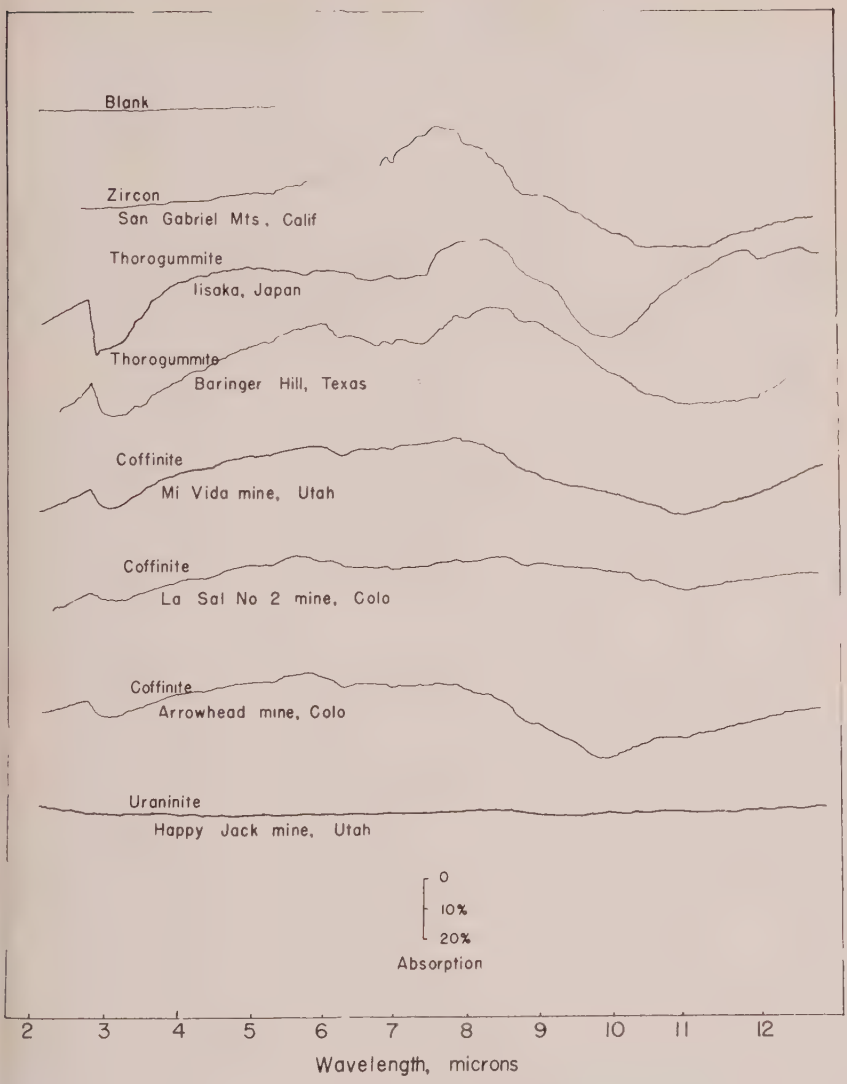


FIG. 1 Infrared absorption spectra of zircon, thorogummite, coffinite, and uraninite.

a combination of indirect techniques in order to arrive at the chemical composition of coffinite. Heating, leaching, and alpha-plate studies combined with x-ray and semiquantitative spectrographic analyses strongly suggest the following: silica to uranium ratios are constant but insufficient to satisfy the formula $USiO_4$, arsenic and vanadium are not essential constituents of coffinite, the phase soluble in HNO_3 contains most of the uranium and 20 to 75 per cent of the total silica in the coffinite-bearing speci-

men. Amorphous sexivalent uranium is not present, and the uranium is in the quadrivalent state. Coffinite has a distinctive x-ray diffraction powder pattern of the zircon-type with $a_0 = 6.94$ Å and $c_0 = 6.31$ Å. The close similarity of the infrared absorption spectra of thorogummite, $Th(SiO_4)_{1-x}(OH)_{4x}$, and coffinite indicated that coffinite contains silicon-oxygen bonds in tetrahedral groups as well as bonded hydroxyl groups. Although no single line of evidence is sufficient to establish the identity and composition of this important uranium mineral of the unoxidized ores of the Colorado Plateau, all of the evidence taken together strongly supports the idea that coffinite is tetragonal with a zircon-type structure and has the formula $U(SiO_4)_{1-x}(OH)_{4x}$.

Addendum

Since the preparation of this manuscript H. R. Hoekstra and L. H. Fuchs of the Argonne National Laboratory have synthesized coffinite using uranous chloride and sodium silicate. The oven-dried product gave an x-ray diffraction powder pattern which matched patterns of nautral coffinite. The infrared absorption spectra showed the presence of bonded OH groups. A report of this work is published in *Science*, **123,** 105 (1956).

References

Coffin, R. C. (1921), Radium, uranium, and vanadium deposits of southwestern Colorado: *Colorado Geol. Survey, Bull.* **16,** 1–231.

Fischer, R. P., and Hilpert, L. S. (1952), Geology of the Uravan mineral belt: *U. S. Geol. Survey, Bull.* **988-A,** 1–13.

Fleischer, Michael (1954), New mineral names: *Am. Mineral.*, **39,** 1037.

Frondel, Clifford (1953), Hydroxyl substitution in thorite and zircon: *Am. Mineral.*, **38,** 1007–1018.

Goldschmidt, V. M. (1954), Geochemistry, Oxford University Press, 702 p.

Gruner, J. W., and Smith, D. K., Jr. (1955), Annual report for April 1, 1954, to March 31, 1955: *U. S. Atomic Energy Comm., Tech. Inf. Serv.*, **RME-3020,** 16–24.

Launer, P. L. (1952), Regularities in the infrared absorption spectra of silicate minerals: *Am. Mineral.*, **37,** 764–784.

McConnell, Duncan (1950), The crystal chemistry of montmorillonite: *Am. Mineral.*, **35,** 166–172.

Rosenzweig, A., Gruner, J. W., and Gardiner, Lynn (1954), Widespread occurrence and character of uraninite in the Triassic and Jurassic sediments of the Colorado Plateau: *Econ. Geology*, **49,** 351–361.

Stern, T. W., and Stieff, L. R. (1954), Preliminary description of coffinite—a new uranium mineral (abstract): *Nuclear Science Abstracts*, **8,** 62, abstract 530.

Stieff, L. R., and Stern, T. W. (1952), Preparation of nuclear-track plates and stripping films for the study of radioactive minerals: *Am. Mineral.*, **37,** 184–196.

Stieff, L. R., Stern, T. W., and Sherwood, A. M. (1955), Preliminary description of coffinite—a new uranium mineral: *Science*, **121,** 608–609.

Weeks, A. D., and Thompson, M. E. (1954), Identification and occurrence of uranium and vanadium minerals from the Colorado Plateaus: *U. S. Geol. Survey, Bull.* **1009-B,** 13–62.

Manuscript received Dec. 9, 1955.

A RESTUDY OF BAKERITE, PRICEITE, AND VEATCHITE*

HENRY KRAMER, *U. S. Geological Survey, Washington, D. C.*,†

AND

ROBERT D. ALLEN, *U. S. Geological Survey, Claremont, California.*

ABSTRACT

Complete chemical analyses have been made on six specimens to clarify existing uncertainties in the formulas of bakerite, priceite, and veatchite. Previously published formulas are corroborated for all three minerals. Optical measurements clear up several ambiguities in the literature. Tabulated below are formulas (calculated from analyses), optical properties, specific gravities, and spectrographic determinations.

	Bakerite	*Priceite*	*Veatchite*
Chemical formula	$8CaO \cdot 5B_2O_3 \cdot 6SiO_2 \cdot 6H_2O$	$4CaO \cdot 5B_2O_3 \cdot 7H_2O$	$3(SrO, CaO) \cdot 8B_2O_3 \cdot 5H_2O$
α_{Na}	1.626 ± 0.004*	1.573 ± 0.002	1.550 ± 0.002
β_{Na}	——	1.595 (calc.)	1.553 (calc.)
γ_{Na}	1.655 ± 0.003*	1.597 ± 0.002	1.621 ± 0.002
2V	——	$32° \pm 2°$	$25° \pm 2°$
Optical group	——	Biaxial negative	Biaxial positive
Specific gravity (25° C.)	2.885*	2.415*	Not determined
Trace elements (<1%)	Al, Mg, Fe, Na, Sr, Cu, Sn, Pb, Ag, Mn	Si, Al, Mg, Fe, Sr, Cu, Na	Ca, Si, Al, Mg, Fe, Ba, Cu, Mn

* Average value.

X-ray data confirm a striking similarity between bakerite and datolite patterns; a possible structural formula for bakerite, which agrees with the chemical analyses is $Ca_8B_8(BO_4)_2(SiO_4)_6(OH)_6 \cdot 3H_2O$.

On the basis of mineralogical and chemical associations it is suggested that (1) priceite is sometimes derived from colemanite, (2) bakerite may be deposited by hydrothermal solutions.

INTRODUCTION

Bakerite, priceite, and veatchite are three borates whose reported chemical formulas are subject to review; and optical determinations available on these minerals are incomplete or inconsistent. The experimental results of examining California specimens are reported in this paper to help clarify several of these uncertainties. In addition, spectrographic analyses, *x*-ray diffraction data, and density determinations are included. A brief discussion of the origin of bakerite and priceite is based on mineralogical and chemical associations. Descriptions of the six specimens studied are presented below.

* Publication authorized by the Director, U. S. Geological Survey.

† Present address: Pyrotechnics Laboratory, Samuel Feltman Ammunition Laboratories, Picatinny Arsenal, Dover, New Jersey.

Specimen number	*Locality*	*Occurrence*
Bakerite 1 (Collected by W. T. Schaller)	Corkscrew Canyon, Death Valley area, Inyo County, Calif. (Exact locality not known)	As irregular veins in altered volcanic rock. Pockets among veins are lined with acicular crystals of thomsonite and natrolite
Bakerite 2 (Collected by D. H. Kupfer)	Center of sec. 22, T. 26 N., R. 2 E., San Bernardino base and meridian, DeBely Wash, 1000 feet SW. of DeBely Mine, Death Valley area, Inyo County, Calif.	Float. Encrusted and veined by minute crystals of natrolite and thomsonite
Priceite 1 (Collected by F. M. Byers)	NW¼ sec. 16, T. 26 N., R 2 E., San Bernardino base and meridian, 1450 feet N. 55° E. from U. S. Mineral Monument 40 (elev. 2191 feet); Monte Blanco area, Death Valley area, Inyo County, Calif.	White veins associated with colemanite in basaltic tuff. (Tuff consists of partly devitrified glass with average index of refraction near 1.50, nondescript anisotropic material, and basalt fragments)
Priceite 2 (Collected by J. F. McAllister)	SW¼ sec. 9, T. 26 N., R. 2 E., San Bernardino base and meridian, 3900 feet N. 45° E. from U. S. Mineral Monument 40 (elev. 2191 feet), Corkscrew Wash, Death Valley area, Inyo County, Calif.	White veins in altered basalt
Priceite 3 (Collected by D. F. Hewett)	Same as Priceite 2	Megascopically translucent and pale olive-yellow.* Float presumably derived from veins in altered basalt
Veatchite (Collected by S. J. Muessig)	Center NE¼ sec. 32, T. 5 N., R. 14 W., San Bernardino base and meridian, lower dump, Lang Borate district, Tick Canyon, Los Angeles County, Calif.	Silky fibrous crystals encrusting colemanite and clay on massive howlite

* Pale olive-yellow 10 Y 7/2, Rock-Color Chart, *Geol. Soc. Am.* (1951).

X-ray powder patterns were prepared by Arthur Chodos, Department of Geology, California Institute of Technology. Spectrographic analyses were made by H. W. Johnson, Pacific Spectrochemical Laboratory, Los Angeles, Calif. Datolite specimens were supplied by W. C. Oke of the California Institute of Technology. Borate specimens were collected by members of the U. S. Geological Survey whose names are given above.

The original manuscript was revised in accord with suggestions by W. T. Schaller, C. L. Christ, and members of the Claremont office of the Geological Survey.

Bakerite

Optical Properties

Palache, Berman, and Frondel (1951) describe bakerite as "Optically biaxial with moderate birefringence and a mean index of refraction of 1.642; in part spherulitic." The specimens used in the present investigation have permitted measurement of both alpha and gamma. It was not possible, however, to determine either beta or 2V because of its fine-crystalline habit.

Table 1. Optical Properties of Bakerite

	Bakerite 1	Bakerite 2	Palache, Berman, and Frondel (1951)
α_{Na}	1.624±0.002	1.628±0.002	—
γ_{Na}	1.654±0.002	1.656±0.002	—
Birefringence ($\gamma-\alpha$)	0.030±0.004	0.028±0.004	Moderate
Average index	1.639	1.642	1.642
$Habit_{micro}$	Cryptocrystalline to submicroscopic; spherulitic extinction	Same as bakerite 1	In part spherulitic

Chemical Analyses

From two analyses of bakerite, Giles (1903) derived the following formula: $8CaO \cdot 5B_2O_3 \cdot 6SiO_2 \cdot 6H_2O$. No other published analyses are known to the writers. W. F. Foshag (1954) has obtained two bakerite analyses which are essentially the same as those published by Giles. Contrasting with the above formula is the one proposed by Palache, Berman, and Frondel (1951) "based on the structural resemblance to datolite, herderite, and homilite indicated by *x*-ray powder diffraction study": $Ca_4B_4(BO_4)(SiO_4)_3(OH)_3H_2O$. When the latter formula is recast as oxides and multiplied by two it becomes: $8CaO \cdot 5B_2O_3 \cdot 6SiO_2 \cdot 5H_2O$. Thus, the only difference between the formulas is in the number of molecules of water. Two bakerites have been analyzed to determine the water content as well as the cationic ratios.

The possibility that "H_2O (−)" can be held in bakerite at temperatures in excess of 105° C. has been explored by two methods. (1) A differential

TABLE 2. BAKERITE—CHEMICAL ANALYSES AND CALCULATION OF FORMULA

	Bakerite 1 (per cent)		Bakerite 2 (per cent)		Giles (1903)* (per cent)		Palache Berman, and Frondel (1951) theoretical per cent)
	Orig.	Recalc.	Orig.	Recalc.	Orig.	Recalc.	
CaO	35.14	35.42	34.47	35.24	35.05	35.38	35.97
B_2O_3	27.58	27.79	26.57	27.17	27.30	27.56	27.92
SiO_2	27.90	28.12	28.40	29.03	28.25	28.52	28.89
H_2O (+)	8.60	8.67	8.37	8.56	8.46	8.54	7.22
H_2O (−)	0.30		0.26				
R_2O_3	0.65		1.93		0.94		
Total	100.17		100.00		100.00		
Less H_2O (−) and R_2O_3	0.95		2.19		0.94		
Total	99.22	100.00	97.81	100.00	99.06	100.00	100.00
Specific gravity (25° C.)	2.88		2.89				2.88

Analyst: Henry Kramer

	Molecular proportions (Bakerite 1)	Oxygen atoms	Atomic ratios		Atomic ratios on basis of 40 O's
CaO	0.632	0.632	Ca	0.632	7.788
B_2O_3	0.399	1.197	B	0.798	9.833
SiO_2	0.468	0.936	Si	0.468	5.767
H_2O	0.481	0.481	H	0.962	11.854

Atomic ratios and formula on basis of 41 O's

Ca	7.983
B	10.080
Si	5.911
H	12.151

$Ca_8B_{10}Si_6O_{35} \cdot 6H_2O$

or

$8CaO \cdot 5B_2O_3 \cdot 6SiO_2 \cdot 6H_2O$

* Average of two analyses.

thermal analysis curve of bakerite 2 was prepared with a portable apparatus, using maximum sensitivity and a heating rate of 30° C. per minute to obtain maximum thermographic response from the instrument. A single endothermic peak was recorded which commenced at an indefinite point between 400 and 500° C. and reached a maximum at 590° C. The sample was not heated above 600° C. (2) Bakerite 1 was heated in a muffle furnace at 200° C. for 30 minutes. Water loss was not appreciably greater than at 105° C. These results would indicate that the usual procedure for determination of "H_2O (−)" is applicable to bakerite.

The assumption of 41 oxygen atoms in the formula fits the analysis of bakerite 1 and verifies Giles' formula for bakerite. Although bakerite 2 was unsuitable for formula calculation because of impurities, its B_2O_3/H_2O ratio, calculated from weight per cents, also substantiates this formula:

	Bakerite 1	*Bakerite 2*
B_2O_3/H_2O	3.205	3.174

Priceite

Optical Properties

Although the indices of refraction of priceite are known with reasonable accuracy (Larsen, 1917; Foshag, 1924), the measured and calculated values of 2V are discordant (Palache, Berman, and Frondel, 1951). In fact, 2V has been previously measured only on priceite from Panderma, Turkey (also known as pandermite).

The direct measurement of beta on grains of priceite is exceptionally difficult because the orientation of the optical indicatrix is uncertain. Beta was determined, therefore, by calculation from alpha, gamma, and 2V measured on the universal stage, as well as by direct measurement.

Cryptocrystalline varieties of priceite (priceite 2 and 3) whose crystal diameter averages less than 5 microns appear to have a lower gamma index, and consequent lower birefringence, than the coarser crystallized type (priceite 1), whose crystal diameter averages more than 20 microns. This effect is probably caused by the nearly submicroscopic particle size rather than by variations in the chemistry of the mineral. Optical data from the coarser material are believed to be superior. The 2V measured on priceite 1 is exactly the same as that reported for priceite from Panderma (Larsen, 1917). Beta calculated is the same as beta measured (on grains "on edge"), limits of error considered.

Chemical Analyses

Foshag (1924) gives two possible formulas for priceite: (1) $4CaO \cdot 5B_2O_3 \cdot 7H_2O$ (after Van't Hoff); (2) $5CaO \cdot 6B_2O_3 \cdot 9H_2O$. Either one

Table 3. Optical Properties of Priceite

	Priceite 1	Priceite 2	Priceite 3	Foshag (1924)
α_{Na}	1.573±0.002	1.573±0.003	1.573±0.003	1.571
β_{Na} calc	1.595	—	—	—
β_{Na} meas.	1.594±0.002	—	—	1.590
γ_{Na}	1.597±0.002	1.595±0.003	1.591±0.003	1.593
Birefringence ($\gamma-\alpha$)	0.024±0.004	0.022±0.006	0.018±0.006	0.022
Optic sign	Negative	—	—	Negative
$2V_{measo.}$	32°±2°	—	—	Medium
$Habit_{micro.}$	Tiny "books" of plates with rhombic outline	Cryptocrystalline	Cryptocrystalline	—
Orientation	α angle long dimension of "plates on edge" varies between 60° and 70°. γ is at an angle with the bisectrix of the obtuse angle of a rhomb of about 5°	—	—	—

is in approximate agreement with published analyses. In this investigation three extremely pure priceites have been analyzed in an attempt to refine our knowledge of the stoichiometry. All three priceites gave negative tests for SO_3 and CO_2. Priceites 1 and 2 contained virtually no insoluble material whereas priceite 3 contained a trace of insoluble material, microscopically identified as volcanic glass and clay. Calculations based on analyses of priceites 1 and 2 support the formula $4CaO \cdot 5B_2O_3 \cdot 7H_2O$.

Veatchite

Optical Properties

Published optical measurements on veatchite (Switzer, 1938; Stewart, Chalmers, and Phillips, 1954) present the following inconsistency: 2V (measured?) is reported as 37°±2°, but 2V calculated from the indices of refraction would be 20.4°.

The indices of refraction found for veatchite are close to those determined by Switzer, but 2V was measured as 25°, which is consistent with these indices. Because of its perfect side pinacoidal cleavage, beta was determined by calculation from alpha, gamma, and measured 2V.

TABLE 4. PRICEITE—CHEMICAL ANALYSES AND CALCULATION OF FORMULA

	Priceite 1 (per cent)		Priceite 2 (per cent)		Priceite 3 (per cent)		Priceites 1 and 2 Average (per cent) Recalc.
	Orig.	Recalc.	Orig.	Recalc.	Orig.	Recalc.	
B_2O_3	49.87	49.88	49.64	49.92	48.95	49.20	49.90
CaO	32.04	32.05	31.90	32.08	32.06	32.43	32.06
H_2O (+)	18.07	18.07	17.90	18.00	18.28	18.37	18.04
H_2O (−)	0.20		0.69		0.41		
Total	100.18		100.13		99.70		
Less H_2O	(−0.20)		0.69		0.41		
Total	99.98	100.00	99.44	100.00	99.29	100.00	100.00
Specific gravity (25° C.)	2.41		N.D.		2.42		

Analyst: Henry Kramer

	Molecular proportions	Oxygen atoms	Atomic ratios		Atomic ratios and formula on basis of 26 O's	
B_2O_3	0.713	2.139	B	1.426	9.988	$Ca_4B_{10}O_{19}\cdot 7H_2O$
CaO	0.572	0.572	Ca	0.572	4.006	or
H_2O	1.001	1.001	H	2.002	14.022	$4CaO\cdot 5B_2O_3\cdot 7H_2O$

TABLE 5. OPTICAL PROPERTIES OF VEATCHITE

	Allen	Switzer (1938)	Stewart, Chalmers, and Phillips (1954)
α_{Na}	1.550±0.002	1.551	1.551
β_{Na}	1.553 (calc.)	1.553	1.553
γ_{Na}	1.621±0.002	1.621	1.621
Birefringence (γ–α)	0.071±0.004	0.070	0.070
Optic sign	Positive	Positive	Positive
$2V_{meas.}$	25°±2°	37°±2°	37°
$Habit_{micro}$	Platy cleavage fragments (parallel to 010)	—	—
Orientation	Angle between γ and "c" is about 30°	Angle between γ and "c" is −38°	Angle between γ and "c" is −30°

Chemical Analyses

An average of three analyses of veatchite from the Lang district indicates the formula $3SrO \cdot 8B_2O_3 \cdot 5H_2O$ (Switzer and Brannock, 1950). A microchemical analysis of veatchite from Aislaby, Yorkshire, gives the formula $SrO \cdot 3B_2O_3 \cdot 2H_2O$ (Stewart, Chalmers, and Phillips, 1954).

The present veatchite analysis is essentially in agreement with the average analysis of Switzer and Brannock (1950), and agrees approximately with the formula they proposed. Unfortunately, our veatchite specimen, which contained less than one per cent clay, was not sufficient for a second analysis or specific gravity measurement.

TABLE 6. VEATCHITE—CHEMICAL ANALYSES AND CALCULATION OF FORMULA

	Veatchite (per cent)		Switzer and Brannock (1950) (average of three recalculated analyses (per cent)	Stewart, Chalmers and Phillips (1954) (per cent)	
	Orig.	Recalc.		Orig.	Recalc.
SrO	30.50	30.72	30.0	30.0*	29.8*
CaO	1.68	1.69	1.6		
B_2O_3	57.56	57.96	58.5	60.3	59.8
H_2O (+)	9.56	9.63	9.6	10.5	10.4
H_2O (−)	0.30				
CO_2	nil				
SO_3	nil				
Insoluble	N.D.				
Total	99.69				
Less H_2O (−)	0.39				
Total	99.30	100.00	99.7	100.8	100.0

Analyst Henry Kramer

	Molecular proportions	Oxygen atoms		Atomic ratios	Atomic ratios and formula on basis of 32 O'S
SrO	0.296	0.296	Sr	0.296	2.821 } 3.107
CaO	0.030	0.030	Ca	0.030	0.286 }
B_2O_3	0.832	2.496	B	1.664	15.861
H_2O	0.535	0.535	H	1.070	10.199
					$(Sr, Ca)_3B_{16}O_{27} \cdot 5H_2O$ or $3(SrO, CaO) \cdot 8B_2O_3 \cdot 5H_2O$

* Includes SrO and CaO.

Spectrographic Analyses

Spectrographic analyses for minor elements in bakerite, priceite, and veatchite are presented in Table 7.

Table 7. Spectrographic Analyses

Concentration range (per cent)	Bakerite		Priceite			Veatchite
	1	2	1	2	3	
0.X	Mg Al Fe	Mg Na	Si	Si Mg Sr	Si Mg Al Fe Na	Si Mg Ca
0.0X	Sr Cu Pb Na	Al Fe Pb	Mg Al Fe Sr	Al Fe	—	Al Fe Ba
0.00X	Ag Mn	Cu Sn	Cu	Cu	Cu	—
0.000X	—	—	—	—	—	Cu Mn

X-Ray Diffraction Data

X-ray powder patterns were prepared for all three minerals with nickel-filtered copper radiation over the range $2\theta = 0°$ to 90°, the spectrum being scanned with a Geiger counter spectrometer at 1° per minute.

The similarity between powder patterns of bakerite and datolite has been noted by Palache, Berman, and Frondel (1951). In Table 8 the bakerite pattern is compared with patterns prepared from (1) finely crystalline datolite from Keweenaw Peninsula, Michigan (datolite 1), and (2) coarsely crystalline datolite from Hampden Quarry, Springfield, Maine (datolite 2). With respect to spacing, the patterns nearly coincide for all major peaks and for many minor peaks. The bakerite pattern, however, apparently represents a slight contraction of either datolite pattern. If the bakerite structure can be derived from that of datolite by partial substitution of B for Si, contraction would be expected. Undoubtedly, bakerite and datolite structures are nearly identical, but a structural formula must account for the bakerite composition. If the formula proposed by Palache, Berman, and Frondel (1951) were modified

TABLE 8. *X*-RAY DATA: INTERPLANER SPACINGS AND RELATIVE INTENSITIES
Nickel-filtered copper radiation

Priceite 1		Priceite 2		Bakerite 1		Datolite 2		Datolite 2		Veatchite	
d(Å)	*I*	*d*(Å)	*I*	*d*(Å)	*I*	*d*(Å)	*I*	*d*(Å)	*I*	*d*(Å)	*I*
10.92	10	10.85	10	6.01	1	5.99	2	—		10.53	10
5.99	2	6.01	3	4.82	2	4.83	2	4.85	1	8.27	1
5.46	8	5.47	3	3.74	5	3.75	4	3.76	10	6.94	1
4.49	1	4.51	2	3.38	3	3.40	4	3.41	3	5.63	1
4.29	4	4.30	3	3.10	9	3.12	10	3.11	10	5.22	3
3.63	10	3.63	10	3.04	1	—		—		4.20	1
3.49	7	3.49	9	2.98	3	2.98	5	3.00	5	3.93	1
3.39	1	3.40	1	2.84	10	2.86	6	2.86	5	3.69	1
3.33	1	—		2.50	3	2.52	5	2.53	1	3.47	10
3.30	1	3.30	1	2.45	1	—		—		3.32	2
3.07	1	—		2.39	1	2.41	3	2.42	1	2.88	3
2.98	1	2.98	2	2.28	1	2.30	2	2.30	1	2.79	1
2.88	2	2.89	2	2.23	6	2.25	5	2.24	3	2.76	1
2.79	1	2.79	2	2.18	5	2.19	5	2.19	3	2.67	1
2.72	6	2.72	3	2.15	2	2.16	2	2.16	2	2.61	10
2.67	1	2.67	1	2.07	1	2.08	2	2.08	1	2.40	1
2.59	1	2.59	1	2.03	1	2.04	1	2.04	1	2.21	1
2.52	1	2.51	1	1.983	3	1.996	2	1.998	2	2.17	1
2.47	1	2.46	2	1.895	1	—		1.903	2	2.16	1
2.42	1	2.42	1	1.828	2	1.873	3	1.872	3	2.08	9
2.39	1	2.39	1	1.760	1	1.771	2	1.774	1	1.924	1
2.33	2	2.33	2	1.735	1	1.746	2	1.749	1	1.833	1
2.31	1	2.32	2	1.704	2	1.720	3	1.722	2	1.735	2
2.28	1	—		—		1.664	2	1.664	1	1.488	2
2.23	1	2.23	1	1.634	3	1.645	3	1.647	1	1.406	1
2.18	5	2.18	5	1.603	1	1.621	1	1.622	1	1.301	2
2.16	2	—		1.551	1	—		—		1.156	1
2.14	1	2.14	1	1.512	1	1.526	2	1.528	1		
2.08	1	—		—		—		1.499	1		
2.06	1	2.06	1	—		1.481	2	1.481	1		
2.03	1	2.03	1	—		—		1.429	1		
1.977	1	1.977	1	1.315	1	1.323	1	—			
1.953	1	—		—		1.305	1	—			
1.939	2	1.941	2			1.228	1	1.229	1		
1.852	1	1.852	1	1.107	1	1.191	1	—			
1.836	1							1.122	1		
1.815	2	1.814	2	—		—		1.097	5		
1.801	1	1.797	2								
1.757	1	1.755	1								
1.731	1	1.729	1								
1.695	1	—									
1.658	1	1.656	1								
1.629	1	1.629	1								
1.576	1	1.576	1								
1.556	1	1.556	1								
1.540	1	—									
1.453	1	—									
1.375	1	1.375	1								
1.352	1	1.352	1								
1.308	1										
1.269	1	1.270	1								
1.109	1	1.109	1								

as follows it would satisfy the water requirements indicated by oxide analysis: $Ca_8B_8(BO_4)_2(SiO_4)_6(OH)_6 \cdot 3H_2O$.

The pattern for priceite 1 is apparently more completely developed than the pattern for priceite 2, probably because the former is more coarsely crystallized.

The veatchite pattern agrees fairly well with a pattern reported by Stewart, Chalmers, and Phillips (1954), especially with respect to diffraction maxima of strong and moderate intensity.

Origin of Bakerite and Priceite

Mineralogic and chemical evidence suggests that bakerite is deposited by hydrothermal or late-magmatic solutions: (1) bakerite is veined and encrusted with the zeolites natrolite and thomsonite; (2) bakerite contains trace quantities of such typically hydrothermal elements as Pb, Sn, Ag, and Mn, all of which are generally absent from borates.

Mineralogic and petrographic evidence suggests that priceite is derived from colemanite. A white translucent coating sometimes found on "cauliflower" colemanite in Gower Gulch, Death Valley, is characterized by an average index of refraction near 1.585 and moderate birefringence; this material is believed to be priceite, probably an alteration of the colemanite. White pisolitic nodules from the Thompson mine which is located 2.55 miles N. 83° W. of U. S. Mineral Monument 47, Death Valley, consist of comparatively fresh colemanite mingled with finely crystalline transulcent alteration material with fibrous habit and indices of refraction intermediate between those of colemanite and priceite; if the alteration process had reached completion the end-product might have been priceite. Thin sections of priceite from the Monte Blanco area, Death Valley, show corroded euhedral inclusions of colemanite surrounded by fine-crystalline priceite.

Colemanite and priceite from the Death Valley area contain the same trace elements: Si, Al, Fe, Mg, Sr, Ma, and Cu. Principal differences in concentration are shown by Si and Cu as follows:

Per cent	0.X	0.0X	0.00X	0.000X
Colemanite		Si		Cu
Priceite	Si		Cu	

If priceite is derived from colemanite, the process might bring about enrichment in these elements.

References

Foshag, W. F. (1924), Priceite from Furnace Creek, Inyo County, California: *Am Mineral.*, **9**, 11–13.

Foshag, W. F. (1954), Personal communication.

GILES, W. B. (1903), Bakerite (a new borosilicate of calcium) and howlite from California: *Mineral. Mag.*, **13,** 353–355.

LARSEN, E. S. (1917), Proof that priceite is a distinct mineral species: *Am. Mineral.*, **2,** 1–3.

PALACHE, C., BERMAN, H., AND FRONDEL, C. (1951), Dana's System of Mineralogy, 7th ed., vol. 2, pp. 341–343, 348–349, 363.

STEWART, F. H., CHALMERS, R. A., AND PHILLIPS, R. B. (1954), Veatchite from the Permian evaporites of Yorkshire: *Mineral. Mag.*, **30,** 389–392.

SWITZER, G. (1938), Veatchite, a new calcium borate from Lang, California: *Am. Mineral.*, **23,** 409–413.

SWITZER, G., AND BRANNOCK, W. W. (1950), Composition of veatchite: *Am. Mineral.*, **35,** 90–92.

Manuscript received Dec. 8, 1955.

THERMAL STUDIES OF AMMONIUM FIXATION AND RELEASE IN CERTAIN CLAY MINERALS[1]

A. D. Scott, J. J. Hanway, and G. Stanford.[2]

Abstract

The thermal decomposition of NH_4 ions adsorbed on kaolinite, illite, bentonite and vermiculite occurred over a wide range in temperature. The temperature of decomposition appeared to be influenced by the nature of the exchange site and by the entrapment of NH_4 ions in the lattice. The H ions that remained when NH_4 ions were decomposed interfered with this method of determining the amount of NH_4 held on the different exchange sites or fixed in the lattice of the clay materials.

Wyoming bentonite fixed 15 m.e. of NH_4 per 100 grams when the NH_4 saturated clay material was heated at 300° to 350° C. The loss of NH_3 from these fixed NH_4 ions produced an exothermic peak at 550°C. in the differential thermal analysis curve for NH_4 bentonite.

The thermal decomposition of NH_4 saturated bentonite and a kaolinite clay has been investigated by Bottini (6, 7) and Cornet (9). They have shown that NH_3 is volatilized from these clays as the NH_4 ions are decomposed at high temperatures. Furthermore, from the relative rate of NH_3 loss at different temperatures, Cornet concluded that the site of the NH_4 ions on the clay determined the temperature at which they were decomposed. Working with NH_4 saturated bentonite, Cornet suggested that temperatures up to 125° C. decomposed NH_4 ions on the broken bond surfaces, while the rapid loss of NH_3 at 275° and 400 ° C. was due to NH_4 on exterior planar and interplanar surfaces, respectively.

In a study of vermiculite and its relation to biotite, Barshad (2) determined the weight loss due to NH_3 and water when NH_4 vermiculite was heated. Up to 255° C. the weight loss was due to water alone. Apparently the NH_4 ions on the vermiculite were not decomposed at this temperature. Between 255° and 500° C. a small amount of NH_3 was lost, whereas temperatures of 550° to 600° C. decomposed all of the NH_4 on the exchange.

It would appear from these investigations that NH_4 saturated clay minerals differ in the manner in which they lose NH_3 at elevated temperatures. Some of these differences are probably associated with the type of exchange sites holding the NH_4 ions on the clay. It is, however, also possible that differences arise because NH_4 ions are fixed in some clay minerals and not in others. The difference in thermal decomposition of NH_4 vermiculite and NH_4 bentonite, for instance, may be due to the fact that NH_4 ions are fixed in vermiculite but generally not in bentonite. If fixed

[1] Journal Paper No. J-2867 of the Iowa Agricultural Experiment Station, Ames, Iowa. Project No. 1234, Department of Agronomy.

[2] Agronomy Department, Iowa State College, Ames, Iowa.

NH_4 ions are decomposed at a characteristic temperature that is different from the exchangeable NH_4 ions, it is possible that thermal decomposition measurements could be used to determine fixed NH_4 in clays as well as to identify the presence of NH_4 fixing clay minerals. The objective of this study, therefore, was to determine whether a relationship existed between the thermal decomposition of adsorbed NH_4 and its fixation in clay minerals.

Differential thermal analyses are commonly used as one means of characterizing clay minerals. While each clay mineral group has in general a characteristic differential thermal curve, the individual curves obtained vary with the cation adsorbed on the clay. The differential thermal curves of NH_4 saturated clay minerals are of particular interest since the loss of NH_3 as well as water will influence the shape of the curve. It is evident from the differential thermal curves of vermiculite and bentonite obtained by Barshad (2, 3) that the effect of the adsorbed NH_4 varies with the clay mineral involved. Since these differences are probably related to the manner in which the clay minerals hold the NH_4 ions, differential thermal analyses were made in the present study to gain further information about the relationship between the thermal properties of adsorbed NH_4 and its fixation in the clay minerals. Differential thermal curves of the clays saturated with other ions were also obtained to further identify the clay minerals used in this study.

Materials and Methods

Samples of the two vermiculites investigated by Allison, *et al.* (1) were obtained from Dr. F. E. Allison for this study. One vermiculite was from Libby, Montana; the other, from Greenville, South Carolina. According to Allison, *et al.*, both materials are actually vermiculite-biotite mixtures. Wyoming (Volclay) bentonite from the American Colloid Company and Goose Lake Grundite from the Illinois Clay Products Company were used as sources of montmorillonite and illite, respectively. Kaolinite of unknown origin was also used in this investigation.

The vermiculite flakes were about 0.25 inch in diameter. In some cases, therefore, the vermiculite was ground in a Christy-Norris Laboratory hammermill using a screen with round holes 1/16-inch in diameter. The other clay materials were used without previous fractionation except as noted in the individual experiments.

Fifty to 100 grams of the clay minerals was placed on a Buchner funnel and leached with 1000 ml. of 1 *N* NH_4Cl to saturate them with NH_4. They were washed with 70 per cent methanol until the leachate gave a negative test with Nessler reagent and then air dried. The dry NH_4 saturated clays were placed in a muffle furnace on a raised platform near

the thermocouple to be heated at different temperatures and for varying lengths of time. The temperature fluctuated within plus or minus 20° C. of the desired temperature.

To determine the amount of exchangeable and fixed NH_4 on the clays, both before and after the heat treatment, the systems were made alkaline with NaOH or KOH and the NH_3 distilled into a measured amount of 0.05 *N* HCl. The excess acid was titrated with a standard NaOH solution. Blank controls were included in each set of distillations. The NH_4 on the clay mineral displaced by K will be regarded as exchangeable, while that displaced by Na but not by K will be regarded as fixed in this investigation. In some cases the total NH_4 in vermiculite was determined by first digesting the sample in concentrated H_2SO_4.

Differential thermal analyses were made with automatic recording equipment. The sample holders and covers were made of 18-8 chrome-nickel steel. Pt—Pt (10% Rh) thermocouples were used to measure the differential temperature. The furnace temperature was measured with a chromel-alumel thermocouple in the center of the sample block. Powdered alumina was used as the inert material. The temperature was increased at the rate of 10° C. per minute.

Time of Heating

A study was first made to determine how long the NH_4 clay minerals should be heated at any one temperature. There is no evidence in the literature to indicate the stability of the adsorbed NH_4 to prolonged heating. It was, therefore, entirely possible that all of the NH_4 could be decomposed even at a relatively low temperature if the NH_4 clay mineral were heated long enough.

To determine the effect of time of heating, one gram samples of NH_4 saturated vermiculite, bentonite and illite were heated at a few specified temperatures for different periods of time. The NH_4 remaining on the clay mineral after the heating period was determined by distillation in 200 ml. of 1 *N* NaOH for 1 hour. In some cases, duplicate samples were distilled in 200 ml. of 1 *N* KOH for 1 hour.

Bentonite. The NH_4 saturated bentonite contained 74 m.e. NH_4 per 100 grams prior to heating. All of this NH_4 was displaced by distillation in either NaOH or KOH. That is, there was no fixed NH_4 in the initial NH_4 bentonite.

The heated bentonite was distilled only in NaOH. In each case the NaOH displaced all of the NH_4 on the bentonite. The results shown in Fig. 1 therefore indicate the total amount of NH_4 remaining on the bentonite after it was heated at different temperatures for different periods of time. It is apparent from these results that there was a rapid initial loss

of NH_3 at any one temperature followed by a slow but consistent loss as the heating period was extended.

Since NH_4 on the bentonite continues to be decomposed as the heating time is increased, it may be concluded that the fractions of NH_4 held on the different exchange sites cannot be sharply distinguished by this meth-

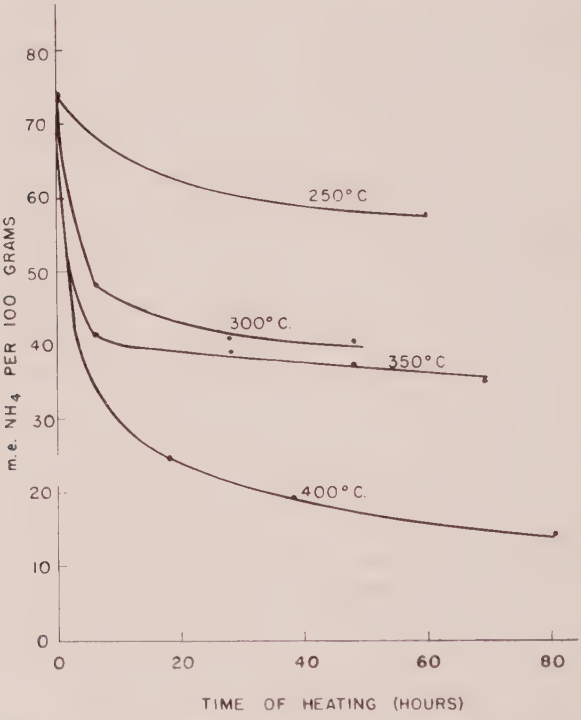


FIG. 1. NH_4 released from Wyoming bentonite by a one hour distillation in 200 ml. of 1 *N* NaOH after the NH_4 saturated bentonite has been heated at different temperatures for varying lengths of time.

od. This does not preclude the possibility that the decomposition temperature of the NH_4 ions varies with the exchange site occupied. In fact, the temperature dependence of the rapid initial loss of NH_3 would suggest that the NH_4 ions on the bentonite do vary in their decomposition temperature. The difficulty in distinguishing between the different NH_4 exchange sites is probably due to the H ions that remain on the exchange sites when the NH_3 is driven off. These H ions may interchange with exchangeable NH_4 ions on other sites. By this process, NH_4 ions that would normally not be decomposed at the temperature employed may be transferred to sites where they can be decomposed. Thus, the process involved

in these prolonged heating experiments is probably not merely a volatilization of NH_3 from the NH_4 ions on certain exchange sites at a specific temperature but one of H—NH_4 exchange as well.

Evidence that H ions are left on the bentonite when NH_4 bentonite is heated was obtained by Cook (8), who prepared a H saturated bentonite by heating NH_4 bentonite at 450° C. for 48 hours. In the present study, the pH of the NH_4 bentonite was determined before and after heating at 400° C. for 24 hours. The pH determinations were made with a glass electrode and a 1:5 bentonite to water ratio. The pH of the unheated sample was 7.3 and of the heated sample was 4.0.

Vermiculite. Unground Montana vermiculite which had been exfoliated with H_2O_2 prior to NH_4 saturation was used in this experiment. The NH_4 saturated vermiculite contained 83 m.e. of NH_4 per 100 grams. Distillation for 1 hour in 200 ml. of 1 *N* NaOH released 69 m.e. of NH_4 per 100 grams, whereas a similar distillation with KOH released only 3 m.e. of NH_4 per 100 grams. Data reported elsewhere[3] show that a longer distillation with NaOH would release all of the NH_4 but the KOH would release no more if the time of distillation were increased. Thus, according to the procedure of Barshad (4), the vermiculite contained 80 m.e. of fixed NH_4 per 100 grams.

When the NH_4 vermiculite was heated at temperatures up to 400° C. and for as long as 80 hours, there was little or no loss of NH_3 as shown in Fig. 2. Apparently, temperatures greater than 400° C. are needed to decompose the NH_4 on vermiculite. These results, therefore, cannot be used to evaluate the effect of time of heating. That is, it is not known if there would be a gradual loss of NH_3 with time once the decomposition temperature of at least part of the adsorbed NH_4 is exceeded.

The results of this study do, however, show that the relative ease of NH_4 displacement by Na is influenced by the temperature at which the samples were previously heated. With temperatures up to 250°C. a one hour NaOH distillation continued to replace about 69 out of the 83 m.e. of NH_4 on the vermiculite. When the samples were heated at 300° or 350° C., however, more of the NH_4 on the vermiculite was displaced by NaOH. Although the vermiculite used in this experiment was exfoliated with H_2O_2 before it was NH_4 saturated, it exfoliated even more when it was heated at 300° C. or higher. The increase of NH_4 displacement by NaOH is, apparently, the result of this exfoliation. Since NH_4 was not lost at these temperatures (see the constancy of the total NH_4 values in Fig. 6 also) the exfoliation observed must have been due to the volatilization

[3] Hanway, J. J., Scott, A. D., and Stanford, G., Replaceability of ammonium fixed in clay minerals as influenced by ammonium and potassium in the extracting solution. Submitted for publication.

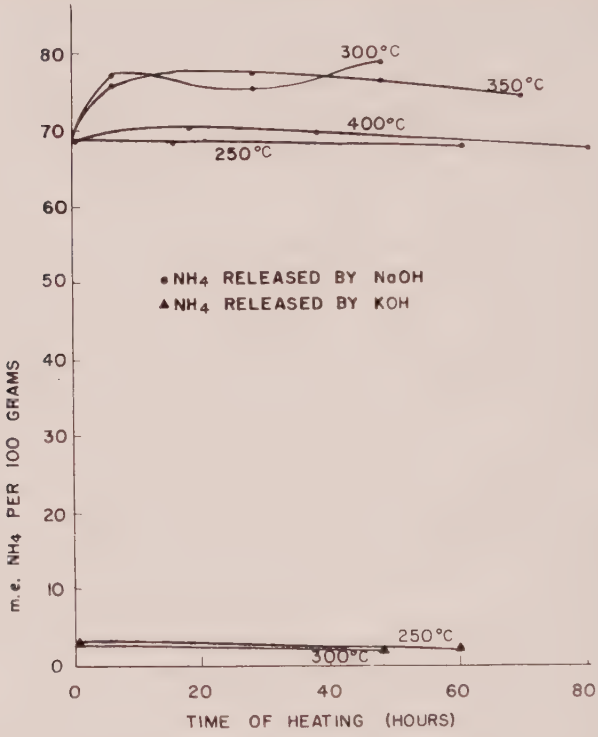


FIG. 2. NH_4 released from Montana vermiculite by a one hour distillation in 200 ml. of 1 *N* NaOH or KOH after the NH_4 saturated vermiculite has been heated at different temperatures for varying lengths of time.

and loss of water alone. It should be noted that the amount of NH_4 replaced by KOH distillation was not influenced by this exfoliation. That is, the NH_4 would still be considered as being fixed.

Samples heated at 400° C. did not release as much NH_4 to NaOH in one hour as those heated at 300° C. even though exfoliation occurred in both cases. As the heating temperature was increased from 350° C. to 400° C., it is possible that K was released from the biotite present in the sample. Kolterman and Truog (10) have shown that heating NH_4 biotite to 500° C. does release K. Such a release of K in the present study would account for the decrease in NH_4 displacement since Hanway, *et al.*[3] have shown that very small amounts of K interfere with the release of fixed NH_4 by NaOH. The fact that the samples heated at 400° C. released the same amount of NH_4 as those heated at 250° C. is probably coincidental.

Results from a similar experiment with unground South Carolina

vermiculite are given in Fig. 3. This vermiculite sample was not exfoliated with H_2O_2. The results are quite similar to these obtained with the Montana vermiculite. In this case there is a more pronounced decrease in the NH_4 displaced by Na as the time of heating at 400° C. was increased. This decrease is probably not due to a loss of NH_3 since the total NH_4 data given in Fig. 7 shows that there is no loss of NH_3 after heating for 24 hours at 400° C. The decrease is more likely due to a gradual release of

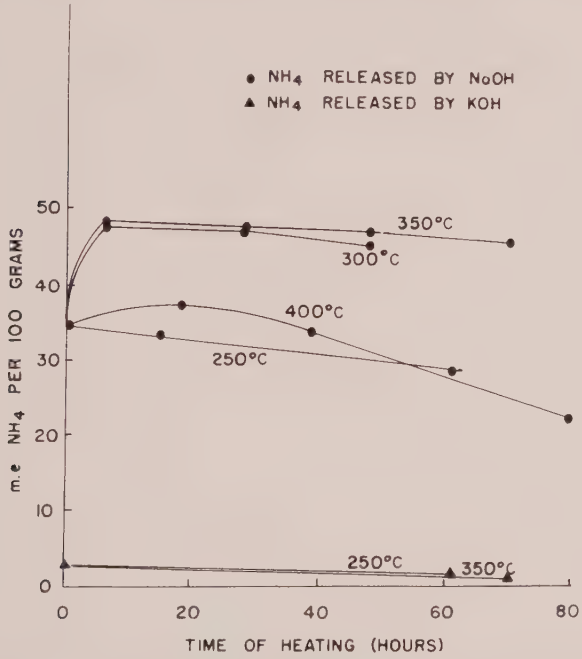


FIG. 3. NH_4 released from South Carolina vermiculite by a one hour distillation in 200 ml. of 1 *N* NaOH or KOH after the NH_4 saturated vermiculite has been heated at different temperatures for varying lengths of time.

K from the biotite which renders the fixed NH_4 less and less easily replaced by Na.

Illite. Prior to heating, the NH_4 saturated illite used in this study contained 26 m.e. of adsorbed NH_4 per 100 grams which could be displaced by distillation in NaOH. Distillation in KOH displaced all but 1 m.e. of this adsorbed NH_4. The heated illite was distilled only in NaOH.

The effect of heating the NH_4 illite at different temperatures for varying lenths of time is shown in Fig. 4. These results are similar to those obtained with bentonite in that NH_3 was lost rapidly at first and then grad-

ually as the heating time was extended. However, essentially all of the NH_4 on the illite was decomposed by heating at 300° C., while a considerable portion of the NH_4 remained on the bentonite even after prolonged heating at 400° C. This difference must be associated with the interlayer NH_4 ions that are present in the bentonite but not in the illite. It will be shown later that some of these interlayer NH_4 ions in bentonite are fixed when the clay mineral is heated to about 350° C. and that these fixed NH_4 ions in bentonite resist decomposition at temperatures below 400° C. There was little or no NH_4 fixation in the illite. It is,

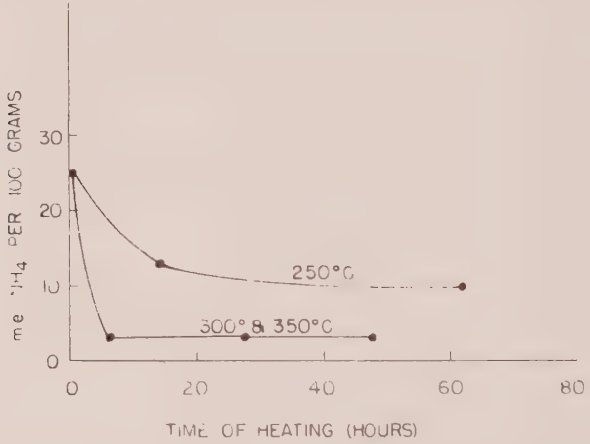


FIG. 4. NH_4 released from illite by a one hour distillation in 200 ml. of 1 *N* NaOH after the NH_4 saturated illite had been heated at different temperatures for varying lengths of time.

therefore, apparent from the illite results that prolonged heating at 300° C. will decompose most of the adsorbed NH_4 as long as it is exchangeable.

TEMPERATURE OF HEATING

To determine the relationship between the decomposition of NH_4 on various clay minerals and the temperature of heating, one or two gram samples of NH_4 saturated minerals were heated for 24 hours. This time of heating was selected because it was beyond the period in which the initial rapid loss of NH_3 occurred and should provide for reasonably reproducible results. The total NH_4 remaining on the clay minerals was determined by boiling a sample for 1 hour in concentrated H_2SO_4, making the digest alkaline with NaOH and distilling. NH_4 released by NaOH and KOH was determined by distilling a sample in 200 ml. of 1 *N* solutions of the hydroxides for one hour.

Bentonite. The amount of NH_4 released from the bentonite by NaOH

distillation was the same in all cases as that released by the H_2SO_4 digestion; therefore, in Fig. 5 a curve for the release to NaOH is not given. The curve showing the total NH_4 retained by the bentonite at various temperatures is similar to those obtained by other workers (5, 6, 7). Little NH_3 was lost at temperatures up to 200° C. The loss of NH_3 increased

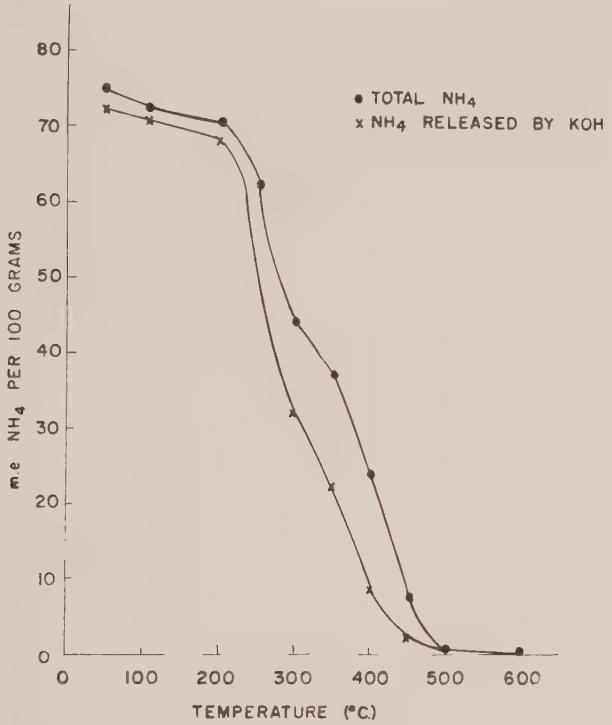


FIG. 5. Fixation and release of ammonium by Volclay bentonite as influenced by heating for 24 hours at different temperatures.

rapidly as the temperature increased from 200° to 300° C. and again from 350° to 450° C. with a decreased rate of NH_3 loss as the temperature increased from 300° to 350° C. Very little NH_4 remained on the bentonite after heating at 500° C. for 24 hours.

Barshad (3) has proposed that adsorbed NH_4 not replaced by distillation in KOH may be considered to be fixed. After heating at temperatures up to 200° C., KOH released all but 2 m.e. of the NH_4 on the bentonite. However, after heating at temperatures above this, and especially at temperatures from 300° to 400° C., a considerable portion of the NH_4 on the mineral was fixed; i.e., it was not replaced by KOH. As much as 15 m.e. of NH_4 per 100 grams was fixed at these higher temperatures.

Since the bentonite sample used in this study was not fractionated, the question arose as to whether the NH_4 fixation which occurred represented fixation by a normally expanding lattice mineral like montmorillonite or was due to the presence of a degraded micaceous mineral such as illite in the bentonite. In this case, since the essentially non-expanding micaceous materials would tend to exist in larger particle sizes, the <.2 micron fraction of the bentonite should be relatively free of these materials. A suspension of the Volclay bentonite, which is normally Na saturated, was therefore run through a Sharples super centrifuge to separate out some of the <.2 micron fraction. This fraction was NH_4 saturated by passing the suspension through an NH_4 saturated Amberlite IR-100 resin exchange column.

The NH_4 released by NaOH and KOH distillation from this NH_4 saturated <.2 micron fraction following different heating treatments is shown in Table 1. There was no fixed NH_4 in the unheated samples or in the sample dried at 110° C. However, just as in the original unfractionated bentonite sample, there was 15 m.e. of NH_4 per 100 grams fixed in the <.2 micron clay material after it was heated at 350° C. for 24 hours.

TABLE 1. EFFECT OF HEATING NH_4 SATURATED <.2 MICRON VOLCLAY BENTONITE ON NH_4 RELEASED BY DISTILLATION IN NaOH AND KOH SOLUTIONS

Heating temperature	Time of heating, hrs.	m.e. NH_4 released per 100 grams of bentonite by:		m.e. NH_4 fixed per 100 grams of bentonite (NaOH—KOH)
		NaOH	KOH	
Unheated	0	126	126	0
110° C.	24	118	118	0
350° C.	24	38.8	23.6	15.2

The distillation was continued for 4 hours to assure complete release of all the NH_4 that would be released, but very little was released after the first hour. It was observed that the NH_4 clay, after drying and heating at 350° C. consisted of large flakes. These flakes broke up and the clay was completely dispersed in the NaOH solution whereas the large flakes persisted in the KOH solution. These results suggest that NH_4 is fixed in montmorillonite at this higher temperature because the contracted lattice resists re-expansion by KOH.

Vermiculite. The vermiculites lost no NH_3 at temperatures up to 400° C. as shown in Figs. 6 and 7. At temperatures above 500° C. the Montana vermiculite lost large amounts of NH_3 but still retained 9 m.e. of NH_4 per 100 grams after heating at 600° C. for 24 hours. The South Carolina vermiculite started to lose NH_3 at a slightly lower temperature, and after heating at 550° C. it contained essentially no NH_4.

After heating at temperatures up to 250° C., NaOH distillation failed to replace 2 to 3 m.e. of the total NH_4 per 100 grams during a one-hour distillation. However, heating at 300° C. resulted in essentially complete release of the NH_4 by NaOH. As discussed earlier, the exfoliation of vermiculite at 300° C. definitely resulted in the NH_4 being more easily

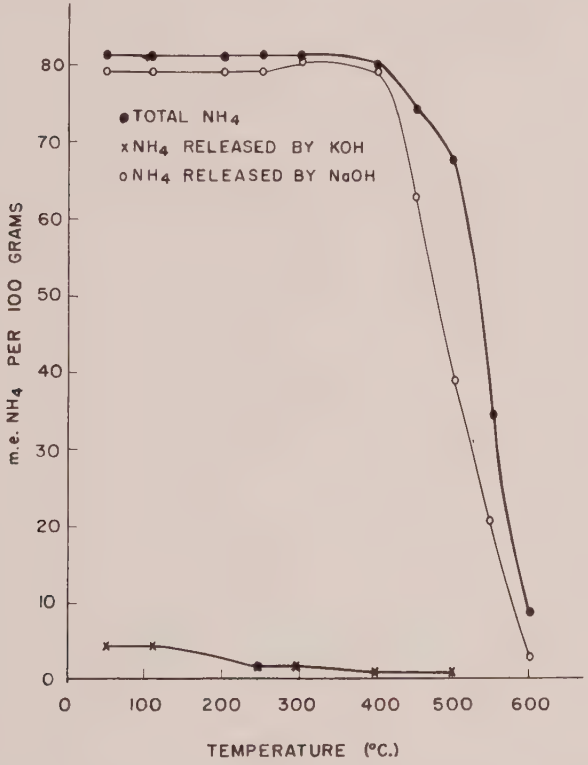


FIG. 6. Fixation and release of ammonium by Montana vermiculite as influenced by heating for 24 hours at different temperatures.

replaced by NaOH. After heating at temperatures greater than 400° C., a one hour distillation in NaOH failed to release considerable quantities of the NH_4 present. This reduction in the amount released by Na was probably due to a release of K at these high temperatures from the biotite present in the sample. This conclusion was substantiated by the observation that prolonged distillation, which has been shown to be effective when small amounts of K were present (10), resulted in complete release of the NH_4. Furthermore, removal of the potassium by precipitation resulted in a complete replacement of the NH_4 by Na in one hour.

The KOH distillation removed very little NH_4 from the vermiculite,

but it continued to release some NH_4 even when the samples were heated at 500° C. There was no increase in the release of NH_4 by KOH even though on heating at temperatures of 300° or above the vermiculite exfoliated, with an expansion of two to three times its orginal volume This expansion of the lattice obviously did not make the NH_4 ions more easily replaced by K.

Illite. The NH_4 saturated illite used in this study released 20 m.e. of

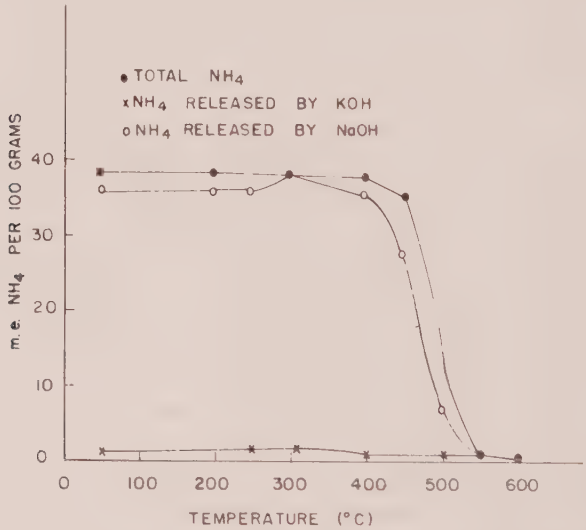


FIG. 7. Fixation and release of ammonium by South Carolina vermiculite as influenced by heating for 24 hours at different temperatures.

NH_4 when it was distilled in NaOH. When it was digested in concentrated H_2SO_4 for 1 hour and then distilled in NaOH it released a total of 24 m.e. of NH_4. The difference in NH_4 released is probably due to the presence of organic matter since the original untreated illite contained nitrogen equivalent to 4.7 m.e. of NH_4 per 100 grams as determined by Kjeldahl analysis. The NH_4 displaced by distillation in NaOH alone is probably a good measure of the NH_4 adsorbed on the illite. In any case, both the total NH_4 and NaOH released NH_4 values given in Fig. 8 show the same general change in the NH_4 retained at different temperatures. Up to 200° C., there was a slow but gradual loss of NH_3, a more rapid loss between 200° and 350° C., and by 400° C. essentially all of the NH_4 was decomposed.

The amount of NH_4 released by KOH was consistently 1 to 2 m.e. per 100 grams less than that released by NaOH. Thus, there was little NH_4

fixed in this illite, and the amount fixed was not influenced by heating at higher temperatures. The relative absence of NH_4 fixation is probably due to the fact that the illite received no pretreatment, such as electrodialysis, that would remove fixed K. Thus, all positions capable of fixation were already occupied by K ions.

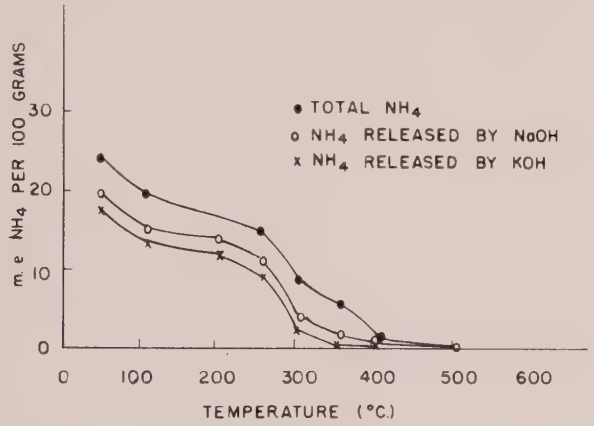


FIG. 8. Fixation and release of ammonium by illite as influenced by heating for 24 hours at different temperatures.

Kaolinite. The NH_4 saturated kaolinite contained 7.5 m.e. of NH_4 per 100 grams. NaOH distillation, KOH distillation and H_2SO_4 digestion prior to alkaline distillation all released the same amount of NH_4 from kaolinite. Therefore, only the total NH_4 values have been used in Fig. 9 to show the effect of heating NH_4 kaolinite. From these results, it appears that the NH_4 on kaolinite is gradually decomposed as the temperature is increased from 50° to 400° C.

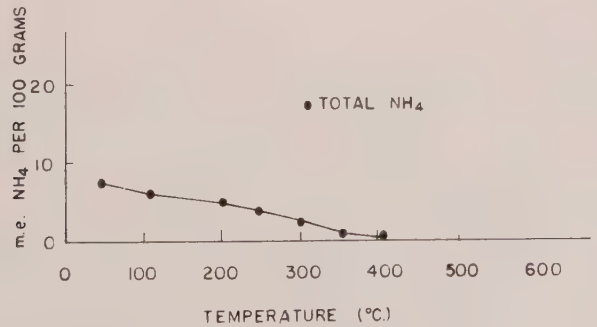


FIG. 9. Release of ammonium by kaolinite as influenced by heating for 24 hours at different temperatures.

Comparison of different minerals. The percentage of the total NH_4 lost by each of the minerals at different temperatures is given in Fig. 10. In general each of the minerals loses NH_3 over a wide range of temperatures. One of the biggest differences between minerals is that illite, kaolinite and bentonite begin to lose NH_3 at 100° C., while vermiculite loses

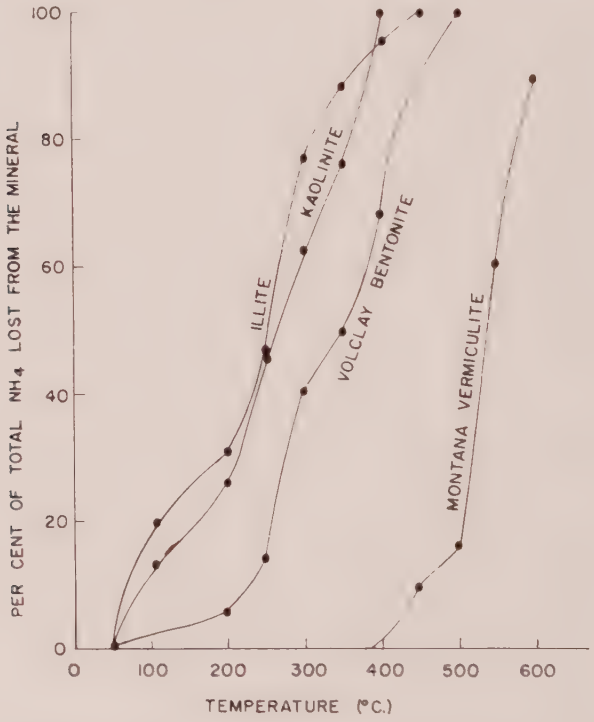


FIG. 10. Percentage of the total NH_4 lost from different minerals on heating for 24 hours at different temperatures.

little or no NH_3 until 400° C. Illite and kaolinite lose all of their NH_3 by 400° C.; thus their curves do not overlap the vermiculite curve. The NH_4 bentonite thermal decomposition curve, however, overlaps both the illite and vermiculite curves. These differences appear to be primarily determined by the presence of fixed NH_4.

Illite and kaolinite with NH_4 primarily on external surfaces and in an exchangeable location readily lose NH_3 by thermal decomposition. The illite curve conforms with the suggestion of Cornet (9) that NH_4 on broken bond surfaces is decomposed by 125° C., while the maximum evolution of NH_3 from exterior planar surfaces occurs at 275° C. The NH_4 on kaolinite, which is presumably all on broken bond surfaces, however, was not entirely decomposed by 125° C. Instead, there was a gradual loss

of NH_3 up to 400° C. with only a slight indication of a decrease in slope of the curve between 100° and 200° C. It should also be noted that this kaolinite curve is very different from the curve Bottini (7) obtained with a kaolinite clay.

The inflections in the bentonite curve showing a more rapid loss of NH_3 at temperatures of about 275° C. and 400° C. are similar to those observed by Cornet (9). The inflection at 275° C. is probably associated with the loss of NH_3 from planar surfaces as Cornet has suggested, since illite also shows an inflection at this temperature. The results of this investigation, however, indicate that the fixation of NH_4 on bentonite caused the decrease in the slope of the total NH_4 curve between 300° and 350° C., which gave rise to another distinct inflection at 400° C. The exchangeable NH_4 ions, on the other hand, continued to decrease at a fairly constant rate over the temperature range of 300° to 400° C. It may be concluded that the interplanar exchangeable NH_4 ions on bentonite are not more resistant to thermal decomposition than the exterior planar ions. It is expected that in the absence of NH_4 fixation the curve for the decrease in total NH_4 on bentonite would be similar to that of illite. In fact, a plot of the decrease in exchangeable NH_4 only does show very little indication of separate inflections at 275° and 400° C.

It is apparent from Fig. 5 that the fixed NH_4 ions resisted thermal decomposition until the temperature exceeded 400° C. The NH_3 loss at higher temperatures was, however, partly due to exchangeable NH_4 ions. Since the exchangeable NH_4 ions were not entirely decomposed before the fixed NH_4 ions started to decompose, the fixed and exchangeable NH_4 on bentonite cannot be distinguished by this method. It is entirely possible that the observed exchangeable NH_4 at these higher temperatures become exchangeable because of a H displacement of the fixed NH_4 during the cooling period. This point is being investigated at the present time.

The NH_4 in vermiculite resists decomposition until 400° C. The high temperature of decomposition is probably due to the fact that essentially all of the NH_4 on vermiculite is fixed. A comparison of the vermiculite and bentonite curves shows that most of the fixed NH_4 in vermiculite required a higher temperature for decomposition than fixed NH_4 in bentonite. This observation is in line with the ease with which NH_4 is fixed in the two minerals. While vermiculite will fix NH_4 under moist conditions, NH_4 bentonite must be dehydrated at 300° to 350° C. before the lattice is sufficiently contracted to fix the NH_4.

In general it may be concluded from these results that NH_4 held on sites where it is fixed required a higher decomposition temperature than NH_4 ions on sites where they were not fixed. There was, however, no case where heating at one temperature resulted in the loss of NH_3 from

the exchangeable NH_4 leaving just the fixed NH_4 on the clay. The temperature of decomposition, therefore, cannot be used to distinguish sharply between fixed and exchangeable NH_4.

Differential Thermal Analysis

The differential thermal curves obtained for the various clay minerals are given in Figs. 11, 12, 13 and 14. The curves obtained with the natural

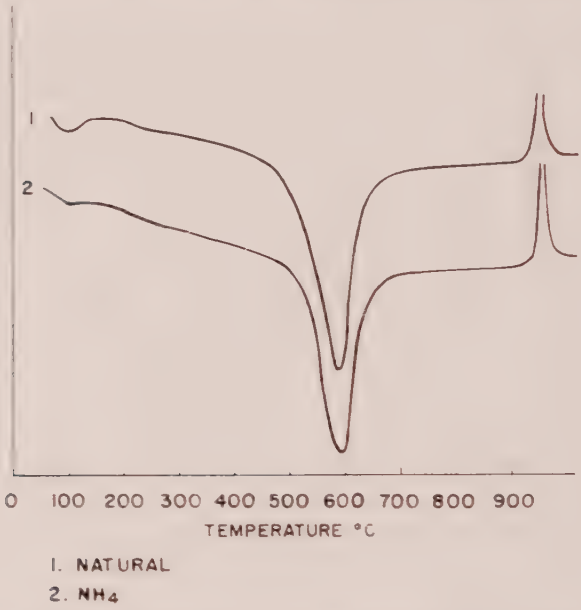


Fig. 11. Influence of adsorbed cation on the differential thermal curve for kaolinite.

material; that is, the first curve in each figure, are quite typical for the mineral concerned. It is apparent from Fig. 11 that adsorbed NH_4 had no effect on the kaolinite curve.

The large ill-defined exothermic peak with a maximum at 400° C. in the illite curve, Fig. 12, is not usually observed. This peak is probably due to the presence of organic matter as indicated by the nitrogen content of the untreated illite. This exothermic peak detracts from the usefulness of the differential thermal curve in the thermal study of NH_4 on the clay. Curve 3 in Fig. 11 indicates that the NH_4 does influence the curve, either by its own decomposition, or by its effect on the impurity giving rise to the peak.

The curves for the natural (Na saturated) and K saturated bentonite in Fig. 13 are characteristic of those generally obtained for montmorillonite clay. The two endothermic troughs were not affected by any of the

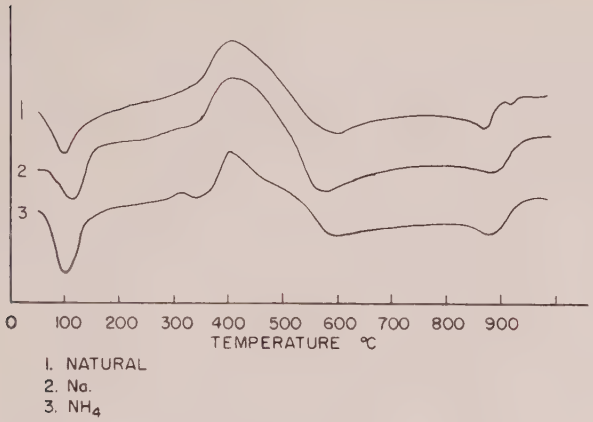


FIG. 12. Influence of adsorbed cation on the differential thermal curve for illite.

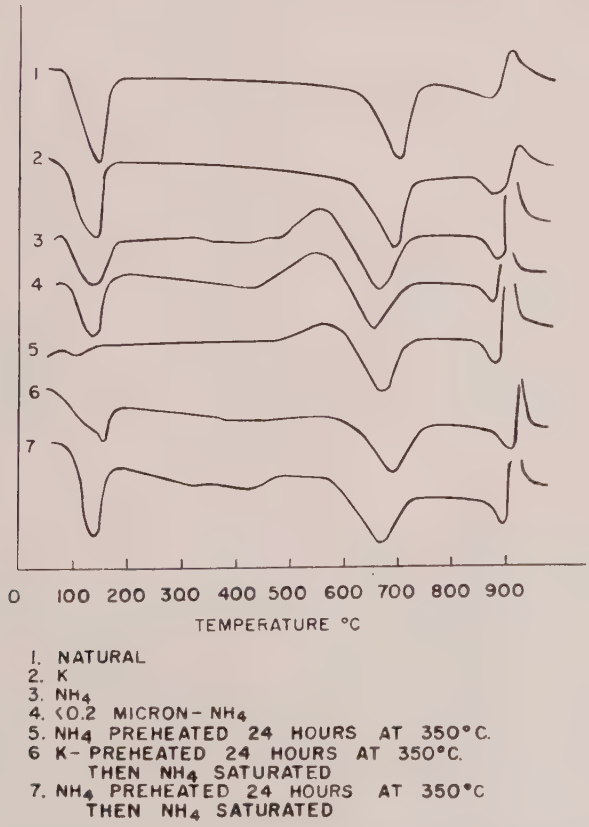


FIG. 13. Influence of adsorbed cation on the differential thermal curve for Wyoming (Volclay) bentonite.

other treatments except that shown by curve 5. In this case, the differential thermal analysis was made soon after the bentonite had been heated at 350° C. and the clay mineral apparently had not had time to become rehydrated. Since the bentonite was not protected from the atmosphere during the intervening period, it apparently does not exhibit the rapid rehydration Barshad (2) observed with vermiculite.

Saturating the bentonite with NH_4 resulted in the production of an exothermic peak at about 550° C. This was observed with both the unfractioned and the <.2 micron material. Curves obtained for an NH_4 saturated Mississippi bentonite were similar except that the exothermic peak occurred at 425° C. These results differ from those of Barshad (3) in that only one exothermic peak was found, whereas the NH_4 bentonites he studied showed two peaks, one at 360° C. and another at 470° C.

It is evident from curves 5, 6 and 7 that the NH_4 fixed in bentonite at 300° to 350° C. is responsible for the 550° C. exothermic peak in the differential thermal curve. The peak was still evident in curve 5 for NH_4 bentonite that had been previously heated at 350° C. for 24 hours even though the sample retained only 31 of the original 80 m.e. of NH_4 per 100 grams after the preheating. On the other hand, when a K saturated bentonite was heated at 350° C. for 24 hours and then leached with NH_4Cl to saturate the clay with NH_4, the differential thermal curve exhibited no exothermic peak. Preheating the K bentonite at 350° C. apparently fixed K ions in those sites capable of fixing NH_4 ions. As a result the 66 m.e. of NH_4 per 100 grams adsorbed by this sample of clay prior to the differential thermal analysis were exchangeable ions that were decomposed without influencing the differential thermal curve. Curve 7 was obtained with bentonite that had been previously heated at 350° C. for 24 hours to fix NH_4 ions and then saturated with NH_4. In this case the sample was found to contain 66 m.e. of exchangeable NH_4 per 100 grams.

The exothermic peak in the bentonite differential thermal curves occurred in all cases where fixed NH_4 was present. If the NH_4 ions were blocked from the fixing sites by prior fixation of K, the curve exhibited no exothermic effects from NH_4 ions on the bentonite. Apparently any exothermic effect due to the loss of NH_3 from the exchangeable NH_4 ions is counteracted by a concurrent loss of water. On the other hand, the fixed NH_4 ions are decomposed and NH_3 lost without a concurrent loss of water, since an exothermic peak occurs. This indicates that the exchangeable NH_4 ions in bentonite are closely associated with water molecules while the fixed NH_4 ions are not.

The differential thermal curves obtained for Montana vermiculite, Fig. 14, correspond with those obtained by Barshad (2). In the curve for

the natural vermiculite there are low temperature endothermic troughs characteristic of Ca or Mg on the exchange complex. When the Ca and Mg were replaced by NH_4 ions, these low temperature troughs were eliminated. In this regard, vermiculite is different from bentonite which exhibits a low temperature endothermic trough even with NH_4 on the exchange complex. Apparently there is much more water associated with the exchangeable NH_4 ions in bentonite which gives rise to this endothermic effect as it is lost.

According to Barshad (2), each NH_4 ion in vermiculite is associated with

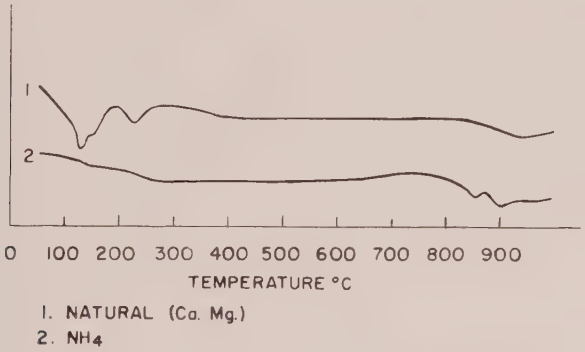


FIG. 14. Influence of adsorbed cation on the differential thermal curve for Montana vermiculite.

one molecule of water. Furthermore, he has shown that the NH_3 lost from vermiculite by heating is accompanied by an equivalent loss of water. Any exothermic effects from the loss of NH_3 are apparently counteracted by the endothermic effect of the concurrent water loss since the NH_4 vermiculite differential thermal curve has the appearance of an anhydrous material.

CONCLUSIONS

The NH_4 ions on the kaolinite and illite used in this study were largely exchangeable. These exchangeable NH_4 ions started to decompose at temperatures below 100° C. and were completely decomposed by heating for 24 hours at 400° C. On the other hand, fixed NH_4 ions on vermiculite were stable until nearly 400° C. and required 24 hours of heating at 600° C. to decompose them entirely. The thermal decomposition curve for the NH_4 ions on bentonite was unique because some of the NH_4 ions which were initially exchangeable were fixed when the clay was heated at 300° to 350° C. Like kaolinite and illite the exchangeable NH_4 ions on bentonite started to decompose below 100° C., and like vermiculite the fixed NH_4 did not decompose until the temperature exceeded 400° C.

From these results it may be concluded that fixed NH_4 ions are not as readily decomposed as the exchangeable ions.

The thermal decomposition curve for the NH_4 adsorbed on illite supports Cornet's (9) suggestion that the exchange site of the NH_4 ions influences the temperature at which they are decomposed. In the case of NH_4 bentonite, however, the two distinct inflections in the curve between 200° and 500° C. does not occur because of the decomposition of NH_4 ions on different exchange sites. Instead, the two inflections occur because there is a decrease in the amount of NH_3 lost as NH_4 ions are fixed in the bentonite when this clay material is heated at 300° to 350° C.

While the fixed NH_4 ions appears to resist thermal decomposition more than the exchangeable NH_4 ions, no sharp distinction could be made between the two forms by the method used. In bentonite, some exchangeable NH_4 remained on the clay up to 500° C. where the fixed NH_4 was also decomposed. Likewise, a sharp distinction between the fractions of exchangeable NH_4 ions held on different sites could not be made because there was a slow but consistent loss of NH_3 when NH_4 saturated illite or bentonite was heated at one temperature for an extended period of time. The difficulty in both cases was that H ions remained when the NH_4 ions were decomposed. By exchange these H ions caused NH_4 ions that were normally not decomposed at the temperature employed to be transferred to sites where they were decomposed.

An exothermic peak occurred at 550° C. in the differential thermal analysis curve for NH_4 bentonite. This peak was due to the loss of NH_3 from the NH_4 ions fixed in bentonite at 300° to 350° C. The fixed NH_4 ions in vermiculite on the other hand produced no exothermic effects. It is apparent that the fixed NH_4 ions in bentonite do not have water associated with them like they do in vermiculite.

References

1. Allison, F. E., Roller, E. M., and Doetsch, J. H. (1953), Ammonium fixation and availability in vermiculite: *Soil Sci.*, **75,** 173–180.
2. Barshad, I. (1948), Vermiculite and its relation to biotite as revealed by base exchange reactions, *x*-ray analyses, differential thermal curves and water content: *Am. Mineral.*, **35,** 655–678.
3. ——— (1950), The effect of the interlayer cations on the expansion of the mica type of crystal lattice: *Am. Mineral.*, **35,** 225–338.
4. ——— (1951), Cation exchange in soils. I. Ammonium fixation and its relation to potassium fixation and to determination of ammonium exchange capacity: *Soil Sci.*, **72,** 361–371.
5. ——— (1954), Cation exchange in micaceous minerals. II. Replaceability of ammonium and potassium from vermiculite, biotite and montmorillonite: *Soil Sci.*, **78,** 57–76.
6. Bottini, Von O. (1937), Über die Thermische Zersetzung von Ammoniumpermutit, Ammoniumbentonite und Ammoniumton: *Kolloid Zeits.*, **78,** 68–71.

7. ——— (1937), Über die Thermische Zersetzung Gemischter "Ammonium-Kalzium"-Permutite, -Bentonite und -Tone: *Kolloid Zeits.*, **80**, 56–59.
8. Cook, R. L. (1935), Divergent influence of degree of base saturation of soils on the availability of native soluble and rock phosphates: *Jour. Am. Soc. of Agron.*, **27**, 297–311.
9. Cornet, I. (1943), Sorption of NH_3 on montmorillonitic clay: *J. Chem. Phys.*, **11**, 217–226.
10. Kolterman, D. W., and Truog, E. (1953), Determination of fixed soil potassium: *Soil Sci. Soc. Am. Proc.*, **17**, 347–351.

Manuscript received Dec. 23, 1955.

THE CHEMICAL FORMULA OF EMPRESSITE

GABRIELLE DONNAY, F. C. KRACEK, AND W. R. ROWLAND, JR.,
Geophysical Laboratory, Carnegie Institution of Washington, Washington, D. C.

ABSTRACT

Ag_5Te_3 is synthetic empressite. $Ag_{5-x}Te_3$ is the formula deduced, for the mineral, from cell dimensions and density of analyzed crystals.

Empressite was described by Bradley (1914, 1915) as a silver telluride AgTe and by Schaller (1914) as the silver end-member of the phase (Ag,Au)Te, which occurs as the mineral muthmannite. The formula rested on three determinations of type-locality material, two by Bradley (1914) and one by E. J. Dittus (*in* Bradley, 1915), which gave values $Ag_{0.97\pm0.01}Te_{1.00}$ in excellent agreement with one another. Nevertheless, in the light of later analyses and syntheses, it appears likely that native tellurium was admixed in the analyzed samples in such finely divided form that it was not recognized under the microscope. More recently a careful analysis by R. N. Williams, also on material from the type locality, gave the composition $Ag_{1.18}Te_{1.00}$ as reported by Thompson *et al.* (1951). These authors found the specific gravity to be 7.61 ±0.01. They took *x*-ray patterns of powders as well as synthetic single crystals and showed that the empressite powder pattern is identical with that of a homogeneous fusion product of composition Ag_5Te_3. They concluded, however, that the general formula should be written $Ag_{2-x}Te_{1-x}$ with $0.1 \leqq x \leqq 0.5$, thus implying that silver and tellurium substitute for each other over an appreciable range of solid solution. Because of the difference in electronegativity of silver and tellurium and because these two elements are known to play very different roles in related compounds, this formula is unsatisfactory.

A recent study of the silver-tellurium phase diagram by Kracek and Ksanda (1955) establishes the existence of two and only two compounds in the Ag-Te system, namely: Ag_2Te, identical with hessite, and Ag_5Te_3, to which the compositions AgTe, Ag_7Te_5, Ag_3Te_2, $Ag_{12}Te_7$ and Ag_7Te_4 had previously been ascribed.

Professor Berry kindly sent us the single crystals of empressite which Thompson *et al.* (1951) had obtained by hydrosynthesis. We confirmed their cell dimensions on the precession camera, using CuKα radiation ($\lambda = 1.5418$ Å); $a = 13.49$ Å, $c = 8.47_4$ Å, all ±0.3 per cent. The diffraction aspect is P^{***}, with a pronounced pseudo-aspect $P6_3^{**}$ (all reflections $000l$ are missing when l is odd, except 0003). Unfortunately, because of scarcity of material, it was not possible to determine the specific gravity of these single crystals, and since their exact composition was not certain either, we proceeded with the *x*-ray and density studies of synthetic samples prepared by Kracek and Ksanda. A least-square analysis of the powder pattern of Ag_5Te_3 (62.50 at. per cent Ag) gives cell dimensions

$a=13.46$ Å, $c=8.47$ Å, all ± 0.3 per cent, V = 1328 Å^3. The observed specific gravity is 7.96 ± 1 per cent. Assuming 7 Ag_5Te_3 per cell the calculated specific gravity is 8.07. The intensities and cell dimensions of Ag_5Te_3 check those of the powder pattern of type-locality material given by Thompson *et al.* (1951, p. 468), namely: $a=13.49$ Å (13.46 kX), $c=8.48$ Å (8.46 kX), V = 1336 Å^3. Although the silver/tellurium ratio in this material, as noted above, is 1.43, not 1.67, and the specific gravity is 7.61 instead of 7.96, there is no doubt that the two patterns come from isostructural compounds, so that the ideal formula for empressite can only be Ag_5Te_3.

Because both composition and specific gravity are known for the sample from the Empress Mine, it is straightforward, once the ideal formula is established, to decide between the three possible types of solid solution.

1. Substitution solid solution. The formula is to be written $Ag_{5-x}Te_{3+x}$; $x=0.29$. With seven formula units of $Ag_{4.71}Te_{3.29}$ per cell and a measured cell volume of 1336 Å^3, the calculated specific gravity is 8.1.

2. Addition solid solution. The formula is to be written Ag_5Te_{3+x}; $x=0.50$. With seven formula units of $Ag_5Te_{3.50}$ and a measured cell volume of 1336 Å^3, the calculated specific gravity is 8.6.

3. Omission solid solution. The formula is to be written $Ag_{5-x}Te_3$; $x=0.71$. With seven formula units of $Ag_{4.29}Te_{3.00}$ and a measured cell volume of 1336 Å^3, the calculated specific gravity is 7.4. Reasonable agreement between this value and the observed one (7.61) establishes the formula of empressite as $Ag_{5-x}Te_3$. Powder patterns of synthetic samples whose composition ranges from Ag_5Te_3 to $Ag_{4.50}Te_3$ show only the $Ag_{5-x}Te_3$ phase. Hessite lines are observed when as little as 0.66 at. per cent excess silver is present.

Cell dimensions calculated for $Ag_{4.74}Te_3$ and $Ag_{4.50}Te_3$ show no significant changes. The cell volume remains constant within experimental limits of error. If tellurium forms a hexagonal close-packed framework, random vacancies in the silver positions would not be expected to lead to measurable changes in cell dimensions.

References

Bradley, W. M. (1914), Empressite, a new silver-tellurium mineral from Colorado: *Am. Jour. Sci.*, **38**, 163–165.

——— (1915), On the mineral empressite: *Am. Jour. Sci.*, **39**, 223.

Kracek, F. C., and Ksanda, C. J. (1955), Phase relations in the system silver-tellurium, in manuscript.

Schaller, W. T. (1914), The identity of empressite with muthmannite: *J. Wash. Acad. Sci.*, **4**, 497–499.

Thompson, R. M., Peacock, M. A., Rowland, J. F., and Berry, L. G. (1951), Empressite and "stuetzite:" *Am. Mineral.*, **36**, 458–470.

Manuscript received Dec. 24, 1955.

CLINOPYROXENES OF ALKALI OLIVINE-BASALT MAGMA

J. F. G. Wilkinson, *The University of New England, Armidale, N.S.W., Australia.*

Abstract

In representatives of alkali olivine-basalt magma, as contrasted to tholeiitic rocks, only one common pyroxene, a clinopyroxene close to diopside or salite, appears. The clinopyroxene crystallization trend is parallel to the Di-He join, principally in the fields of diopside or salite. Analytical data indicates that alkali olivine-basalt clinopyroxenes having compositions more iron-rich than $Ca_{45}Mg_{25}Fe_{30}$ must be comparatively rare.

The contrasting behavior of the pyroxene assemblage of alkali olivine-basalt and tholeiitic magma depends principally on the undersaturated or saturated nature of the respective residual magmatic solutions, which determine whether or not orthopyroxene as a product of magmatic reaction with early-formed olivine will appear. The higher modal pyroxene content of tholeiites, their more varied pyroxene assemblage, and the greater variation in clinopyroxene composition with differentiation compared with alkali olivine-basalt clinopyroxenes, are important consequences of this reaction.

Introduction

While much has been written on the crystallization trends and mutual relationships of clinopyroxenes from tholeiitic rocks, clinopyroxenes of under-saturated basic alkaline rocks have been comparatively neglected. Except for Murray's (1954) investigation of the Garbh Eilean clinopyroxenes, little attention has been directed to crystallization trends of clinopyroxenes from a single intrusion of alkali olivine-basalt type.

Several of the concepts in the present paper result from the investigation of the Black Jack teschenite sill, near Gunnedah, New South Wales. This differentiated five hundred foot thick intrusion of Tertiary age is a typical representative of alkali olivine-basalt magma. The principal mineralogical (modal) variations in the sill are expressed in a progressive decrease in olivine with increasing height above the lower contacts, while clinopyroxene and iron ore are slightly more abundant in the upper levels of the intrusion. During differentiation, the olivine becomes more fayalitic (Fa_{21} to Fa_{60}) while the plagioclase feldspar is enriched in albite (An_{72} to An_{13}) (Table 1). The homogeneous iron-titanium ores also reveal considerable compositional changes. In strong contrast, the associated bulk clinopyroxene (usually strongly zoned) undergoes little change in composition during differentiation ($Ca_{48}Mg_{37}Fe_{15}$ to $Ca_{47}Mg_{34}Fe_{19}$). The limits of clinopyroxene composition are close to the range, $Ca_{49}Mg_{37}Fe_{14}$ to $Ca_{47}Mg_{33}Fe_{20}$ (Table 2), based on analyses of the Mg- and Fe-rich fractions of the analyzed bulk clinopyroxene.

The writer follows Poldervaart and Hess (1951, Fig. 1*B*) on clinopyroxene nomenclature. The clinopyroxene compositions, except in certain instances where they have been derived from a previous source, are

expressed in atomic percentages of Ca, Mg and Fe (following Hess, 1949).

The following concepts are fundamental to any discussion dealing with the nature and crystallization histories of the pyroxenes:

(i) The recognition of certain magma types.

(ii) Clinopyroxene nomenclature based on optical properties, allied with the use of optics for compositional purposes.

(i) The concept of magma types, proposed by the authors of the Mull memoir (Bailey *et al.*, 1924) is now well known. It is "a permanent contribution to petrologic thought" (Tilley, 1950, p. 38). In their definition of the Plateau and Non-Porphyritic Central magma types, the Mull authors (1924, p. 14) state that "a purple colour is characteristic of the augite" in the Plateau rocks. The highly calcic diopsidic nature of the clinopyroxene in the Mull Plateau (=olivine-basalt) magma, compared with the enstatite-augite varieties in the the Non-Porphyritic (=tholeiitic) magma type, was pointed out by Kennedy (1931, p. 63; 1933, pp. 240–241). Similar mineralogical differences had been recognized earlier by Washington (1922, p. 800) in the "cone-" and "plateau-basalts" respectively. The ambiguity arising from usage of the terms "olivine-basalt" and "tholeiite" as applied to magma types, has been discussed by Tilley (1950, pp. 40–41), who uses as an alternative for the former, the term "alkali olivine-basalt."

(ii) There is no analytical evidence indicating that the lime content (usually greater than 20 weight per cent) of clinopyroxenes from alkali olivine-basalt magma ever approaches that of pigeonite, as defined by Poldervaart and Hess (1951, p. 473), despite the fact that such pyroxenes may have low 2V's in the range 30–38 degrees (cf. Yagi, 1953, p. 780). Yet many writers, following Kuno (1936*a*, p. 141) have referred to these clinopyroxenes as "pigeonites" or "pigeonitic," with a consequent erroneous composition. The clinopyroxenes under discussion are usually richer in TiO_2 (Table 2), Al_2O_3, Fe_2O_3 and CaO than common tholeiitic clinopyroxenes (see Hess, 1949, p. 633). There appears to be little agreement in the literature as to the exact variation in $\gamma \wedge c$, 2V, refractive indices, etc. to be ascribed to a particular constituent, whose presence in many cases cannot be diagnosed optically. The effects of TiO_2 on the optics are most uncertain (Dittler, 1929; Kuno, 1936; Segnit, 1953). The variable optics of the clinopyroxenes listed in Table 2 should be noted. Optical properties of titania-rich clinopyroxenes indicate a higher Fe and lower Ca content than revealed by analysis. Until other methods e.g. the correlation of cell dimensions with variation in Al^{3+}, Fe^{3+}, Ti^{4+} and Na^{+} (Kuno and Hess, 1953) become available, chemical analyses provide the safest means of deriving accurate compositions of titaniferous clinopyroxenes.

Clinopyroxene Crystallization Trends in Alkali Olivine-Basalt Magma

Hess (1941, pp. 574–578) summarized the work of Barth (1931; 1936), Tsuboi (1932) and Wager and Deer (1939) and drew up a course of crystallization for tholeiitic clinopyroxenes, a trend substantiated later by Edwards (1942) and Walker and Poldervaart (1949). The varying crystallization trends suggested by these workers are shown in Fig. 1. In certain cases it is clear that the suggested trends applied to clinopyroxenes from both tholeiitic and alkali olivine-basalt magmas.

Basic data on the crystallization trends of the clinopyroxenes from a

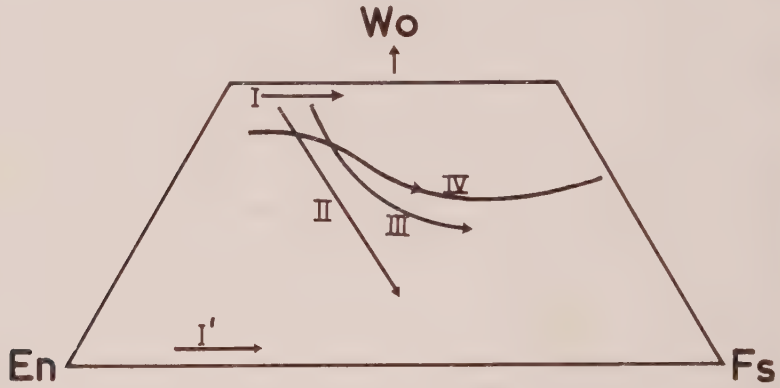


Fig. 1. Schematic representation of pyroxene crystallization trends in basic rocks. I Tsuboi (1932), followed by Kuno (1936*a*); II Barth (1936); III Wager and Deer (1939), integrating data from Kennedy (1933) and Kuno (1936*a*); IV Hess (1941, 1951).

single differentiated intrusion of alkali olivine-basalt type is now supplied by the Garbh Eilean and Black Jack pyroxenes. The principal compositional relationships of the main mineral series in the latter intrusion have already been summarized. In the former sill, the range in clinopyroxene composition is from $Ca_{47}Mg_{42}Fe_{11}$, the pyroxene in the picrite, to $Ca_{44}Mg_{30\cdot5}Fe_{25\cdot5}$, the iron-rich fraction of the clinopyroxene in the crinanite 325 feet above sea level (Murray, 1954, Table 1). In both intrusions, the modal olivine decreases with progressive magmatic evolution, a feature shown by other differentiated intrusions of this magma (Table 4). The olivines in the Garbh Eilean (Murray, 1954, Fig. 2) and Black Jack rocks are richer in ferrous iron and undergo considerably greater iron enrichment than the associated clinopyroxene. The crystallization trend of the latter minerals in both instances is parallel to the diopside-hedenbergite join (Fig. 2), principally in the fields of diopside and salite.

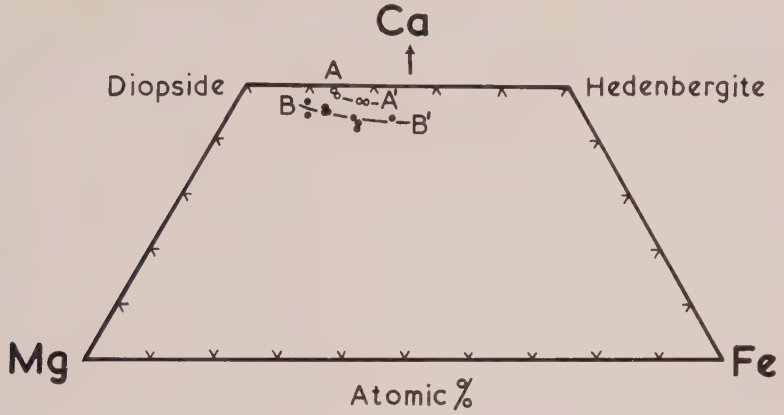


FIG. 2. Clinopyroxene crystallization trends in intrusions of alkali olivine-basalt type. Open circles—clinopyroxenes from the Black Jack sill, near Gunnedah, New South Wales trend *AA'*. Solid circles—clinopyroxenes from the Garbh Eilean sill, Shiant Isles, trend *BB'* (Murray, 1954).

One of the most striking features of the Garbh Eilean and Black Jack clinopyroxenes is their relatively small range in composition, for in this respect they lag strongly behind the associated minerals and parent rocks (see Murray, 1954, Fig. 3). Such relationships provide marked contrast to tholeiitic intrusions showing medium or strong fractionation, where the principal pyrogenetic minerals all undergo comparable compositional changes (Table 1).

To stabilize the trend indicated by the Garbh Eilean and Black Jack

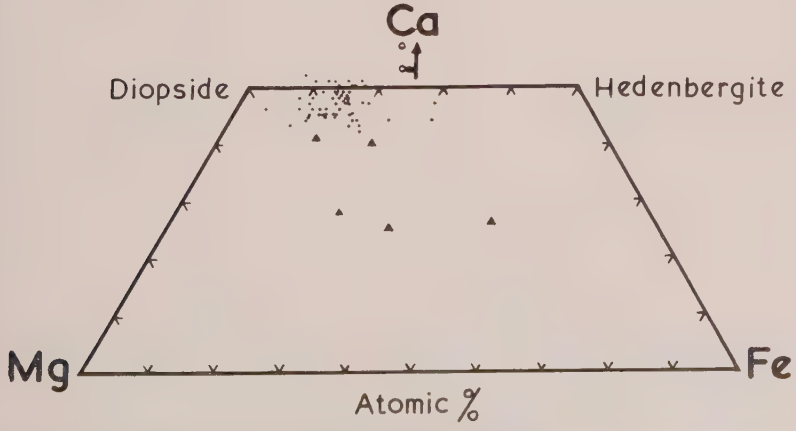


FIG. 3. Compositions of titaniferous clinopyroxenes. Solid circles—clinopyroxenes from alkali olivine-basalt magma. Solid triangles—titaniferous clinopyroxenes from tholeiitic magma. Open circles—titaniferous clinopyroxenes from contaminated basic magma.

TABLE 1. COMPOSITIONAL VARIATION WITHIN THE PRINCIPAL MINERAL SERIES OF SOME DIFFERENTIATED INTRUSIONS

Intrusion	Clinopyroxene	Ortho-pyroxene	Olivine	Plagioclase	Remarks	Reference
Black Jack sill, Gunnedah, N. S. W.	$Ca_{39}Mg_{37}Fe_{14}$ to $Ca_{47}Mg_{33}Fe_{20}$	—	Fa_{21}–Fa_{60}	An_{72}–An_{43}	Olivine and feldspar compositions refer to the cores of the crystals	
Garbh Eilean sill, Shiant Isles	$Ca_{..}Mg_{42}Fe_{14}$ to $Ca_{41}Mg_{..}Fe_{..}$	—	Fa_{17}–Fa_{90}	An_{88}–An_{30}	Upper composition limits of olivine and feldspar on zoned crystals	Johnston (1953) Murray (1954)
Skaergaard* intrusion East Greenland	$Ca_{36}Mg_{42}Fe_{22}$ to $Ca_{30}Mg_{2}Fe_{68}$	Of_{40}–Of_{76}	Fa_{24}–Fa_{97}	An_{60}–An_{30}		Wager and Deer (1939) Muir (1951)
New Amalfi sheet,* Matatiele	$Wo_{..}En_{..}Fs_{..}$ to $Wo_{38}En_{9}Fs_{53}$	Of_{15}–Of_{100}	Fa_{15}–Fa_{100}	An_{70}–An_{60} $\rightarrow(An_{31})$	Pyroxene composition from optics. Plagioclase (An_{31}) from upper fayalite-hedenbergite-granophyre	Poldervaart (1944)
Palisade sill,* New Jersey	"hypersthene-augite to iron-rich pigeonite"	Of_{55}–Of_{10}	Fa_{20}–Fa_{35}	An_{76}–An_{48}	Upper limit of olivine composition on zoned crystals	Walker (1940)
Mount Wellington* sill Tasmania	$Wo_{35}En_{60}Fs_{5}$ to $Wo_{27}En_{18}Fs_{55}$; pigeonite $Wo_{10}En_{20}Fs_{70}$	Of_{15}–Of_{39}	rare	An_{75}–An_{65} $\rightarrow An_{26}$ (outer zones)	Clinopyroxene compositions from optical measurements	Edwards (1942)
Dillsburg sill,* Penn.	$Ca_{39}Mg_{..}Fe_{..}$ to $Ca_{43}Mg_{16.5}Fe_{40.5}$	—	Fa_{20} ?	An_{70}–An_{35}	Clinopyroxene composition from optics. Olivine rare	Hotz (1953)

* Products of tholeiitic magma.

minerals, additional clinopyroxenes have been plotted in Fig. 3. Since alkali olivine-basalt clinopyroxenes generally possess relatively high titania contents, attention was directed to clinopyroxenes containing more than average amounts of this constituent. Relevant pyroxene data concerning composition, optics and literature are listed in Table 2. The references in this table are not listed at the end of the paper.

The plotted analyses include nearly sixty clinopyroxenes from non-tholeiitic igneous rocks (Table 2, Analyses 1 -48). To save repetition, the Garbh Eilean clinopyroxenes (Murray, 1954, Table 1) have not been included in the tabulation. The parent rocks are undersaturated (alkalic) types, usually with olivine and/or feldspathoids, and include many representatives of alkali olivine-basalt magma. The debatable question of the possible genetic interrelationships of certain of the listed rocks is outside the scope of the present investigation.

The additional analyses include titaniferous clinopyroxenes from tholeiitic magma (Table 2, Analyses 49–53), and from basic feldspathoidal rocks produced by reaction of basic magma with carbonate sediments (Analyses 54–56).

The plot of the clinopyroxenes from basic alkaline magmas (Fig. 3) yields important results, especially when one considers the variation in age, location and most important, the magmatic histories of the parent rocks themselves. As a group, these minerals reveal little variation in composition. The majority plots in the field of salite; a small number fall in the augite field but close to the augite-salite boundary. There is an absence of any marked trend extending through ferrosalite to hedenbergite, only three analyses revealing significant iron enrichment (Table 2, Analyses 40 and 46; Murray, 1954, Table 1, Analysis 31 *H*).

The titaniferous clinopyroxenes from both tholeiitic and contaminated basic rocks plot outside the field of clinopyroxenes from alkaline rocks, the tholeiitic examples behaving in a manner similar to their titania-poor equivalents in differentiated tholeiitic magma, with appreciable replacement of both Ca^{2+} and Mg^{2+} by Fe^{2+}. The carbonate-basic magma reaction types in the three instances reveal lime enrichment.

Comparing Figs. 2 and 3, it is seen that the compositional trends of the Garbh Eilean and Black Jack clinopyroxenes embrace the normal compositional limits of alkali olivine-basalt clinopyroxenes, i.e. the trend is dominantly parallel to the diopside-hedenbergite join, within the field embraced by Fe_9-Fe_{21} and Ca_{50}-Ca_{43}. There is no tendency for a pyroxene trend from diopside to ferrosilite, a trend demonstrated in certain tholeiitic rocks (Kuno, 1955), but often considered to apply to basaltic magmas in general (Fig. 1).

Murray (1954, Fig. 1) has extended the crystallization course of the

TABLE 2. OPTICAL PROPERTIES AND COMPOSITIONS OF TITANIFEROUS CLINOPYROXENES PLOTTED ON FIG. 3

Analysis number	Weight per cent TiO_2	Composition in atom per cent	Optical properties	Rock type	Locality	Reference
1	3.04	$Ca_{49}Mg_{37}Fe_{14}$	$\alpha = 1.699–1.704$ $\beta = 1.704–1.708$	teschenite, 20 feet above lower contact (1) Mg-rich fraction	Black Jack sill, Gunnedah, N. S. W.	J. F. G. Wilkinson (1956), *Geol. Mag.*, (in press)
2	3.21	$Ca_{48}Mg_{37}Fe_{15}$	$\gamma = 1.725–1.731$ $2V = 44–52$; $\gamma \wedge c$ 42–45	(2) Bulk clinopyroxene		
3	2.42	$Ca_{47}Mg_{34}Fe_{19}$	$\alpha = 1.699–1.707$ $\beta = 1.704–1.711$ $\gamma = 1.725–1.732$ $2V = 49–59$; $\gamma \wedge c$ 42–45	teschenite approx. 500 feet above lower contact (3) bulk clinopyroxene	Black Jack sill, Gunnedah, N. S. W.	*Geol. Mag.*, (in press)
4	2.15	$Ca_{47}Mg_{33}Fe_{20}$		(4) Fe rich fraction		
5	4.28	$Ca_{51}Mg_{37}Fe_{12}$	—	nepheline-basalt	Black Mountain, Uvalde Quadrangle, Texas	F. W. Clarke, (1910), *U. S. Geol. Surv., Bull.* **419,** 43
6	3.03	$Ca_{46}Mg_{49}Fe_{5}$	—	wyomingite	Leucite Hills, Wyoming	W. Cross, (1897), *Am. J. Sci.*, (Ser. 4), **4,**, 130
7	1.67	$Ca_{46}Mg_{42}Fe_{12}$	$\alpha 1.690$ $\beta 1.698$ $\gamma 1.720$ $2V = 48$; $\gamma \wedge c$ 45	camptonite	Skaergaard area, East Greenland	E. A. Vincent, (1953), *Q.J.G.S.*, **109,** 34
8	1.52	$Ca_{45}Mg_{43}Fe_{12}$	β 1.700–1.711 $\gamma \wedge c$ ca 45	leucite-tephrite	Vesuvius	H. S. Washington and H. E. Merwin, (1921), *Am. J. Sci.*, (Ser. 5), **1,** 22
9	2.11	$Ca_{48}Mg_{41}Fe_{11}$	$\alpha 1.704$ $\beta 1.711$ $\gamma 1.732$	alkali andesite (?)	Monti Rossi, Etna	H. S Washington, and H. E. Merwin, *op. cit.*, 29
10	2.86	$Ca_{50}Mg_{34}Fe_{16}$	$\alpha 1.699$ $\beta 1.718$ $\gamma 1.742$ $2V = 66–67$; $\gamma \wedge c$ 46	missourite	Villa Senni, Italy	H. S. Washington, and H. E. Merwin, (1927), *Am. J. Sci.*, (Ser. 5), **14,** 185
11	2.85	$Ca_{48}Mg_{33}Fe_{19}$	—	leucitite	Ticchiena, Hernican District, Italy	H. S. Washington, (1906), *Carnegie Publ. No.* **57,** 134
12	1.19	$Ca_{51}Mg_{36}Fe_{13}$	$\alpha 1.703$ $\beta 1.710$ $\gamma 1.727$	leucitite	Alban Hills, Italy	H. S. Washington, and H. E. Merwin, (1923), *Am. Mineral.*, **8,** 105
13	3.78	$Ca_{45}Mg_{37}Fe_{15}$	$\alpha 1.714$ $\gamma 1.740$ $\gamma \wedge c 47$	syenite	d'Almeida Barranco, Tenerife	W. Kunitz, (1936), *N. Jb. Min.*, **70,** 409–410

TABLE 2—(*continued*)

Analysis number	Weight per cent TiO_2	Composition in atom per cent	Optical properties	Rock type	Locality	Reference
14	4.09	$Ca_{48}Mg_{37}Fe_{16}$	α1.719 γ1.745 2V=46 $\gamma \wedge c$ 47	"nepheline-dolerite"	Lobauer Berg	W. Kunitz, *op. cit.*
15	3.57	$Ca_{48}Mg_{38}Fe_{14}$	α1.716 γ1.742 2V=58 $\gamma \wedge c$ 48	phonolite	Kaiserstuhl	W. Kunitz, *op. cit.*
16	4.62	$Ca_{47}Mg_{36}Fe_{17}$	α1.724 γ1.752 2V=46 $\gamma \wedge c$ 52	nephelinite	Meiches	W. Kunitz, *op. cit.*
17	1.67	$Ca_{45}Mg_{39}Fe_{16}$	α1.698 γ1.728 $\gamma \wedge c$ 44	tephrite	Tenerife	W. Kunitz, *op. cit.*
18	5.02	$Ca_{47}Mg_{36}Fe_{17}$	α1.731 γ1.758	nepheline rock	Los Siete, Funentes	W. Kunitz, *op. cit.*
19	2.83	$Ca_{49}Mg_{37}Fe_{14}$	α1.712 γ1.740	nepheline-basalt	Stöffelskuppe	W. Kunitz, *op. cit.*
20	2.05	$Ca_{45}Mg_{41}Fe_{14}$	α1.690 β1.697 γ1.715 2V=52–54 $\gamma \wedge c$ 42	teschenite	Brocken Ra., Eastern Wellington, N. Z.	C. O. Hutton, (1943), *Trans. Proc. Roy. Soc. N. Z.*, **72,** 354
21	2.88	$Ca_{50}Mg_{32}Fe_{18}$	α1.698 β1.704 γ1.724 2V=48–63	theralite	L. Waihola, Otago, New Zealand	C. O. Hutton, (1942), *Trans. Proc. Roy. Soc. N. Z.*, **72,** 182
22	2.25	$Ca_{48}Mg_{43}Fe_{9}$	α1.695 β1.701 γ1.721 2V=60$\gamma \wedge c$46	potash ankaratrite	Nyamunuka Crater, S. W. Uganda	Th. G. Sahama, (1952), *Am. J. Sci.* (Bowen Vol.), 466
23	2.49	$Ca_{47}Mg_{38}Fe_{15}$	β1.696 2V=48	dolerite with nepheline and analcime	Mauritius	F. Walker, and L. O. Nicolaysen, (1954), *Col. Geology and Min. Res.*, **4,** 19
24	4.84	$Ca_{51}Mg_{34}Fe_{15}$	α1.725 γ1.746 $\gamma \wedge c$42	"Augitite" assoc. with nepheline-syenite	Ice River, Brit. Columbia	C. H Warren, J. A. Allen, and M. F. Connor, (1917), *Am. J. Sci.* (Ser. 4), **43,** 77
25	2.78	$Ca_{52}Mg_{40}Fe_{8}$	$\gamma \wedge c$46.5 2E=86	leucite-nepheline-basanite	Laacher See, Rhineland	R. Brauns, (1928), *N. Jb. Min., Abt. A*, **57,** 133
26	2.91	$Ca_{51}Mg_{39}Fe_{10}$	—	alkali trachyte	Gleeser Feld, Laacher See, Rhineland	R. Brauns, *op. cit.*
27	2.06	$Ca_{43}Mg_{47}Fe_{10}$	α1.704 γ1.729 2V=54 $\gamma \wedge c$45	atlantite (?)	Azores	P. Esenwein, (1929), *Zeits. Vulk.*, **12,** 120
28	1.87	$Ca_{50}Mg_{36}Fe_{14}$	2V=57 $\gamma \wedge c$45–47	"basalt-tuff"	Mount Medves, Hungary	L. Jugovics, (1934), *M.A.*, **6,** 120
29	2.05	$Ca_{48}Mg_{36}Fe_{16}$	—	lamprobolite-bearing basalt	Liebhards, Rhön	X. Galkin, (1910), *N. Jb. Min.*, **29,** 687

TABLE 2—(*continued*)

Analysis number	Weight per cent TiO_2	Composition in atom per cent	Optical properties	Rock type	Locality	Reference
30	1.24	$Ca_{48}Mg_{37}Fe_{15}$	—	lamprobolite-bearing basalt	Gehulfensberg, Rhön	X. Galkin, *op. cit.*
31	1.44	$Ca_{46}Mg_{38}Fe_{16}$	—	lamprobolite-bearing basalt	Sparbrod, Rhön	X. Galkin, *op. cit.* 688
32	2.09	$Ca_{46}Mg_{41}Fe_{13}$	$2V = 61$ $\gamma \wedge c 43$	phenocrysts in theralite	Bo Ploi, Siam	O. Weigel, and E. Krueger, (1934), *M.A.*, **7**, 331
33	2.53	$Ca_{48}Mg_{36}Fe_{16}$	$n1.734$ $2V = 59$ $\gamma \wedge c 46$	groundmass in theralite	Bo Ploi, Siam	O. Weigel, and E. Krueger, *op. cit.*
34	2.92	$Ca_{49}Mg_{36}Fe_{15}$	$\alpha 1.721$ $\beta 1.725$ $\gamma 1.746$ $2V = 51 \gamma \wedge c 50$	monzonitic teschenite	Marklowice, Poland	W. Wawryk, (1935), *M.A.*, **6**, 212
35	1.77	$Ca_{45}Mg_{37}Fe_{18}$	—	leucite-tephrite (?)	Vesuvius	K. Muller, (1936), *M.A.*, **6**, 536
36	4.86	$Ca_{49}Mg_{37}Fe_{14}$	$\alpha 1.701$ $\gamma 1.728$ $2V = 49$ $\gamma \wedge c 43–52$	monchiquite	Turja, Kola	E. H. Kranck, (1928), *Fennia*, **51**, No. 5, Table IX
37	1.53	$Ca_{49}Mg_{39}Fe_{12}$	—	analcime-basalt	The Basin, Colorado	W. Cross, (1897), *Jour. Geol.*, **5**, 687
38	1.91	$Ca_{46}Mg_{44}Fe_{10}$	—	analcime-basalt	Scano, Sardinia	H. S. Washington, (1914), *Jour. Geol.*, **22**, 747
39	2.10	$Ca_{44}Mg_{44}Fe_{12}$	$\alpha 1.695$ $\beta 1.706$ $\gamma 1.720$ $2Vca 60$ $\gamma \wedge c 46$	limburgite	Hopi Buttes, Arizona	H. Williams, (1936), *Bull. Geol. Soc. Am.*, **47**(1), 166, Analysis 15
40	2.18	$Ca_{17}Mg_{23}Fe_{36}$	$\gamma \wedge c 32–38$	ijolite	Ice River, Brit. Columbia	J. A. Allen, (1914), *Can. Geol. Surv., Mem.* **55**, 171
41	2.34	$Ca_{45}Mg_{39}Fe_{16}$	$\alpha 1.703$ $\beta 1.714$ $\gamma 1.731$ $2V = 48 \gamma \wedge c 55$	alkaline olivine-basalt	Old Pallas area, Co. Limerick, Eire	D. F. Ashby, (1946), *Mineral. Mag.*, **27**, 196
42	1.59	$Ca_{44}Mg_{37}Fe_{19}$	$\alpha 1.695$ $\beta 1.706$ $\gamma 1.726$ $2V = 52 \gamma \wedge c 44–49$	alkaline olivine-trachy-basalt	Old Pallas area, Co. Limerick, Eire	D. F. Ashby, *op. cit.*
43	4.33	$Ca_{49}Mg_{35}Fe_{16}$	$\alpha 1.719$ $\beta 1.722$ $\gamma 1.742$ $2V = 42$	"essexite-porphyry"	Stöffel, Westerwald	J. Holzner, (1934), *Zeits. Krist.*, **87**, 10
44	4.50	$Ca_{51}Mg_{32}Fe_{17}$	$\alpha 1.718$ $\beta 1.723$ $\gamma 1.738$ $2V = 46$	nepheline-dolerite	Löbauer Berg	J. Holzner, *op. cit.*
45	5.50	$Ca_{50}Mg_{34}Fe_{16}$	$\alpha 1.725$ $\beta 1.730$ $\gamma 1.750$ $2V = 40$	nepheline-dolerite	Meiches, (Vogelsberg)	J. Holzner, *op. cit.*

TABLE 2—(*continued*)

Analysis number	Weight per cent TiO_2	Composition in atom per cent	Optical properties	Rock type	Locality	Reference
46	2.98	$Ca_{44}Mg_{25}Fe_{31}$	2Vca58 $\gamma \wedge c$48	alkaline dolerite	Kaersut, Greenland	E. K. Drescher, and H. K. E. Krueger, (1927), *N. Jb. Min.*, **57,** 587
47	2.83	$Ca_{45}Mg_{39}Fe_{16}$	α1.699 γ1.727 2V = 33.5 –41 $\gamma \wedge c$36–43	analcime-dolerite	Moroto District, Sakhalin	K. Yagi, (1953), *Bull. Geol. Soc. Am.*, **64,** 780
48	2.96	$Ca_{45}Mg_{37}Fe_{18}$	α1.690 γ1.715 2V = 38–53 $\gamma \wedge c$36–43	analcime-dolerite	Moroto District, Sakhalin	K. Yagi, *op. cit.*, 780
49	4.42	$Ca_{26}Mg_{25}Fe_{49}$	α1.721 β1.728 γ1.749 2V = 44 $\gamma \wedge c$39	hortonolite-quartz-gabbro (1907)	Skaergaard intrusion, East Greenland	W. A. Deer, and L. R. Wager, (1938), *Mineral. Mag.*, **25,** 16
50	3.75	$Ca_{28}Mg_{47}Fe_{25}$	α1.695 β1.701 γ1.728 2V = 46 $\gamma \wedge c$39	coarse basalt	Valley of Atuana, Hiva Oa, Marquesa Islands	T. F. W. Barth, (1931), *N. Jb. Min., Abt. A*, **64,** 218
51	2.37	$Ca_{41}Mg_{44}Fe_{15}$	2V = 53–55	olivine-augite-basalt	Mt. Bullengarook, Gisborne area, Victoria	A. B. Edwards, and W. Crawford, (1940), *Proc. Roy. Soc. Vict.*, **52,** Pt. II, 303
52	2.40	$Ca_{25}Mg_{41}Fe_{34}$	2V = 38 $\gamma \wedge c$45	doleritic vein	Portrush sill, Co. Antrim	N. Harris, (1937), *Proc. Roy. Irish Acad.*, **43,** 103
53	1.62	$Ca_{40}Mg_{36}Fe_{24}$	γ1.732 2V = 51	olivine-gabbro	Camas Mòr, Muck	C. E. Tilley, (1952), *Am. J. Sci.* (Bowen Vol.), 533
54	3.85	$Ca_{53}Mg_{25}Fe_{22}$	α1.74 γ1.76	melilite-nepheline-dolerite	Scawt Hill, Co. Antrim	C. E. Tilley, and H. F. Harwood, (1931), *Mineral. Mag.*, **22,** 454
55	2.85	$Ca_{52}Mg_{24}Fe_{23}$	—	titanaugite-pyroxenite	Camphouse, Ardnamurchan	S. O. Agrell (unpubl. analysis)
56	5.72	$Ca_{57}Mg_{23}Fe_{20}$	$\alpha = \beta$ = 1.741 γ1.762 $\gamma \wedge c$32	segregation in plagioclase-diopside-hornfels xenolith	Schivas, Aberdeenshire	B. E. Dixon and W. Q. Kennedy, (1933), *Zeits. Krist.*, **86,** 112

Garbh Eilean clinopyroxenes into the field of ferroaugite, mainly on an analysis of clinopyroxene ($Ca_{41}Mg_{14}Fe_{45}$) from an orthophyre vein in the Portrush sill, County Antrim. Of the many analyses studied, only one falls in the ferroaugite field, and then practically on the ferrosalite boundary (Fig. 3). The Portrush clinopyroxene should find no place in determining the trends of the present pyroxenes for the following reasons:

1. The origin of the orthophyre vein is related in part to reaction and rheomorphic injection. Consequently it is doubtful if the associated clinopyroxene is a "normal" type in that its precipitation occurred under strictly magmatic conditions.
2. It appears that the Portrush sill and its veins are the products of the consolidation of undersaturated tholeiitic magma (cf. Tilley, 1950, pp. 40–41). In his original account of the Portrush rocks, Harris (1937, pp. 102–104) recognized hypersthene (Of_{52}) in addition to clinopyroxene. His descriptions include two clinopyroxene analyses, one of "enstatite-augite" ($Ca_{42}Mg_{44}Fe_{14}$), the other poor in lime and approaching subcalcic augite ($Ca_{25}Mg_{41}Fe_{34}$). The olivine-dolerites themselves carry normative hypersthene and are low in alkalies. The clinopyroxene in question plots very close to the trend of the Skaergaard clinopyroxenes from the ferrohortonolite-ferrogabbros, a point commented on by Murray.

In tholeiitic magma rarely is fractionation so extreme that the composition of the clinopyroxene passes $Wo_{29}En_{30}Fs_{41}$, i.e. the intersection of the course of clinopyroxene crystallization (after Hess, 1941) and the two-pyroxene boundary (Poldervaart and Hess, 1951, p. 483; Fig. 5). Although only one common pyroxene occurs in alkali olivine-basalt magma, it is important to note that only two clinopyroxenes in Table 2 pass the two-pyroxene boundary in the direction of hedenbergite. Examples of clinopyroxenes of the diopside-hedenbergite series showing iron enrichment in excess of $Ca_{45}Mg_{25}Fe_{30}$ must be rare in alkaline basic rocks. The retention of a large percentage of the available iron in the ferrous state in a reducing (relatively anhydrous) magmatic environment (Kennedy, 1948), and the continued crystallization of clinopyroxene after the disappearance of olivine under conditions of continual Fe/Mg enrichment would be fundamental conditions for such iron enrichment. Extreme fractionation of ijolitic types may furnish examples. However at compositions more iron-rich then approximately $Ca_{44}Mg_{36}Fe_{20}$, continued fractionation of alkali olivine-basalt clinopyroxenes may result in progressive enrichment in the acmite molecule (Yagi, 1953), a trend often observed on a small scale in basic alkaline rocks as the zonal series, salite→aegirine-augite→aegirine, especially where the normal clinopyroxene (diopside or salite) abuts against a micro-crystalline alkaline residuum.

The Contrasting Behavior of the Pyroxenes from Both Magma Types

The pyroxene assemblage in representatives of alkali olivine-basalt magma differs markedly from its equivalent in tholeiitic rocks in two important aspects, namely in the absence of orthopyroxene and pigeonite, and in the much more limited degree of clinopyroxene iron enrichment (Fig. 4), particularly in the replacement of Ca^{2+} by Fe^{2+}.

(i) In tholeiitic rocks, the frequently described mantling of olivine by orthopyroxene provides petrological testimony to the reaction relation between early-formed olivine and liquid (Bowen and Schairer, 1935).

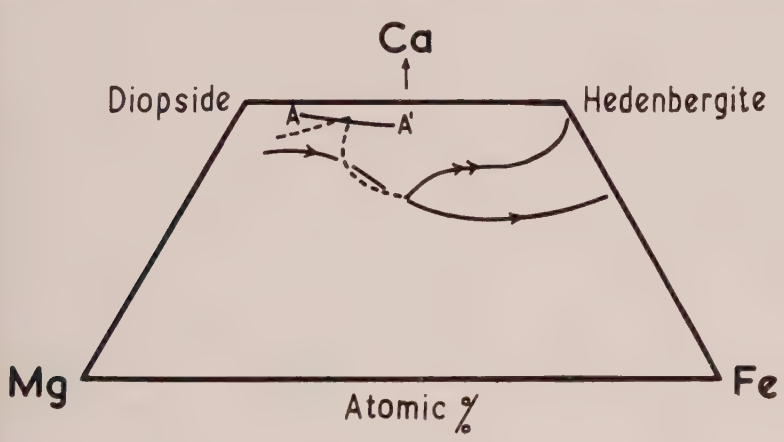


Fig. 4. Clinopyroxene trends in basaltic magmas.

$A-A'$ Alkali olivine-basalt clinopyroxene trend.
———→ Clinopyroxene course of crystallization in tholeiitic rocks (Poldervaart and Hess, 1951).
– – –→ Clinopyroxene trend of the tholeiitic Skaergaard intrusion (Muir, 1951).

Although these authors consider the relation does not hold for certain "iron-rich basalts" which yield undersaturated differentiates, they regard the phenomenon as independent of the parental magma.

In the magma types under discussion, the presence or absence of orthopyroxene depends on the chemistry of the residual liquids formed during crystallization and subsequent fractionation. In many basic alkaline rocks (essexites, theralites, teschenites, lugarites), a microcrystalline mesostasis, often analcimic, consisting of alkali feldspar microlites, clinopyroxene and dusty iron ore, is frequently present, even in the early stages of magmatic evolution (Flett, 1910, p. 298; Browne, 1927, p. 375; Lehmann, 1930, Figs 3 and 4; Walker, 1930, p. 370; 1936, p. 280; Benson, 1942, p. 166). Such a mesostasis is widespread in the teschenites from all levels of the Black Jack sill (Table 3, Analysis 1). Under suitable condi-

TABLE 3. ANALYSES OF ANALCIME—SYENITES

	I	II	III	IV	V
SiO_2	50.71	50.01	56.86	58.36	52.33
TiO_2	0.59	2.00	0.53	0.48	1.17
Al_2O_3	16.72	17.98	20.19	15.82	17.86
Fe_2O_3	3.26	3.05	3.63	4.87	3.12
FeO	5.49	3.26	1.40	2.53	3.89
MnO	0.01	0.10	0.13	0.27	0.08
MgO	0.42	3.13	0.33	0.59	3.61
CaO	3.27	7.09	1.64	1.99	1.88
Na_2O	6.42	4.43	7.42	7.47	3.04
K_2O	5.75	4.82	4.39	4.31	7.79
H_2O+	4.07	2.95	3.29	2.62	3.05
H_2O-	0.49	0.27	0.07	0.72	1.02
P_2O_5	0.12	0.67	0.07	0.35	0.46
CO_2	2.94	0.09	—	n.f.	0.26
etc.	—	0.12	—	0.04	0.21
Total	100.26	99.97	99.95	100.42	99.77
Norm.					
or	33.92	28.4	26.13	25.6	46.1
ab	33.01	20.4	47.67	49.8	23.8
ne	11.36	9.1	7.95	4.0	1.0
an	—	15.0	8.06	—	5.3
c	—	—	0.31	—	2.4
ac	—	—	—	5.1	—
di	—	11.7	—	6.0	—
hy	—	—	—	0.2	—
ol	4.37	1.9	0.56	—	8.5
il	1.22	3.8	1.06	0.9	2.3
mt	4.87	4.4	3.25	4.6	4.4
hm	—	—	1.44	—	—
ap	0.34	1.7	—	1.0	1.0
cc	5.50	—	—	—	—
siderite	1.28	—	—	—	—

Analysis I: Microcrystalline mesostasis, occurring as vein in teschenite, Black Jack sill, Gunnedah, New South Wales. Anal. J.F.G.W.

Analysis II: Analcime-syenite, forming felsic part of 80 foot sill, Utah. Anal. J. G. Fairchild (Gilluly, 1927, p. 205).

Analysis III: Analcime-syenite (1501), Morotu District, Sakhalin. Anal. K. Yagi (Yagi, 1953, Table 16).

Analysis IV: Segregation in analcime-syenite, Eilean Mhuire, Shiant Isles. Anal. E. G. Radley (Walker, 1930, p. 387).

Analysis V: Syenitic segregation (potash alkali-syenite) in upper teschenite of Lugar Sill boring, Mortonmuir, Cronberry, Ayrshire. Anal. G. A. Sergeant (Tyrrell, 1948, p. 165).

tions, this type of residuum may crystallize as internal cross-cutting analcime-syenite (Table 3). The chemistry of this liquid prohibits any reaction relation involving olivine. In strong contrast the oversaturated nature of late-stage tholeiitic liquids is indicated by two analyses of tholeiitic residua (Walker, 1935; Vincent, 1950), containing 31–36 per cent normative quartz. Fractionation of alkali olivine-basalt magma does however occasionally yield syenitic products with normative quartz (Yagi, 1953, Table 16) and in certain instances, modal quartz (Raggart and Whitworth, 1932, p. 223). At just what stage this divergence to yield an acid alkali (pantelleritic) end product (Tilley, 1950, p. 43) occurs is not precisely known, but it is not believed to materially affect the pyroxene assemblage in relation to the non-appearance of orthopyroxene since olivine generally disappears before this stage is reached, and the ferromagnesian assemblage is dominated by sodic clinopyroxenes and alkaline amphiboles.

In both magma types, the nature of the olivine (where present) reflects the presence or non-appearance of orthopyroxene. The olivines in tholeiitic rocks are unzoned or rarely show slight zoning, indicating the readiness with which this mineral reacts with the magma, compared with the associated clinopyroxene or plagioclase which may be strongly zoned. Widespread normal zoning is a feature of the olivines of alkali olivine-basalt derivatives (Tomkeieff, 1939; Benson, 1942, p. 164; Johnston, 1953). The nature of the strongly fayalitic outer zones is analogous with the compositional relationships between the co-existing olivine and orthopyroxene in tholeiitic rocks, where the orthopyroxene may be the most iron-rich ferromagnesian silicate (Muir, 1951, p. 711; Ramberg and de Vore, 1951, Fig. 2). However as progressive iron enrichment occurs, the olivine may be the most iron-rich mineral (Muir, 1954, p. 382; Ramberg and de Vore, *op cit.*), a relationship in harmony with the experimental data of Bowen and Schairer (1935).

(ii) Edwards (1942), Walker and Poldervaart (1949) and Muir (1951) have correlated the observed crystallization trend in tholeiitic clinopyroxenes with atomic structure. The higher titania content of alkali olivine-basalt clinopyroxenes cannot be the reason for their relatively inert behavior, since during fractionation, tholeiitic titaniferous clinopyroxenes behave similarly to their titania-poor equivalents.

The following explanation of the two differing clinopyroxene trends is based mainly on petrological and mineralogical data, although physicochemical and crystal chemical reasoning may well be applied.

In tholeiitic magma, even in its early undersaturated stages, the reaction relation between olivine and liquid results in the continuous formation of "hypersthene molecules." While these are potential ortho-

pyroxene or pigeonite, a variable percentage combines with highly diopsidic clinopyroxene (the "primitive" clinopyroxene of both magma types) to give augite, so that the modal pyroxene of tholeiites is greater than that of alkali olivine-basalts for the major part of their differentiation histories, even though in both cases a similar amount of lime is available for pyroxene formation.

Relevant data on medium grained differentiated intrusions (where more reliance can be placed on micrometric data) is set out in Table 4. These intrusions possess compositions representative of their parental magma types (see Walker, 1940, Table 3; Walker and Poldervaart, 1949, Table 24; Nockolds and Allen, 1954, Table 17). Pegmatitic facies or rocks with appreciable amphibole or mica are not included in the tabulation. The tholeiitic types possess a higher modal pyroxene content, averaging 30–45 per cent (see Turner and Verhoogen, 1951, p. 183), compared with alkali olivine-basalt rocks where the modal pyroxene varies from 18–24 per cent (see also Walker, 1934, Table 1). There is no notable divergence in the CaO content of both series, each carrying 50–60 per cent of modal plagioclase of similar basicity.

The principal pyroxene relationships visualized are as follows:

$$\text{olivine} + SiO_2 \rightarrow \text{orthopyroxene}$$
$$\text{orthopyroxene} + \text{diopside} \rightarrow \text{augite}$$
$$\text{olivine} + SiO_2 + \text{diopside} \rightarrow \text{augite (tholeiite)}$$
$$\text{In silica-deficient basic rocks} - SiO_2 \rightarrow \text{olivine} + \text{diopside (alkali olivine-basalt)}$$

Thus in the early magmatic stages, the tholeiitic clinopyroxene (augite) shows replacement of Ca^{2+} by Fe^{2+}, compared with the diopsidic type in alkali olivine-basalt at an equivalent stage. In its subsequent differentiation, tholeiitic magma may involve nearly double the amount of clinopyroxene in alkali magma.

While fractionation results in enrichment in iron relative to magnesium (and in certain instances, absolute iron enrichment), the response of the principal ferromagnesian mineral series to this enrichment varies in each magma type. In tholeiitic rocks, most of the Fe–Mg enrichment occurs in the olivine (if it still persists), orthopyroxene or pigeonite; the clinopyroxene lags behind these minerals. While falling temperature favors clinopyroxene iron enrichment, the additional and more difficult replacement of Ca^{2+} by Fe^{2+} is induced by the limited amount of available magmatic lime. Exceptions to the relatively high pyroxene content of tholeiite may be noted. The Skaergaard marginal gabbros, considered to represent the parental magma, contain 23 per cent pyroxene, a figure which increases to 41 per cent in the middle gabbros (Wager and Deer, 1939, p. 95 and p. 144). With this increase in pyroxene, which now reveals appreciable replacement of Ca^{2+} by Fe^{2+} (Fig. 4), the modal olivine de-

TABLE 4. COMPARATIVE CHEMICAL AND MODAL DATA ON ROCK TYPES FROM DIFFERENTIATED INTRUSIONS OF ALKALI OLIVINE-BASALT AND THOLEIITIC TYPE

Name of intrusion	Range of CaO (weight per cent)	MgO	FeO	Modal olivine (volume per cent)	Modal pyroxene	Modal plagioclase	Reference
Black Jack sill, Gunnedah, N. S. W.	10.25– 8.12	9.57–2.97	9.57–7.93	23.0– 0.0 (based on 60 modes)	16.4–29.2	52.2 to average around 45	
Garbh Eilean sill, Shiant Isles	12.38– 9.74	14.61–6.60	10.69–9.22	31.0– 8.0	17.0–29.0	60.0–50.0	Walker (1930)
Loch Mealt-Kilt Rock sill, Trotternish, Skye	11.61 11.47	5.98–5.32	7.40–5.77	17.1– 4.6	14.3–25.2	73.7–58.8	Walker (1932)
No. 6 Bore, Mt. Nebo sill, N. S. W.	10.7 – 8.29	10.8 –9.02	9.95–6.3	18.5–12.0	12.0–22.6	not determined	Edwards (1953)
Circular Head laccolith, Tasmania	9.95– 8.20	11.84–5.24	10.94–6.41	24.9– 4.4	13.1–27.3	76.6–49.4 (includes zeolite and mesostasis)	Edwards (1941)
George Washington Bridge section, Palisades sill, N. J.*	10.65– 8.38	17.48–3.47	11.54–7.70	22.0– 0.0	51.8–29.4	65.8–32.6	Walker (1940)
Dillsburg sill, Penn.*	10.18– 8.85	7.3 –4.33	9.19–7.85	2.0– 0.0	57.5–37.4	43.7–30.0	Hotz (1953)
Whin sill (generalized figures)*	9.46– 8.21	5.90–4.42	11.44–8.95	—	38.7–31.6	52.3–49.0	Holmes and Harwood (1928)
Hangnest sill, South Africa*	9.40– 8.89	7.32–5.14	9.12–8.85	—	50.2–40.6 (average 42.9)	49.8–40.7 (average 40.7)	Walker and Poldervaart, (1941)
Elephant's Head dyke and New Amalfi sheet, Matatiele, South Africa*	13.86 8.4	9.77–4.76	11.18–8.74	12.3– 0.0	40.4–37.2 →(26.5)	45.5–40.5 →(33.4)	Poldervaart (1944)

* Products of tholeiitic magma.

creases. Tholeiites may retain their initial moderately low pyroxene content (when no great degree of iron enrichment would be anticipated), if reaction is prevented by the residual liquids diffusing through the crystal interstices. However olivine frequently disappears at a relatively early stage in tholeiitic evolution, and indeed this mineral may be antipathetic with orthopyroxene (Walker and Poldervaart, 1941*a*, p. 143). In the later stages of pyroxene fractionation when re-entry of Ca^{2+} occurs (Edwards, 1942), and the replacement is dominantly Fe^{2+} for Mg^{2+}, the additional withdrawal of lime is reflected in a decrease in modal pyroxene, despite albite enrichment in the plagioclase e. g. decrease in modal pyroxene occurs at this stage in the Palisades, Hangnest and Dillsburg sills. Possibly the two-pyroxene boundary is reached about this stage and the main Fe/Mg enrichment now occurs in the clinopyroxene.

In alkali olivine-basalt magma, the ferromagnesian assemblage consists of diopsidic clinopyroxene and olivine. In the initial stages, the early separation of forsteritic olivine greatly increases the normative Wo content of the magma (Kennedy, 1933, p. 252). In the absence of *possible* localized crystal accumulation, the failure of the reaction relation results in a moderately low near-constant amount of clinopyroxene. With decreasing temperature, the bulk of Fe/Mg enrichment is borne by an ever-diminishing quantity of olivine, which becomes more fayalitic (and in many instances, more strongly zoned). Exsolution lamellae are uncommon in alkali olivine-basalt clinopyroxenes. The absence of the reaction relation limits the amount of En-Fs in solid solution (cf. Poldervaart and Hess, 1951, p. 488). In these clinopyroxenes, the lack of alteration in the presence of residual magmatic solutions (except in dykes of "white trap"), (Flett, 1931, p. 47; 1932, p. 145; Browne, 1924, p. 244; Raggatt and Whitworth, 1932, p. 217; Campbell, Day and Stenhouse, 1932, p. 352) may well be consequent on the greater structural stability resulting from more limited replacement of Ca^{2+} by Fe^{2+}, compared with their tholeiitic equivalents (see also Harry, 1954, p. 85).

Acknowledgments

The bulk of this study was carried out in the Department of Mineralogy and Petrology, Cambridge, during the writer's tenure of a Royal Dutch/Shell Commonwealth Post-Graduate Scholarship. This financial assistance is gratefully acknowledged.

The writer expresses his thanks to Professor C. E. Tilley and Dr. S. R Nockolds for helpful discussions on pyroxene problems, and to Professor H. H. Hess and Dr. G. M. Brown for critically reading the manuscript. Dr. S. O. Agrell gave permission to quote the analysis of the Camphouse titaniferous clinopyroxene, carried out by Mr. J. H. Scoon.

References

Bailey, E. B., *et al* (1924), Tertiary and post-Tertiary geology of Mull, Loch Aline and Oban: *Mem. geol. Surv. Scot.*, 445 pp.

Barth, T. F. W. (1931), Crystallization of pyroxenes from basalts: *Am. Mineral.*, **16,** 195–208

Barth, T. F. W. (1936), The crystallization process of basalt: *Am. J. Sci.*, **31,** 321–351.

Benson, W. N. (1942), The basic igneous rocks of eastern Otago and their tectonic environment, Part III: *Trans. roy. Soc. N.Z.*, **72,** 160–185.

Bowen, N. L., and Schairer, J. F. (1935), The system MgO. FeO. SiO_2: *Am. J. Sci.*, **29,** 151–217.

Browne, W. R. (1924), Notes on the petrology of the Prospect intrusion, with special reference to the genesis of the so-called secondary minerals: *J. roy. Soc. N.S.W.*, **58,** 240–254.

Browne, W. R. (1927), Petrological notes on some New South Wales alkaline basic rocks: *J. roy. Soc. N.S.W.*, **61,** 371–382.

Campbell, R., Day, T. C., and Stenhouse, A. G. (1932), The Braefoot outer sill, Fife, Part I: *Trans. Edinb. Geol. Soc.*, **12,** 342–375.

Dittler, E. (1929), Zur frage der oxydationstufe des titans in den sillikaten: *S.B. Acad. Wiss. Wien, Abt. I*, **138,** 371–411.

Edwards, A. B. (1941), The crinanite laccolith of Circular Head, Tasmania: *Proc. roy. Soc. Vict.*, **53,** 403–415.

Edwards, A. B. (1942), Differentiation of the dolerites of Tasmania: *J. Geol.*, **50,** 451–480, 579–610.

Edwards, A. B. (1953), Crinanite-picrite intrusions in the Nebo district of New South Wales: *Proc. roy. Soc. Vict.*, **65,** 9–29.

Flett, J. S. (1931), The Saline No. 1 teschenite: *Summ. Progr. geol. Surv. London*, for 1930, pt. iii, 44–50.

Flett, J. S. (1932), The Stankards sill: *Summ. Progr. geol. Surv. Lond.* for 1931, pt. ii, 141–156.

Gilluly, J. (1927), Analcite-diabase and related alkaline syenite from Utah: *Am. J. Sci.*, **14,** 199–221.

Harris, N. (1937), A petrological study of the Portrush sill and its veins: *Proc. R. Irish Acad.*, **33,** 95–134.

Harry, W. T. (1954), The clinopyroxene—hornblende equilibrium in thermal metamorphism: some data from Carlingford, Eire: *Geol. Mag. Lond.*, **91,** 79–85.

Hess, H. H. (1941), Pyroxenes of common mafic magmas: *Am. Mineral.*, **26,** 515–535, 573–594.

Hess, H. H. (1949), Chemical composition and optical properties of common clinopyroxenes, Part I: *Am. Mineral.*, **34,** 621–666.

Holmes, A., and Harwood, H. F. (1928), The age and composition of the Whin sill and the related dykes of the north of England: *Mineral. Mag.*, **21,** 493–542.

Hotz, P. (1953), Petrology of granophyre in diabase, near Dillsburg, Pennsylvania: *Bull. Geol. Soc. Am.*, **64,** 675–704.

Johnston, R. (1953), The olivines of the Garbh Eilean sill, Shiant Isles: *Geol. Mag. Lond.*, **90,** 161–171.

Kennedy, G. C. (1948), Equilibrium between volatiles and iron oxides in igneous rocks: *Am. J. Sci.*, **246,** 529–549.

Kennedy, W. Q. (1931), The parent magma of the British Tertiary Province: *Summ. Progr. Geol. Surv. Lond.* for 1930, part ii, 61–73.

KENNEDY, W. Q. (1933), Trends of differentiation in basaltic magmas: *Am. J. Sci.*, **25**, 239–256.

KUNO, H. (1936), Petrological notes on some pyroxene andesites from Hakone volcano, with special reference to some types with pigeonite phenocrysts: *Jap. J. Geol. Geogr.*, **13**, 107–140.

KUNO, H. (1936*a*), On the crystallization of pyroxenes from rock magmas, with special reference to the formation of pigeonite: *Jap. J. Geol. Geogr.*, **13**, 141–150.

KUNO, H. (1955), Ion substitution in the diopside-ferro-pigeonite series of clinopyroxenes: *Am. Mineral.*, **40**, 70–93.

KUNO, H., AND HESS, H. H. (1953), Unit cell dimensions of clinoenstatite and pigeonite in relation to other common clinopyroxenes: *Am. J. Sci.*, **251**, 741–752.

LEHMANN, E. (1930), Der basalt vom Stöffel (Westerwald) und seine essexitich—theralithichen differentiate: *Chem. d. Erde*, **5**, 319–372.

MUIR, I. D. (1951), The clinopyroxenes of the Skaergaard intrusion, eastern Greenland: *Mineral. Mag.*, **29**, 690–714.

MUIR, I. D. (1954), Crystallization of pyroxenes in an iron-rich diabase from Minnesota: *Mineral. Mag.*, **30**, 376–388.

MURRAY, R. J. (1954), The clinopyroxenes of the Garbh Eilean sill, Shiant Isles: *Geol. Mag. Lond.*, **91**, 17–31.

NOCKOLDS, S. R., AND ALLEN, R. S. (1954), The geochemistry of some igneous rock series —Part II: *Geoch. Cosm. Acta.*, **5**, 245–285.

POLDERVAART, A. (1944), The petrology of the Elephant's Head dike and the New Amalfi sheet (Matatiele): *Trans. roy. Soc. S. Afr.*, **30**, 85–119.

POLDERVAART, A., AND HESS, H. H. (1951), Pyroxenes in the crystallization of basaltic magma: *J. Geol.*, **59**, 472–489.

RAGGART, H. G., AND WHITWORTH, H. F. (1932), The intrusive igneous rocks of the Muswellbrook—Singleton district: Part II The Savoy Sill: *J. roy. Soc. N.S.W.*, **66**, 194–223.

RAMBERG, H., AND DE VORE, C. (1951), The distribution of Fe^{2+} and Mg^{2+} in co-existing olivines and pyroxenes: *J. Geol.*, **59**, 193–210.

SEGNIT, E. R. (1953), Some data on synthetic aluminous and other pyroxenes: *Mineral. Mag.*, **30**, 218–226.

TILLEY, C. E. (1950), Some aspects of magmatic evolution: *Quart. J. geol. Soc. Lond.* (*Pres. Add.*), **106**, 37–61.

TOMKEIEFF, S. I. (1939), Zoned olivines and their petrogenetic significance: *Mineral. Mag.*, **25**, 229–251.

TSUBOI, S. (1932), On the course of crystallization of pyroxenes from rock magmas: *Jap. J. Geol. Geogr.*, **10**, 67–82.

TURNER, F. J., AND VERHOOGEN, J. (1951), Igneous and Metamorphic Petrology: McGraw-Hill Book Co. Inc., N.Y., 602 pp.

TYRRELL, G. W. (1948), A boring through the Lugar Sill: *Trans. geol. Soc. Glasg.*, **21**, 157–202.

VINCENT, E. A. (1950), The chemical composition and physical properties of the residual glass of the Kap Daussy tholeiite dyke, east Greenland: *Mineral. Mag.*, **29**, 46–62.

WAGER, L. R., AND DEER, W. A. (1939), Geological investigations in E. Greenland, Part III: The petrology of the Skaergaard intrusion, Kangerdluqssuaq, East Greenland: *Medd. Grønland*, **105**, 335 pp.

WALKER, F. (1930), The geology of the Shiant Isles, (Hebrides): *Quart. J. geol. Soc. Lond.*, **86**, 355–398.

WALKER, F. (1932), Differentiation in the sills of northern Trotternish, (Skye): *Trans. roy. Soc. Edinb.*, **57,** 241–257.

WALKER, F. (1934), The term 'crinanite': *Geol. Mag. Lond.*, **71,** 122–128.

WALKER, F. (1935), The late-Palaeozoic quartz—dolerites and tholeiites of Scotland: *Mineral. Mag.*, **24,** 131–159.

WALKER, F. (1936), The geology of the Isle of May: *Trans. geol. Soc. Edinb.*, **13,** 275–285.

WALKER, F. (1940), Differentiation of the Palisade diabase, New Jersey: *Bull. geol. Soc. Am.*, **51,** 1059–1106.

WALKER, F., AND POLDERVAART, A. (1941), The Hangnest dolerite sill, S.A.: *Geol. Mag. Lond.*, **78,** 429–450.

WALKER, F., AND POLDERVAART, A. (1941*a*), The Karroo dolerites of the Calvinia district: *Trans. geol. Soc. S. Afr.*, **44,** 127–148.

WALKER, F., AND POLDERVAART, A. (1949), Karroo dolerites of the Union of South Africa: *Bull. geol. Soc. Am.*, **60,** 591–706.

WASHINGTON, H. S. (1922), Deccan traps and other plateau basalts: *Bull. geol. Soc. Am.*, **33,** 765–803.

YAGI, K. (1953), Petrochemical studies on the alkali rocks of the Morotu district, Sakhalin: *Bull. geol. Soc. Am.*, **64,** 769–810.

Manuscript received Dec. 23, 1955.

EXPERIMENTAL DETERMINATION OF CALCITE-ARAGONITE EQUILIBRIUM RELATIONS AT ELEVATED TEMPERATURES AND PRESSURES*

GORDON J. F. MACDONALD, *Department of Geology and Geophysics, Massachusetts Institute of Technology, Cambridge, Mass.*

ABSTRACT

Calcite-aragonite equilibrium relations have been investigated using the "simple squeezer" high pressure apparatus of Griggs and Kennedy. Samples of natural calcite and synthetic aragonite were subjected to pressures up to 30,000 bars in the temperature range 200° C. to 600° C. The equilibrium curve as determined by this study is given by the equation $P=16T+2400$, where P is in bars and T is in degrees Centigrade. Calcite inverts to aragonite at pressures greater than those given by this equation; aragonite inverts to calcite at lower pressures. The equilibrium curve determined by direct experiment is at a pressure about 1500 bars lower than the curve obtained by Jamieson based on a thermochemical study. The reason for this apparent discrepancy is not known, though several possibilities are discussed. These results confirm the metastability of aragonite at 25° C. and one bar.

The effect of other components on the equilibrium is considered. Thermodynamic arguments show that small amounts of $PbCO_3$, $SrCO_3$, etc., in natural aragonites will not stabilize aragonite relative to calcite. The geologic conditions controlling the deposition of aragonite are as yet uncertain.

INTRODUCTION

Two phases of $CaCO_3$, calcite and aragonite, are found in a wide range of geologic environments. The conditions under which aragonite forms in nature are a puzzling problem in many respects. Aragonite (density 2.95) is denser than calcite (density 2.71) and should thus be a higher pressure form of $CaCO_3$ than calcite. Natural aragonite on heating converts to calcite, the conversion being very rapid at temperatures above 400° C. This would indicate that calcite is a higher temperature form than aragonite, a conclusion substantiated by heat capacity measurements which show that calcite has a higher entropy than aragonite (Anderson, 1934). In addition, thermochemical studies of Backstrom (1925), Roth and Chall (1928), Kobayashi (1951 *a*, *b*) and Jamieson (1953) demonstrate that pressures on the order of several thousand bars would be required for the equilibrium formation of argonite at 25° C. Since aragonite is forming today in nature at or near atmospheric pressure, it has been

* Publication No. 59, Institute of Geophysics, University of California, Los Angeles 24. A report on research carried out under the auspices of the Office of Naval Research. Reproduction in whole or in part is permitted for any purpose of the United States Government.

suggested that the presence of components other that $CaCO_3$, principally $SrCO_3$ and $PbCO_3$, "stabilize" natural aragonite relative to calcite.

The present study is concerned with the direct experimental determination of the calcite—aragonite equilibrium relations. Calcite has been converted to aragonite at high pressures; the reverse transition of aragonite to calcite has also been studied. The results establish the need of high pressures for the equilibrium formation of aragonite. On the basis of the experimental results on pure $CaCO_3$, theoretical calculations of the effect of other components on the stability of aragonite indicate that the percentages of these components found in natural aragonite are too small to account for an equilibrium formation of aragonite.

This investigation was further motivated by a desire to test the applicability of the "simple squeezer" to the study of solid-solid transitions. The "simple squeezer" is a high pressure apparatus designed by Professors Griggs and Kennedy and described by Griggs, Kennedy and Fyfe (1955). In the "simple squeezer" the pressure is not directly measured but is calculated from the force applied to the confining pistons. The sample between the pistons may not be under a hydrostatic pressure and the strain energy resulting from shearing the sample might conceivably affect the position of the equilibrium curve. The uncertainty in the pressure acting on the sample and the uncertainty of the effect of shear on the equilibrium relations made it desirable to compare the "simple squeezer" results on a solid-solid transition with results obtained by independent methods. The calcite-aragonite equilibrium was chosen for this purpose because Jamieson's (1953) careful thermochemical study provided an independent check on the results of the "simple squeezer," at least at relatively low pressures.

Experimental Details

Apparatus

The experimental work was carried out on the "simple squeezer." Since this high pressure system is being described in detail by Griggs and Kennedy elsewhere, the present description will outline only the major features of the apparatus. The confining pressure is produced by pressing two pistons together. The piston faces that come in contact have a diameter of $\frac{1}{4}$ inch. The pistons are pressed together by a commercial hydraulic jack, supported by a framework of plates and tie rods. The sample is placed between the piston faces and is separated from each face by a layer of platinum-10% rhodium foil. The foil is used to prevent adhesion of the sample to the piston faces. The pressure can then be raised by means of the jack, a gauge measuring the pressure on the hydraulic fluid in the jack. The sample is heated by an external furnace enclosing the

pistons and sample. The pistons used in the experiments described here were made of high-speed steel. These pistons were adequate for pressures up to 30,000 bars and temperatures up to 600° C.

The temperature was measured by placing a chromel-alumel thermocouple in a hole in one of the pistons. The tip of the thermocouple came within $\frac{1}{4}$ inch of the piston face. The temperature readings of this thermocouple were calibrated against the readings of a thermocouple placed between the piston faces in the normal position of the sample.

The pressure was determined from the readings on the jack pressure gauge and the area of the pistons. The areas of the piston faces were measured before and after a run. If the area changed significantly during the run, the run was discarded. Effects of friction within the jack were measured by a load cell calibration of the force acting on the pistons.

Materials used and identification

Natural calcite and artificial aragonite were used as starting materials. These were chosen since natural calcite containing only traces of components other than $CaCO_3$ is readily available, while analyzed natural aragonite was not available at the time of the investigation.

The calcite used was optical grade calcite from Chihuahua, Mexico. A spectrographic analysis of identical material has been published by Miller (1952) and this analysis shows that this calcite contains less than 0.1% $SrCO_3$, the major impurity, and less than 0.01% magnesium.

The aragonite was prepared using the method of Keyser and Dequeldre (1952). In this method 1N $CaCl_2$ is slowly mixed with 1N Na_2CO_3 at 100° C. The resulting precipitate is then thoroughly washed to remove the remaining NaCl. The resulting aragonite is extremely fine-grained. The *x*-ray pattern shows very much broadened lines. A fresh batch of aragonite was prepared for each day's runs, since it was observed that the artificial aragonite slowly converted to calcite on standing. The rate of conversion differed from one preparation to another, but in several batches of aragonite, calcite was detected in the *x*-ray pattern after the aragonite had aged for a period of a week.

The samples were identified by comparing the *x*-ray patterns obtained on a Norelco high-angle diffractometer with standard patterns of natural calcite and aragonite and artificial aragonite. Since the patterns are quite distinctive no difficulty was encountered in identifying relatively small amounts of either phase.

Procedure

A sample to be exposed to high pressures is placed on the platinum foil in the form of a dry powder with a small amount of water. The presence

of water does not appear to affect either the position of the equilibrium curve or the rate at which equilibrium is attained. An original thickness of powder of about .02 inch results in a wafer of about .005 inch thick in the center. The wafer tends to be disk-shaped, thicker in the middle and tapering to the edges.

The order of applying the pressure and temperature depends on whether aragonite or calcite is the initial material. If calcite is the original material, the temperature is first raised to the desired value and then the pressure is applied. In this way the sample is at a high pressure only at the desired temperature, and the high pressure form, in this case aragonite, can form only at the required temperature and not at some lower temperature. Similarly, if the original charge is aragonite, the pressure is first increased to the desired value and then the temperature is raised. The sample in this case is at a high temperature only at the pressure of the experiment, and the high temperature form, calcite, can form only at the given pressure. This careful cycling of the experiment is essential since the reaction proceeds rapidly. One hour is in general sufficient to convert calcite to argonite at 400° C. and 12,000 bars. Since raising the temperature to 400° C. takes about 15 minutes in the present apparatus, the sample has time to convert partially to aragonite at lower temperatures than 400° C. if the pressure were at or near 12,000 bars while the temperature is being raised.

After the sample is held at the required conditions of pressure and temperature for a suitable time, ranging from one to 17 hours, depending on the conditions of the experiment, the sample is quenched by releasing the pressure and placing the sample in water. In this way the pressure and temperature are reduced to room values in five seconds or less. This rapid quenching is essential in preserving any aragonite formed at high temperatures, since aragonite converts very rapidly to calcite at temperatures above 400–450° C.

Results

The useful results of the experiments are summarized in Tables 1 and 2. These tables list temperature and pressure conditions of the experiment, length of time at these pressure-temperature conditions and results from *x*-ray examination of resulting products. About ten early runs are not included in this table since these runs were not properly cycled and therefore the results are inconsistent with those listed.

Most of the runs are of about an hour's duration. A few runs at lower temperatures were held at temperature and pressure for 10 20 hours to test whether or not the results obtained represented equilibrium or whether they were due to differences in reaction rates at high and low tem-

TABLE 1. RESULTS OF SUBJECTING CALCITE TO HIGH PRESSURES AND TEMPERATURES

Temperature ° C.	*Pressure, kilobars*	*Time, hours*	*Results of x-ray examination of products*
250	6	10	calcite
300	6	1	calcite
360	6	1	calcite
250	8	10	weak aragonite and calcite
325	8	1	weak aragonite and calcite
340	8	1	aragonite and calcite
380	8	1	calcite
400	9	17	aragonite and calcite
430	9	1	calcite
430	10	1	aragonite and calcite
440	10	1	aragonite and calcite
450	10	1	aragonite and calcite
475	10	1	calcite
490	10	1.5	calcite
500	10	1	calcite
550	10	1	calcite
560	10	1	calcite
520	11	1	calcite
400	12	1	aragonite and calcite
450	12	1	aragonite and calcite
580	14	2.2	aragonite and calcite
300	15	1	aragonite and calcite
380	15	1	aragonite and calcite
400	15	1	aragonite and calcite
420	15	1	aragonite
440	15	1	aragonite and weak calcite
460	15	1	aragonite and weak calcite
470	15	1	aragonite and calcite
520	15	1	aragonite
450	20	1	aragonite and weak calcite
480	20	3.5	aragonite
490	30	.5	aragonite

perature. The longer runs gave results similar to those of the one-hour runs. This evidence, plus the fact that different starting materials give similar results, is taken as indicative that equilibrium was attained.

The points that were used to determine the equilibrium curve are shown in Fig. 1. Only those points near the curve are plotted. The remaining runs listed in Table 1 show that no other phases that can be quenched appear in the system for temperatures up to 600° C. and pressures up to 30,000 bars.

The uncertainties in the individual runs are estimated to be $\pm 10°$ and ± 500 bars. The uncertainty in the temperature is due to the difficulty

TABLE 2. RESULTS OF SUBJECTING ARAGONITE TO HIGH PRESSURES AND TEMPERATURES

Temperature, ° C.	*Pressure kilobars*	*Time, hours*	*Results of x-ray examination of products*
500	8	1	calcite
550	8	1	calcite
400	10	1	aragonite
450	10	1.5	aragonite
500	10	1	calcite
550	10	1	calcite
600	10	1	calcite
550	11	1	calcite
500	12	1	aragonite
600	12	1	aragonite
600	14	1	aragonite
500	15	1	aragonite

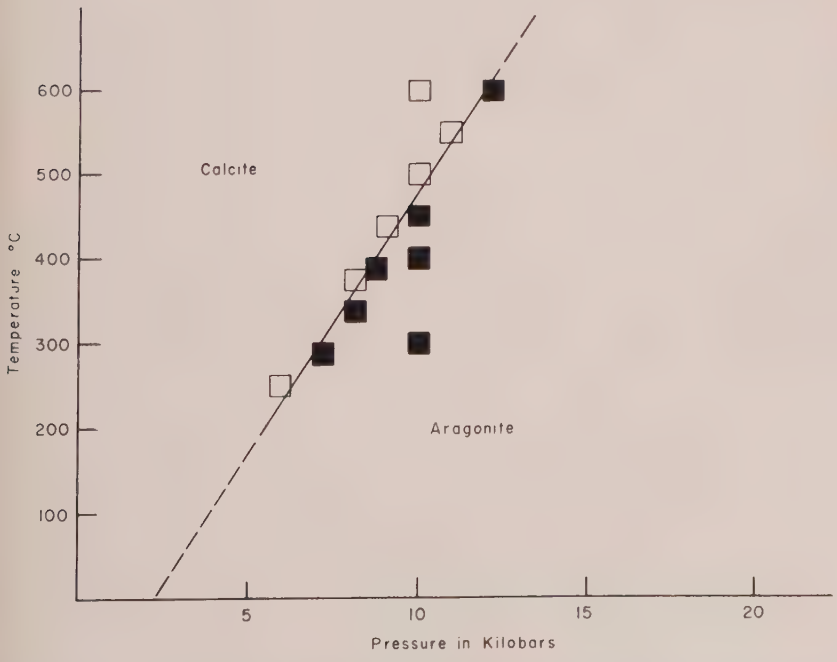


FIG. 1. Plot of runs used in determining calcite-aragonite equilibrium curve. Size of square is approximately proportional to the estimated error in the individual runs. One square may represent two or more runs.

in placing the thermocouple in the identical position relative to the sample. The pressure uncertainty is due to the scale of the pressure gauge on the jack and small fluctuations of the pressure during a run. This estimate of the uncertainty in pressure assumes that the pressure is uniform over the entire sample, an assumption that is certainly unjustified. A better estimate of the uncertainty in pressure is obtained by comparing results obtained by using two similar pieces of apparatus. Such a comparison indicates that the uncertainty in pressure may actually be as large as $\pm 10\%$ of the pressure.

The equation representing the equilibrium curve is $P=16(\pm 3)T+2400(\pm 1000)$ where T is in degrees Centigrade and P is in bars. The estimated uncertainties are derived by examining possible curves that could be drawn without contradicting the experimental determinations, taking into account the uncertainty in the individual points. The position of the curve is reasonably well determined at temperatures above 350° C., but the points at lower temperatures are not closely enough spaced to fix the boundary accurately. The boundary is assumed to be a straight line. The data are not of sufficient accuracy to show minor changes in slope of the equilibrium curve. In general the phase boundary should show curvature, the curvature depending on the differences of heat capacity, thermal expansion and compressibility of calcite and aragonite. Data available on these quantities show that the differences are indeed small.

Thermochemical Considerations

Comparison with earlier results

The thermodynamic properties of calcite and aragonite have been extensively studied. Of particular interest is the work of Jamieson (1953) on the stability relations of aragonite and calcite at temperatures between 25° and 80° C. Jamieson determined the electrical conductivity of aqueous solutions in equilibrium with calcite and the conductivity of solutions in equilibrium with aragonite as a function of temperature and pressure. At equilibrium the solubilities of each phase in water should be equal and therefore the conductivities of the solutions should be equal. This method assumes that the unstable phase does not convert to the stable phase during the course of the experiment, and furthermore, that water does not enter into either solid phase.

On the basis of conductivity measurements at four temperatures between 25° and 80° C. and at various pressures, Jamieson obtained data from which he calculated the equilibrium curve shown in Fig. 2. Using the slope and position of the curve plus the densities of the two minerals, Jamieson obtained the change in entropy for the transition and the heat

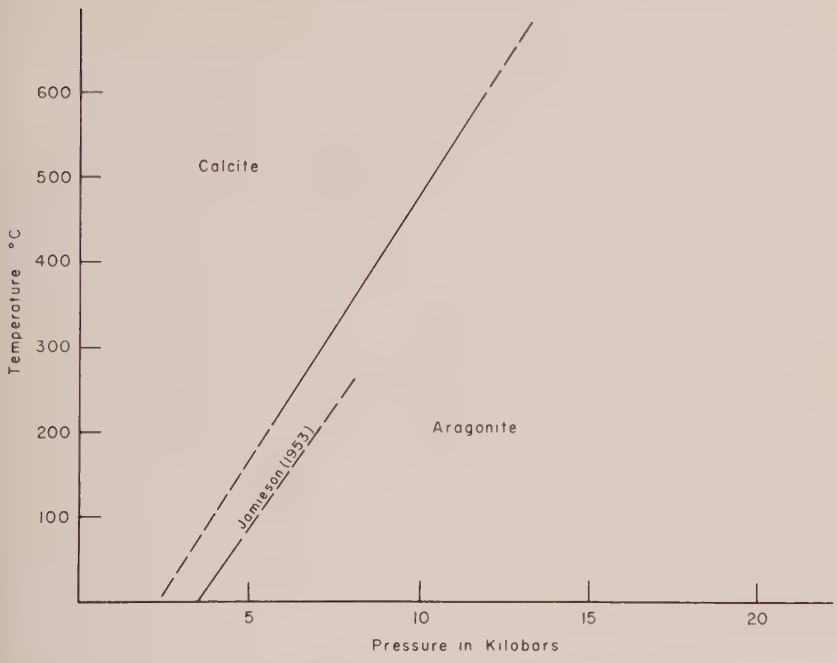


FIG. 2. Comparison of equilibrium curve obtained by Jamieson (1953) and the equilibrium curve obtained in the present study.

of transition at 25° C. and atmospheric pressure. These values are compared with the results of earlier workers in Table 3. Jamieson's value for the change in entropy is in agreeement with Anderson's values obtained by low temperature heat capacity measurements. Similarly, Jamieson's value for the heat of transition is in agreement with the heat of solution measurements of Roth and Chall. The equilibrium curve calculated using Anderson's and Roth and Chall's data would thus lie within a few hundred bars of the curve obtained by Jamieson.

TABLE 3. THERMOCHEMICAL QUANTITIES FOR THE TRANSITION ARAGONITE = CALCITE AT 25° AND ONE BAR

ΔS *cal./deg. mole*	ΔH *cal./mole*	ΔG *cal/mole*	*Investigator*
0.74	30	−180	Backstrom (1925)
	42		Roth and Chall (1928)
1.0 ±0.5			Anderson (1934)
1.1	62	−270	Jamieson (1953)
1.1 ±0.2	160±70	−160±70	MacDonald

The results of the present study are compared with those of Jamieson and earlier workers in Fig. 2 and Table 3. The slope of the equilibrium curve and consequently the entropy of the transition is in agreement with that of earlier workers. However, the equilibrium curve is at a pressure some 1500 bars lower than the curve obtained from Jamieson's data. There are several possible reasons for this discrepancy that should be examined. The mean pressure acting on the sample in the simple squeezer is calculated from the force acting on the piston, this force having been calibrated with a load cell. The actual pressure on the sample might be less than the calculated pressure if the opposing pistons came into contact. This would mean that the pressure would be over-estimated. The observed discrepancy could not be due to such errors, since the present curve lies at *lower* pressures than Jamieson's. The sample in the simple squeezer is under a non-uniform pressure. This shearing stress could affect the position of the equilibrium curve in the desired direction, provided that shear stabilizes aragonite relative to calcite. This possibility cannot at present be ruled out. Finally there is the possibility that Jamieson did not attain equilibrium in his experiments or that he was dealing with partially converted materials in certain of his runs. The agreement of Jamieson's results with those of earlier workers suggests that Jamieson was indeed dealing with equilibrium, but this earlier work should not be taken as decisive. The calculated position of the equilibrium curve depends on the heat of transition. This heat was determined by Roth and Chall by measurement of the heats of solution of the two minerals. Measurements of heats of solution of materials evolving a gas phase are notably difficult, and small errors in the heats of solution would lead to very large errors in the heat of transition.

The above discussion emphasizes the desirability of investigating the aragonite-calcite equilibrium directly in an apparatus in which the pressure is better known than in the simple squeezer, and where the sample is subjected to a uniform hydrostatic pressure. Only such measurements can clear up the discrepancy between the results obtained on the simple squeezer and those obtained from thermochemical data.

Effect of components other than $CaCO_3$ on calcite-aragonite equilibrium

The above results show that aragonite with a composition of $CaCO_3$ is unstable relative to calcite having the same composition at 25° C. and one bar. A measure of this instability at these conditions is the difference in Gibbs free energy of the two phases. The values listed in Table 3 show that at 25° C. and one bar aragonite has a free energy between 90 and 270 calories greater than calcite, depending on the method used to evaluate the free energy difference and taking into account the uncer-

tainties in the data of the present investigation. For the present discussion we will use a free energy difference of 200 ± 100 calories.

Natural aragonites that have formed at conditions near 25° C. and one bar have in general a more complicated composition than $CaCO_3$. It is interesting then to investigate the effects of components other than $CaCO_3$ on the relative stabilities of calcite and aragonite. A necessary condition for equilibrium between the two phases is that the chemical potential of $CaCO_3$ in calcite equal the chemical potential of $CaCO_3$ in aragonite. In general the chemical potentials will be a function of the composition of the phases as well as of temperature and pressure. The condition for equilibrium can then be written

$$\mu^A(T, P, x_1, \cdots, x_n) = \mu^C(T, P, x_1, \cdots, x_n)$$

where μ^A is the chemical potential of $CaCO_3$ in aragonite, and μ^C is the chemical potential of $CaCO_3$ in calcite. The chemical potentials can be written in the form

$$\mu = \mu^0(TP) + RT \ln x\gamma$$

where μ^0 is the chemical potential of the pure component $CaCO_3$ at a given temperature and pressure, x is the mole fraction of $CaCO_3$ in the solution and γ is the activity coefficient of $CaCO_3$ in the solution. The condition for equilibrium is then given by

$$\mu^{0A} + RT \ln x^A\gamma^A = \mu^{0C} + RT \ln x^C\gamma^C$$

which can be written as

$$\ln \frac{x^A\gamma^A}{x^C\gamma^C} = \frac{\mu^{0C} - \mu^{0A}}{RT}.$$

The difference in chemical potentials of the pure components, $\mu^{\circ C} - \mu^{\circ A}$, is just the difference in molar Gibbs free energy. At 25° C. and one bar this difference is -200 ± 100 calories. Substituting this value into the above relation we obtain

$$\frac{x^A\gamma^A}{x^C\gamma^C} = 0.71 \pm 0.15.$$

In order to interpret this result we need to assume something about the activity coefficients γ^A and γ^C. If we assume that $CaCO_3$ forms an ideal solution with other components such as $BaCO_3$, $PbCO_3$, $ZnCO_3$, etc. in both calcite and aragonite, the condition for equilibrium between calcite and aragonite at 25° C. and one bar is given by

$$x^A = 0.71(\pm 0.15)x^C.$$

The mole fraction of $CaCO_3$ in aragonite must be about 0.7 times the mole fraction of $CaCO_3$ in calcite for aragonite to be in equilibrium with calcite. This means that at least 30 mole per cent of components other than

$CaCO_3$ in aragonite are needed to "stabilize" aragonite relative to calcite. Natural aragonite contains at most 8 9 mole per cent of components such as $PbCO_3$, $SrCO_3$, $ZnCO_3$ (Palache, Berman and Frondel, 1951) and most natural aragonites contain much less, so that even considering the errors in the data, it appears very unlikely that aragonite is stabilized by forming solid solutions, provided such solutions are ideal. If the solutions are non-ideal then the activity coefficients are no longer equal to one. A value greater than one for γ^A would mean that even higher concentrations of components other than $CaCO_3$ would be needed to stabilize aragonite. In general an activity coefficient greater than one is associated with solutions having a positive heat of mixing. Solutions of the sort considered here generally have a positive heat of mixing (MacDonald 1954). A negative heat of mixing would favor the stabilization of aragonite by other components. This possibility is considered unlikely but cannot be ruled out except by actual measurements of the heats of mixing.

On the basis of the above thermodynamic argument it is concluded that the amounts of lead, strontium, zinc, etc., found in natural aragonites are not sufficient to stabilize aragonite relative to calcite.

Geologic Problems

The direct experimental study of the calcite-aragonite equilibrium relations confirms Backstrom's conclusion that aragonite near the surface of the earth is unstable relative to calcite. Theoretical considerations indicate that components such as $PbCO_3$, $SrCO_3$, etc., are ineffectual in stabilizing aragonite. This then leaves the major problem of determining what geologic conditions control whether aragonite or calcite is precipitated. One fascinating problem is why certain organisms precipitate aragonite and others calcite to form their shells or skeletons. Of particular interest is the role played by the organic membrane separating the organism from its environment. This membrane undoubtedly sets up an osmotic equilibrium which under certain conditions might lead to the precipitation of aragonite as a stable phase. A great deal of work on the mineralogy and chemistry of shells and conditions for growth of living organisms is needed before a thermodynamic attack on the problem would be profitable.

A further problem of interest is the effect, if any, of the calcite-aragonite transition on the mechanical properties of limestone. There is a definite possibility that plastic flow in limestone might be aided by such a polymorphic transition (Robertson, 1955). Griggs, Turner, Borg and Sosoka (1951) report studies on the deformation of Yule marble at 10,000 bars and 150° C. This is well within the field of stability of aragonite, but at this temperature the reaction would be relatively sluggish.

Similar experiments at 10,000 bars and 300° C. might be expected to show up any effects of the polymorphic transition on the mechanical properties of the marble.

The equilibrium curve shown in Fig. 2 could be interpreted as fixing the maximum pressure to which pure calcite marbles could have been subjected in regional metamorphism. Greater pressures than those given by the equilibrium curve would have resulted in aragonite. However, any aragonite that might have formed could have inverted to calcite at some later time in the history of the marble, erasing in such a process evidence of the original aragonite. The absence of aragonite in metamorphic rocks suggests that these may have formed at pressures lower than those of the equilibrium curve, but certainly nothing more definite can be said.

Acknowledgments

The experimental studies were carried out during the summer of 1955 at the Institute of Geophysics, University of California. The work was supported by the Office of Naval Research. Professor George C. Kennedy introduced me to the techniques of high pressure research and provided all the facilities requisite for successful research. Stimulating discussions of the calcite-aragonite problem with Professor Kennedy and Professor David T. Griggs contributed materially to my understanding of the problem. Special thanks are due to Mr. Don Lyon for his assistance in carrying out the experiments. Particular thanks are due Professor James B. Thompson, who in reviewing the manuscript corrected a major error in the author's analysis of the effect of solid solution on the equilibrium. Professor Kennedy, Eugene C. Robertson and Sydney Clark also reviewed the manuscript and offered helpful suggestions.

References

Anderson, C. T. (1934), The heat capacities at low temperatures of alkaline earth carbonates: *J. Am. Chem. Soc.*, **56,** 340–342.

Backstrom, H. L. (1925), The thermodynamic properties of calcite and aragonite: *J. Am. Chem. Soc.*, **47,** 2432–2472.

Griggs, D. T., Turner, F. J., Borg, I., and Sosoka, J. (1951), Deformation of Yule marble, Part IV: *Geol. Soc. Am. Bull.*, **62,** 1385–1406.

Griggs, D. T., Kennedy, G. C., and Fyfe, W. S. (1955), A simple apparatus for high pressure and temperature: *Am. Geophys. Union Program*, 36th Annual Meeting, 35.

Jamieson, J. C. (1953), Phase equilibrium in the system calcite-aragonite: *J. Chem. Phys.*, **21,** 1385–1390.

deKeyser, W. L., and Dequeldre, L. (1950), Contribution à l'étude de la formation de la calcite, aragonite et vaterite: *Chim. Soc. Belg. Bull.*, **59,** 40–71.

Kobayashi, K. (1951*a*) Heat capacities of inorganic substances at high temperatures, III. Heat capacity of synthetic calcite: *Sci. Rept. ser. I, Tôhoku Univ.*, **35,** 103–110.

Kobayashi, K. (1951*b*) IV. Heat capacity of synthetic aragonite: *Sci. Rept. ser. I, Tôhoku Univ.*, **35,** 111.

MacDonald, G. J. F. (1954), A critical review of geologically important thermochemical data: Ph.D. thesis, Harvard University.

Miller, J. P. (1952), A portion of the system calcium carbonate-carbon dioxide-water, with geological implications: *Am. J. Sci.*, **250,** 161–203.

Palache, C., Berman, H., and Frondel, C. (1952), Dana's System of Mineralogy, volume II: J. Wiley, New York.

Robertson, E. C. (1955), Experimental study of the strength of rocks: *Geol. Soc. Am. Bull.*, **66,** 1275–1314.

Roth, W. A., and Chall, P. (1928), Die thermische Verfolgung einiger metallurgisch wichtiger Reaktionen in einem grosseren Temperatur interval mit Hilfe von zwein neuen calorimeter typen: *Ztschr. Electrochem.*, **34,** 185–199.

Manuscript received Jan. 10, 1956.

APPLICATION OF THE RULE OF GLADSTONE AND DALE TO MINERALS*

HOWARD W. JAFFE, *U. S. Geological Survey, Beltsville, Md.*

ABSTRACT

The relation, $(n-1)/d=K$, the rule of Gladstone and Dale, holds very well for crystalline substances based upon data for 121 minerals selected from modern literature. The specific refractive energy values of the constituents of minerals, determined by Larsen, need very little revision. New values are given for Ce_2O_3, La_2O_3, Nd_2O_3, Pr_2O_3, Sm_2O_3, Sc_2O_3, MoO_3, Y_2O_3, and V_2O_5 in minerals.

To emphasize the relation between index of refraction, density, and chemical composition, Larsen (1921) suggested that the rule of Gladstone and Dale be applied to crystalline substances. Gladstone and Dale (1864) showed that $(n\text{-}1)/d=K$, and $K=(k_1)(p_1/100)+(k_2)(p_2/100)$ +etc., where K is the specific refractive energy of a liquid, k_1, k_2 are the specific refractive energies of the components of the liquid, and p_1, p_2 are the weight percentages of the components. A table of specific refractive energies (k) of the constituents of minerals was published by Larsen (1921 and 1934). Larsen's specific refractive energies are average values calculated from the most reliable mineralogical data available more than 30 years ago. Recently, Prof. Larsen suggested that the author publish a revised set of k values based upon more recent optical, chemical, and density data. With few exceptions, it was found that Larsen's data did not need revision. The few suggested changes are as given at the top of the next page.

When the rule, $(n-1)/d=K$, is applied to minerals, the arithmetical mean index of refraction, $(\alpha+\beta+\gamma)/3$ or $(2\omega+\epsilon)/3$, is used and the relations are stated to hold approximately (Larsen and Berman, 1934).

Mineralogists have made relatively little use of the rule of Gladstone and Dale in the belief that the relations would not hold sufficiently well because of major differences in the manner of combination of the constituents of minerals. Where the optical, chemical, and density data are accurate, the Gladstone and Dale relations hold very well for most minerals, with only slight modifications due to the manner of combination of the constituents. Mineralogists would do well to reexamine their data before deciding that a mineral is an exception to the rule $[(n-1)/d=K]$. This paper was written on the advice of Prof. Larsen and several of the author's colleagues who did not expect that the rule would hold so well for most minerals.

All of the data are presented as a comparison of the calculated mean index of refraction, $dk+1$, with the arithmetical mean index of refraction, $(\alpha+\beta+\gamma)/3$ or $(2\omega+\epsilon)/3$, determined experimentally.

* Publication authorized by the Director, U. S. Geological Survey.

	Larsen and Berman (1934)	Jaffe (1955)
k Ce_2O_3	.160	.149 (*a*)
k La_2O_3	.149	.142 (*a*)
k Nd_2O_3	—	.138 (*a*)
k Pr_2O_3	—	.140 (*a*)
k Sm_2O_3	—	.141 (*a*)
k $(Ce, La, Nd, Pr, Sm)_2O_3$	—	.144 (*b*)
k Y_2O_3	.144	.170 (*c*)
k Fe_2O_3	.308	.290 (*d*)
		.310 (*e*)
		.404 (*f*)
k V_2O_5	.430	.340 (*g*)
k Sc_2O_3	—	.248 (*h*)
k MoO_3	—	.234 (*i*)

(*a*) derived from artificial inorganic compounds and minerals.
(*b*) derived from numerous minerals.
(*c*) derived from $Y_2(SO_4)_3 \cdot 8H_2O$, xenotime and yttrogarnet.
(*d*) derived from silicates.
(*e*) derived from hydrated ferric sulfates.
(*f*) derived from the oxide.
(*g*) derived from rossite and metatyuyamunite.
(*h*) derived from thortveitite.
(*i*) derived from powellite.

In Table 1, the calculated and experimental mean indices of refraction are compared for minerals representative of different silicate structure types.

Regardless of the different linkages of SiO_4 tetrahedra, the silicates in Table 1 show excellent agreement between the calculated and experi-

TABLE 1. COMPARISON OF CALCULATED AND EXPERIMENTAL MEAN INDICES OF REFRACTION FOR MINERALS OF DIFFERENT SILICATE-STRUCTURE TYPES

Mineral	O:Si Ratio	$(\alpha+\beta+\gamma)/3$ or $(2\omega+\epsilon)/3$	$dK+1$	Deviation
Forsterite Mg_2SiO_4	4:1	1.652	1.649	−0.003
Pyrope $Mg_3Al_2(SiO_4)_3$	4:1	1.705	1.705	0.000
Akermanite $Ca_2MgSi_2O_7$	7:2	1.634	1.628	−0.006
Benitoite $BaTiSi_3O_9$	3:1	1.773	1.779	+0.006
Enstatite $MgSiO_3$	3:1	1.654	1.649	−0.005
Talc $Mg_3(OH)_2Si_4O_{10}$	5:2	1.572	1.570	−0.002
Quartz SiO_2	2:1	1.547	1.551	+0.004

mental mean indices of refraction with a maximum deviation of only 0.006. The relations can be shown to hold very well for minerals of extremely complex chemical compositions. This may be demonstrated by a calculation of the mean index of refraction ($dk+1$) of schroeckingerite, $Ca_3Na[UO_2(CO_3)_3(SO_4)F]\cdot 10H_2O$.

Oxide	$p/100$		k		$(k)(p/100)$	
CaO	18.93	×	.225	=	.04259	
Na_2O	3.49	×	.181	=	.00632	
UO_3	32.19	×	.134	=	.04313	
CO_2	14.86	×	.217	=	.03225	
SO_3	9.01	×	.177	=	.01595	
H_2O	20.28	×	.340	=	.06895	
F	2.14	×	.043	=	.00092	
	100.90				.21011	
−O=F	.90	×	.203	=	.00183	
	100.00		K	=	.20828	$\alpha=1.489$
			d	=	2.51	$\beta=1.542$
			dK	=	.52278	$\gamma=1.542$

Mean index, $dk+1=1.523$ (n calculated).
Mean index, $(\alpha+\beta+\gamma)/3=1.524$ (n experimental).

Agreement between the calculated and experimental mean index of refraction is not always as good as $\pm 0.00X$. Some of the calculated and measured values for various minerals show much greater deviations. In some minerals it is thought that the chemical composition or density values are slightly in error inasmuch as the equation $(n-1)/d=K$ is very sensitive to small differences in density.

For example, schroeckingerite with $d=2.51$ and $K=.20828$ gives $dK+1=1.523$ and $(\alpha+\beta+\gamma)/3=1.524$. The calculated mean index of refraction would vary as follows with errors in density:

if $d=2.41$, $dK+1=1.502$ (-0.022)
if $d=2.61$, $dK+1=1.544$ $(+0.020)$.

Similarly small errors in chemical analysis may cause differences of as much as ± 0.02 in the calculated and measured mean indices of refraction. On occasion, however, small chemical errors may balance each other so that they may not be apparent if the constituents involved have similar specific refractive energies. For example, $k_{N_2O}=.181$ and $k_{K_2O}=.189$ and small errors in their determination may be hidden.

Differences in the manner of combination may be expected to modify the relations (Barth, 1930) but the effects are not as pronounced as might

be expected. For example, the relations in calcite and aragonite are illustrative, as follows:

$$\text{calcite } dK+1=1.602\ (2\omega+\epsilon)/3=1.601\ (+0.001)$$
$$\text{aragonite } dK+1=1.652\ (\alpha+\beta+\gamma)/3=1.632\ (+0.020).$$

Assuming that the density and optical data are correct for aragonite, the deviation of 0.020 for the calculated mean index of aragonite must be a function of the different manner of combination of the constituents. In general, it can be expected that, regardless of the manner of combination of the mineral constituents, a deviation of not more than ± 0.020 in the mean index of refraction calculation can be obtained for most minerals from accurate chemical and density data. In most minerals studied by the author the calculated and experimental mean indices of refraction agree within ± 0.009 where the data are known to be reliable. If the relation $[(n-1)/d=K]$ holds so well for pure minerals, what would be the effect of isomorphism in a complex silicate series? There are too few complex mineral groups for which density and index of refraction

Table 2. Comparison of the Calculated and Experimental Mean Indices of Refraction for 7 Members of the Anthophyllite Series

	1	8	9	14	17	29	30
SiO_2	42.90	45.47	46.06	48.38	50.32	57.16	57.05
TiO_2	0.49	0.44	0.53	0.11	0.43	None	None
Al_2O_3	17.82	15.86	14.95	13.23	8.05	1.40	1.94
Fe_2O_3	1.03	2.94	0.62	1.28	2.18	None	None
FeO	18.36	15.34	17.45	14.56	18.34	8.73	11.10
MnO	0.14	0.07	0.04	None	None	0.09	0.11
MgO	15.58	17.62	18.30	20.51	17.55	28.88	26.78
CaO	None	0.14	0.07	0.04	0.74	1.48	0.64
Na_2O	1.52	0.28	0.47	0.11	0.70	0.66	0.27
K_2O	0.03	None	None	None	None	None	0.06
F	0.31	None	None	None	None	None	None
H_2O+	1.95	1.84	1.51	1.48	1.69	1.60	2.05
	100.13						
$-O=F$	0.13						
	100.00	100.00	100.00	100.00	100.00	100.00	100.00
Density	3.277	3.261	3.245	3.259	3.279	3.106	3.102
$(\alpha+\beta+\gamma)/3$	1.667	1.663	1.661	1.655	1.660	1.630	1.628
$dK+1$	1.666	1.672	1.660	1.667	1.670	1.637	1.633
Difference	−0.001	+0.009	−0.001	+0.012	+0.010	+0.007	+0.005

Chemical analyses by F. A. Gonyer (Rabbitt, 1948) after recalculation to 100.00 per cent.

Density and optical data determined by J. C. Rabbitt (Rabbitt, 1948).

measurements were made on analyzed material. Usually the density or indices of refraction are given as a range covering several chemical analyses. One good example of complete data is given by Rabbitt (1948) for a series of seven anthophyllites from Montana. Calculation of the mean index of refraction ($dK+1$) for each anthophyllite is compared with the experimental mean index of refraction, $[(\alpha+\beta+\gamma)/3]$ in Table 2. In calculating the mean index of refraction, all of the minor constituents were included and the analyses were recalculated to 100 per cent. Inasmuch as the analytical totals range from 99.77 to 100.23, the effects of the recalculations to 100.00 are negligible. The recalculation must be made because the relation, $[(n-1)/d=K]$, obviously requires that the specific refractive energy of the compound, K, be based upon 100 per cent. The agreement between the calculated and experimental mean n for each anthophyllite is excellent although the analyses show major variations in silica, alumina, and iron. Thus, if the chemical, optical, and density data are reliable, large-scale isomorphism will not seriously affect the relation $[(n-1)/d=K]$.

In Table 3, the calculated and experimental mean indices of refraction are compared for 121 minerals of widely different chemical composition for which the data seemed most reliable. Several minerals were rejected on the basis of (1) large differences in the calculated and measured density, (2) large amounts of material designated "remainder" in chemical analyses, and (3) poor analytical summations. For example, the measured density of cordylite and that calculated from x-ray data are given as 4.31 and 5.61, respectively (Palache, Berman, and Frondel, 1951). Obviously one of the values is in error for material of a given composition. Application of the rule of Gladstone and Dale suggests the density of cordylite should be near 4.76, assuming that the indices of refraction and chemical composition are correct. Table 3 includes the chemical composition, density, and indices of refraction for each of 121 minerals from which the n values ($dK+1$) were calculated. All of the analyses in Table 3 were recalculated to 100.00 per cent as required by the law of Gladstone and Dale.

Differences of the calculated from the experimental mean indices of refraction are less than ± 0.020 for 92.6 per cent of the entries (Table 3) of which 64.5 per cent are less than ± 0.009. The differences of $dK+1$ from $(\alpha+\beta+\gamma)/3$ or $(2\omega+\epsilon)/3$ are graphically represented in Fig. 1. Some of the 7.4 per cent (9 in 121) of the entries for which $dk+1$ deviates by greater than ± 0.020 obviously result from poor data; others apparently reflect failure of the rule, $[(n-1)/d=K]$, to hold because of marked differences in polarizabilities of the constituents. For example, the data for 16 amphiboles in Table 3 show good agreement between the

(*Continued on page 775*)

TABLE 3. COMPARISON OF EXPERIMENTAL AND CALCULATED MEAN INDICES OF REFRACTION, $[(\alpha+\beta+\omega)]$ OR $[(2\omega+\epsilon)/3]$ WITH $dk+1$ FOR 121 MINERALS

Mineral data	$(\alpha+\beta+\gamma)/3$ or $(2\omega+\epsilon)/3$	$dK+1$	Deviation
Oxides			
1. Periclase, MgO			
MgO 94.03, FeO 5.97			
d 5.72, n 1.745	1.745	1.732	−0.013
2. Bromellite, BeO			
BeO 97.89, CaO 1.03, BaO 0.55, MgO 0.07, Sb_2O_3 0.29, Al_2O_3 0.17			
d 3.017, ω 1.719, ϵ 1.733	1.724	1.715	−0.009
3. Gahnite, $ZnAl_2O_4$			
FeO 1.70, MnO 0.50, ZnO 41.31, Al_2O_3 53.28, Fe_2O_3 2. 51, SiO_2 0.70			
d 4.57, n 1.818	1.818	1.816	−0.002
4. Zincite, ZnO			
ZnO 99.64, MnO 0.27, FeO 0.01, SiO_2 0.08			
d 5.66, ω 2.013, ϵ 2.029	2.018	2.036	+0.018
5. Sassolite, $B(OH)_3$			
B_2O_3 56.39, H_2O 43.61			
d 1.48, α 1.340, β 1.456, γ 1.459	1.418	1.403	−0.015
6. Corundum, Al_2O_3			
Al_2O_3 99.09, Fe_2O_3 0.91			
d 4.0, ω 1.769, ϵ 1.760	1.766	1.775	+0.009
7. Baddelyite, ZrO_2			
ZrO_2 98.93, Fe_2O_3 0.82, CaO 0.06, SiO_2 0.19			
d 5.72, α 2.13, β 2.19, γ 2.20	2.173	2.154	−0.019
8. Quartz, SiO_2			
SiO_2 100.00			
d 2.66, ω 1.544, ϵ 1.553	1.547	1.551	+0.004
9. Tridymite, SiO_2			
SiO_2 100.00			
d 2.30, α 1.469, β 1.470, γ 1.473	1.471	1.476	+0.005
10. Cristobalite, SiO_2			
SiO_2 100.00			
d 2.3, n 1.486	1.486	1.476	−0.010
11. Rutile, TiO_2			
TiO_2 100.00			
d 4.23, ω 2.612, ϵ 2.899	2.708	2.691	+0.017
12. Anatase, TiO_2			
TiO_2 100.00			
d 3.90, ω 2.561, ϵ 2.488	2.537	2.548	+0.011
13. Brookite, TiO_2			
TiO_2 100.00			
d 4.14, α 2.583, β 2.584, γ 2.700	2.622	2.643	+0.021

TABLE 3—(*continued*)

Mineral data	$(\alpha+\beta+\gamma)/3$ or $(2\omega+\epsilon)/3$	$dK+1$	Deviation
14. Portlandite, $Ca(OH)_2$			
CaO 75.64, H_2O 24.31			
d 2.230, ω 1.574, ϵ 1.547	1.565	1.564	−0.001
Carbonates			
15. Calcite, $CaCO_3$			
CaO 56.03, CO_2 43.97			
d 2.710, ω 1.658, ϵ 1.486	1.601	1.602	+0.001
16. Aragonite, $CaCO_3$			
CaO 56.03, CO_2 43.97			
d 2.947, α 1.531, β 1.681, γ 1.685	1.632	1.652	+0.020
17. Magnesite, $MgCO_3$			
MgO 47.81, CO_2 52.19			
d 3.00, ω 1.700, ϵ 1.509	1.636	1.627	−0.009
18. Siderite, $FeCO_3$			
FeO 62.01, CO_2 37.99			
d 3.96, ω 1.875, ϵ 1.633	1.794	1.786	−0.008
19. Rhodochrosite, $MnCO_3$			
MnO 61.71, CO_2 38.29			
d 3.70, ω 1.816, ϵ 1.597	1.744	1.743	−0.001
20. Smithsonite, $ZnCO_3$			
ZnO 64.90, CO_2 35.10			
d 4.43, ω 1.848, ϵ 1.621	1.772	1.777	+0.005
21. Strontianite, $SrCO_3$			
SrO 62.55, CaO 6.10, CO_2 31.35			
d 3.628, α 1.520, β 1.667, γ 1.669	1.618	1.621	+0.003
22. Alstonite, $CaBa(CO_3)_2$			
CaO 17.64, BaO 48.64, SrO 4.25, CO_2 29.47			
d 3.707, α 1.526, β 1.671, γ 1.672	1.623	1.636	+0.013
23. Barytocalcite, $CaBa(CO_3)_2$			
BaO 51.56, CaO 18.85, CO_2 29.59			
d 3.66, α 1.525, β 1.684, γ 1.696	1.632	1.630	−0.002
24. Shortite, $Na_2Ca_2(CO_3)_2$			
Na_2O 20.25, CaO 36.63, CO_2 43.12			
d 2.605, α 1.531, β 1.555, γ 1.570	1.552	1.554	+0.002
25. Thermonatrite, $Na_2CO_3 \cdot H_2O$			
Na_2O 50.03, CO_2 35.45, H_2O 14.52			
d 2.255, α 1.420, β 1.509, γ 1.525	1.485	1.489	+0.004
26. Nesquehonite, $MgCO_3 \cdot 3H_2O$			
MgO 29.11, CO_2 31.65, H_2O 39.24			
d 1.842, α 1.417, β 1.503, γ 1.527	1.482	1.480	−0.002
27. Lansfordite, $MgCO_3 \cdot 5H_2O$			
MgO 23.25, CO_2 25.06, H_2O 51.69			
d 1.694, α 1.456, β 1.469, γ 1.508	1.478	1.469	−0.009

TABLE 3—(*continued*)

Mineral data	$(\alpha+\beta+\gamma)/3$ or $(2\omega+\epsilon)/3$	$dK+1$	Deviation
28. Natron, $Na_2CO_3 \cdot 10H_2O$			
Na_2O 21.66, CO_2 15.38, H_2O 62.96			
d 1.478, α 1.405, β 1.425, γ 1.440	1.423	1.424	+0.001
29. Pirssonite, $Na_2Ca(CO_3)_2 \cdot 2H_2O$			
Na_2O 25.73, CaO 23.41, CO_2 36.11, H_2O 14.75			
d 2.352, α 1.504, β 1.509, γ 1.575	1.529	1.536	+0.007
30. Gaylussite, $Na_2Ca(CO_3)_2 \cdot 5H_2O$			
Na_2O 20.42, CaO 19.03, CO_2 30.05, H_2O 30.50			
d 1.991, α 1.443, β 1.516, γ 1.523	1.494	1.495	+0.001
31. Lanthanite, $(Ce, La)_2(CO_3)_3 \cdot 8H_2O$			
$(Ce, La)_2O_3$ 55.03, CO_2 21.95, H_2O 24.21			
d 2.84, α 1.520, β 1.587, γ 1.613	1.573	1.587	+0.014
32. Artinite, $Mg_2(CO_3)(OH)_2 \cdot 3H_2O$			
MgO 40.99, CO_2 22.37, H_2O 36.64			
d 2.02, α 1.488, β 1.534, γ 1.556	1.526	1.515	−0.011
33. Hydrocerussite, $Pb_3(CO_3)_2(OH)_2$			
PbO 86.33, CO_2 11.35, H_2O 2.32			
d 6.94, ω 2.09, ϵ 1.94	2.040	2.046	+0.006
34. Dawsonite, $NaAl(CO_3)(OH)_2$			
Na_2O 21.81, Al_2O_3 36.01, CO_2 30.51, H_2O 11.61			
d 2.44, α 1.466, β 1.542, γ 1.596	1.535	1.524	−0.011
35. Bastnaesite, $(Ce, La)(CO_3)F$			
Ce_2O_3 38.23, La_2O_3 36.79, CO_2 20.30, F 7.94, H_2O 0.08			
d 5.12, ω 1.717, ϵ 1.818	1.751	1.763	+0.012
36. Ancylite, $(Ce, La)_4(Sr, Ca)_3(CO_3)_7(OH)_4 \cdot 3H_2O$			
CaO 1.54, SrO 21.25, FeO 0.35, Ce_2O_3 22.45, La_2O_3 24.29, CO_2 23.53, H_2O 6.59			
d 3.95, α 1.625, β 1.700, γ 1.735	1.687	1.692	+0.005
37. Tychite, $Na_6Mg_2(SO_4)(CO_3)_4$			
Na_2O 35.58, MgO 15.42, SO_3 15.32, CO_2 33.68			
d 2.588, $n=1.510$	1.510	1.506	−0.004
38. Roentgenite, $Ca_2(Ce, La)_3(CO_3)_5F_3$			
CaO 13.11, $(Ce, La)_2O_3$ 57.32, CO_2 25.71, F 6.66			
d 4.19 (calc.), ω 1.662, ϵ 1.756	1.693	1.694	+0.001
39. Parisite, $(Ce, La)_2Ca(CO_3)_3F_2$			
CaO 10.10, BaO 0.33, $(Ce, La)_2O_3$ 61.57, CO_2 23.95, F 7.00			
d 4.32, ω 1.667, ϵ 1.760	1.698	1.695	−0.003
40. Sahamalite, $(Ce, La)_2(Mg, Fe)(CO_3)_4$			
$(Ce, La)_2O_3$ 59.8, MgO 6.2, FeO 2.0, CO_2 32.0			
d 4.30, α 1.679, β 1.776, γ 1.807	1.754	1.738	−0.016
41. Andersonite, $Na_2Ca(UO_2)(CO_3)_3 \cdot 6H_2O$			
MgO 0.5, CaO 8.1, Na_2O 9.6, UO_3 44.9, CO_2 20.3, H_2O 16.0			
d 2.8, ω 1.520, ϵ 1.540	1.527	1.552	+0.025

TABLE 3—(*continued*)

Mineral data	$(\alpha+\beta+\gamma)/3$ or $(2\omega+\epsilon)/3$	$dK+1$	Deviation
42. Bayleyite, $Mg_2(UO_2)(CO_3)_3 \cdot 18H_2O$			
MgO 9.76, Na_2O 0.21, K_2O 0.10, UO_3 35.29, CO_2 16.72, H_2O 37.92			
d 2.05, α 1.455, β 1.490, γ 1.500	1.482	1.477	−0.005
43. Swartzite, $CaMg(UO_2)(CO_3)_3 \cdot 12H_2O$			
CaO 7.32, MgO 5.47, Na_2O 0.26, K_2O 0.49, UO_3 38.85, CO_2 17.92, H_2O 29.69			
d 2.3, α 1.465, β 1.51, γ 1.540	1.505	1.508	+0.003
44. Leadhillite, $Pb_4(SO_4)(CO_3)_2(OH)_2$			
PbO 82.78, SO_3 7.36, CO_2 8.17, H_2O 1.690			
d 6.55, α 1.87, β 2.00, γ 2.01	1.960	1.982	+0.022
Nitrates			
45. Darapskite, $Na_3(NO_3)(SO_4) \cdot H_2O$			
Na_2O 38.00, N_2O_5 22.10, SO_3 32.65, H_2O 7.25			
d 2.20, α 1.391, β 1.481, γ 1.486	1.453	1.449	−0.004
46. Gerhardtite, $Cu_2(NO_3)(OH)_3$			
CuO 66.12, N_2O_5 22.67, H_2O 11.21			
d 3.43, α 1.703, β 1.713, γ 1.722	1.713	1.750	+0.037
47. Nitrobarite, $Ba(NO_3)_2$			
BaO 58.67, N_2O_5 41.33			
d 3.250, *n* 1.571	1.571	1.564	−0.007
48. Niter, KNO_3			
K_2O 46.58, N_2O_5 53.42			
d 2.109, α 1.332, β 1.504, γ 1.504	1.447	1.456	+0.009
49. Soda-Niter, $NaNO_3$			
Na_2O 36.46, N_2O_5 63.54			
d 2.266, ω 1.587, ϵ 1.336	1.503	1.495	−0.008
50. Nitrocalcite, $Ca(NO_3)_2 \cdot 4H_2O$			
CaO 23.75, N_2O_5 45.75, H_2O 30.50			
d 1.90, α 1.465, β 1.498, γ 1.504	1.489	1.507	+0.018
Iodate			
51. Lautarite, $Ca(IO_3)_2$			
CaO 14.95, I_2O_5 85.04			
d 4.59, α 1.792, β 1.840, γ 1.888	1.840	1.845	+0.005
Borates			
52. Kernite, $Na_2B_4O_7 \cdot 2H_2O$			
Na_2O 22.65, B_2O_3 50.80, H_2O 26.55			
d 1.93, α 1.455, β 1.472, γ 1.487	1.471	1.469	−0.002
53. Probertite, $NaCaB_5O_9 \cdot 5H_2O$			
Na_2O 8.53, CaO 15.45, B_2O_3 50.44, H_2O 25.58			
d 2.141, α 1.514, β 1.524, γ 1.543	1.527	1.531	+0.004

TABLE 3—(*continued*)

Mineral data	$(\alpha+\beta+\gamma)/3$ or $(2\omega+\epsilon)/3$	$dK+1$	Deviation
54. Colemanite, $Ca_2B_6O_{11}\cdot 5H_2O$			
CaO 27.84, B_2O_3 49.61, H_2O 22.55			
d 2.423, α 1.568, β 1.592, γ 1.614	1.591	1.602	+0.011
55. Tincalconite, $Na_2B_4O_7\cdot 5H_2O$			
Na_2O 21.47, B_2O_3 47.42, H_2O 31.11			
d 1.880, ω 1.461, ϵ 1.474	1.465	1.468	+0.003
56. Borax, $Na_2B_4O_7\cdot 10H_2O$			
Na_2O 16.26, B_2O_3 36.51, H_2O 47.23			
d 1.715, α 1.447, β 1.469, γ 1.472	1.463	1.463	0.000
57. Inyoite, $Ca_2B_6O_{11}\cdot 13H_2O$			
CaO 20.5, B_2O_3 37.2, H_2O +26.1, H_2O −16.2			
d 1.875, α 1.495, β 1.510, γ 1.520	1.508	1.510	+0.002
Sulfates			
58. Barite, $BaSO_4$			
BaO 65.70, SO_3 34.30			
d 4.50, α 1.636, β 1.637, γ 1.648	1.641	1.649	+0.008
59. Celestite, $SrSO_4$			
SrO 56.42, SO_3 43.58			
d 3.97, α 1.621, β 1.624, γ 1.631	1.625	1.625	0.000
60. Anhydrite, $CaSO_4$			
CaO 41.19, SO_3 58.81			
d 2.98, α 1.570, β 1.575, γ 1.614	1.586	1.586	0.000
61. Alunite, $KAl_3(SO_4)_2(OH)_6$			
K_2O 10.02, Al_2O_3 39.65, SO_3 35.50, H_2O 14.83			
d 2.752, ω 1.572, ϵ 1.592	1.579	1.574	−0.005
62. Boussingualtite, $(NH_4)_2Mg(SO_4)_2\cdot 6H_2O$			
$(NH_4)_2O$ 14.44, MgO 11.18, SO_3 44.40, H_2O 29.98			
d 1.722, α 1.472, β 1.473, γ 1.479	1.475	1.474	−0.001
63. Ilesite, $MnSO_4\cdot 4H_2O$			
MnO 31.82, SO_3 35.88, H_2O 32.30			
d 2.25, α 1.511, β 1.519, γ 1.521	1.517	1.527	+0.010
Phosphates, Arsenates, Vanadates, Tungstates			
64. Moraesite, $Be_2PO_4(OH)\cdot 4H_2O$			
BeO 25.32, P_2O_5 34.82, H_2O 39.86			
d 1.805, α 1.462, β 1.482, γ 1.490	1.478	1.473	−0.005
65. Svanbergite, $SrAl_3(PO_4)(SO_4)(OH)_6$			
Al_2O_3 36.98, Fe_2O_3 0.24, CaO 3.25, SrO 12.87, P_2O_5 16.74, SO_3 17.38, H_2O 12.54			
d 3.22, ω 1.635, ϵ 1.649	1.640	1.654	+0.014

TABLE 3—(*continued*)

Mineral data	$(\alpha+\beta+\gamma)/3$ or $(2\omega+\epsilon)/3$	$dK+1$	Deviation
66. Arrojadite, $(Na, K)_5(Fe, Mn, Ca)_{16}(PO_4)_{12}(F, OH)\cdot H_2O$			
P_2O_5 40.10, Al_2O_3 2.67, FeO 28.29, MnO 15.82, MgO 1.04, CaO 2.47, Li_2O 0.09, Na_2O 6.41, K_2O 1.74, H_2O 0.91, F 0.80			
d 3.553, α 1.664, β 1.670, γ 1.675	1.670	1.675	+0.005
67. Graftonite, $(Fe, Mn, Ca)_3(PO_4)_2$			
P_2O_5 39.85, Al_2O_3 0.20, FeO 30.85, MnO 21.92, MgO 0.10, Li_2O 0.05, Na_2O 0.28, CaO 6.03, H_2O 0.60, F 0.20			
d 3.775, α 1.709, β 1.714, γ 1.736	1.720	1.725	+0.005
68. Lazulite, $MgAl_2(PO_4)_2(OH)_2$			
MgO 11.96, FeO 2.80, CaO 0.08, Al_2O_3 32.53, Fe_2O_3 0.49, TiO_2 0.16, P_2O_5 46.08, H_2O 5.90			
d 3.118, α 1.610, β 1.634, γ 1.644	1.629	1.629	0.000
69. Scorzalite, $FeAl_2(PO_4)(OH)_2$			
MgO 2.93, FeO 17.07, MnO 0.10, CaO 0.03, Al_2O_3 30.83, Fe_2O_3 0.13, TiO_2 0.10, P_2O_5 42.71 H_2O 6.10			
d 3.327, α 1.636, β 1.666, γ 1.676	1.659	1.666	+0.007
70. Zincian rockbridgeite, $(Fe'', Mn)(Fe'''_{4-y}, Zn_y)(PO_4)_3(OH)_{5-y}\cdot yH_2O$			
P_2O_5 33.74, FeO 10.86, MnO 2.11, Li_2O 0.01, Na_2O 0.13, ZnO 5.20, Fe_2O_3 41.20, H_2O 6.75			
d 3.51, α 1.82, β 1.83, γ 1.88	1.843	1.839	−0.004
71. Montebrasite, $(Li, Na)Al(PO_4)(OH, F)$			
Li_2O 9.68, Na_2O 0.43, Al_2O_3 35.31, P_2O_5 47.70, F 5.42, K_2O 0.10, MgO 0.33, H_2O 3.31			
d 3.085, α 1.594, β 1.608, γ 1.616	1.606	1.615	+0.009
72. Adamite, $Zn_2(AsO_4)(OH)$			
ZnO 57.05, As_2O_5 39.15, H_2O 3.54, SiO_2 0.26			
d 4.435, α 1.722, β 1.742, γ 1.763	1.742	1.736	−0.006
73. Brazilianite, $NaAl_3(PO_4)_2(OH)_4$			
Na_2O 8.29, K_2O 0.20, Al_2O_3 42.77, Fe_2O_3 0.03, TiO_2 0.05, P_2O_5 38.71, H_2O 9.95			
d 2.985, α 1.602, β 1.609, γ 1.623	1.611	1.614	+0.003
74. Ludlamite, $Fe_3(PO_4)_2\cdot 4H_2O$			
FeO 49.59, MgO 0.97, P_2O_5 33.20, H_2O 16.24			
d 3.14, β 1.650, β 1.667, γ 1.688	1.668	1.669	+0.001
75. Monazite, $(Ce, La)PO_4$			
$(Ce, La)_2O_3$ 67.23, ThO_2 2.98, SiO_2 0.70, P_2O_5 28.97, PbO 0.12			
d 4.98, α 1.779, β 1.782, γ 1.833	1.798	1.781	−0.017

TABLE 3—(*continued*)

Mineral data	$(\alpha+\beta+\gamma)/3$ or $(2\omega+\epsilon)/3$	$dK+1$	Deviation
76. Monazite			
$(Ca, La)_2O_3$ 65.28, Y_2O_3 5.13, P_2O_5 29.59			
d 5.173, α 1.785, β 1.787, γ 1.840	1.804	1.822	+0.018
77. Variscite, $AlPO_4 \cdot 2H_2O$			
Al_2O_3 32.38, Fe_2O_3 0.06, Cr_2O_3 0.18, P_2O_5 44.71, H_2O 22.67			
d 2.53, α 1.563, β 1.588, γ 1.594	1.582	1.570	−0.012
78. Scorodite, $Fe'''(AsO_4) \cdot 2H_2O$			
Fe_2O_3 34.75, As_2O_5 49.45, TiO_2 0.02, Sb_2O_5 0.06, SiO_2 0.30, H_2O 15.42			
d 3.278, α 1.784, β 1.795, γ 1.814	1.798	1.779	−0.019
79. Mansfieldite, $Al(AsO_4) \cdot 2H_2O$			
Fe_2O_3 0.88, Al_2O_3 23.30, As_2O_5 56.43, P_2O_5 0.59, Sb_2O_5 0.12, TiO_2 0.91, H_2O 17.77			
d 3.031, α 1.622, β 1.624, γ 1.642	1.629	1.628	−0.001
80. Hurlbutite, $CaBe_2(PO_4)_2$			
CaO 21.99, BeO 21.44, P_2O_5 56.57			
d 2.877, α 1.595, β 1.601, γ 1.604	1.600	1.598	−0.002
81. Fluorapatite, $Ca_5(PO_4)_3F$			
CaO 55.59, P_2O_5 42.22, F 3.78			
d 3.18, ω 1.6325, ϵ 1.630	1.632	1.648	+0.016
82. Chlorapatite, $Ca_5(PO_4)_3Cl$			
CaO 53.85, P_2O_5 40.88, Cl 6.81			
d 3.17, ω 1.6684, ϵ 1.6675	1.669	1.686	+0.017
83. Rossite, $CaV_2O_6 \cdot 4H_2O$			
CaO 18.09, V_2O_5 58.67, H_2O 23.24			
d 2.45, α 1.710, β 1.770, γ 1.840	1.773	1.782	+0.009
84. Scheelite, $CaWO_4$			
CaO 19.47, WO_3 80.53			
d 6.10, ω 1.920, ϵ 1.936	1.925	1.921	−0.004
Silicates			
85. Anthophyllite, $(Mg, Fe, Al)_7(Si, Al)_8O_{22}(OH, F)_2$			
SiO_2 42.90, TiO_2 0.49, Al_2O_3 17.82, Fe_2O_3 1.03, FeO 18.36, MnO 0.14, MgO 15.58, Na_2O 1.52, K_2O 0.03, F 0.31, H_2O 1.95			
d 3.277, α 1.656, β 1.667, γ 1.678	1.667	1.666	−0.001
86. Anthophyllite			
SiO_2 45.47, TiO_2 0.44, Al_2O_3 15.86, Fe_2O_3 2.94, FeO 15.34, MnO 0.07, MgO 17.62, CaO 0.14, Na_2O 0.28, H_2O 1.84			
d 3.216, α 1.655, β 1.663, γ 1.672	1.663	1.672	+0.009

TABLE 3—(*continued*)

Mineral data	$(\alpha+\beta+\gamma)/3$ or $(2\omega+\epsilon)/3$	$dK+1$	Deviation
87. Anthophyllite			
SiO_2 46.06, TiO_2 0.53, Al_2O_3 14.95, Fe_2O_3 0.62, FeO 17.45, MnO 0.04, MgO 18.30, CaO 0.07, Na_2O 0.47, H_2O 1.51			
d 3.245, α 1.652, β 1.660, γ 1.669	1.661	1.660	−0.001
88. Anthophyllite			
SiO_2 48.38, TiO_2 0.41, Al_2O_3 13.23, Fe_2O_3 1.28, FeO 14.56, MgO 20.51, CaO 0.04, Na_2O 0.11, H_2O 1.48			
d 3.259, α 1.648, β 1.654, γ 1.662	1.655	1.667	+0.012
89. Anthophyllite			
SiO_2 50.32, TiO_2 0.43, Al_2O_3 8.05, Fe_2O_3 2.18, FeO 18.34, MgO 17.55, CaO 0.74, Na_2O 0.70, H_2O 1.69			
d 3.279, α 1.654, β 1.659, γ 1.667	1.660	1.670	+0.010
90. Anthophyllite			
SiO_2 57.16, Al_2O_3 1.40, FeO 8.73, MnO 0.09, MgO 28.88, CaO 1.48, Na_2O 0.66, H_2O 1.60			
d 3.106, α 1.618, β 1.637, γ 1.635	1.630	1.637	+0.007
91. Anthophyllite			
SiO_2 57.05, Al_2O_3 1.94, FeO 11.10, MnO 0.11 MgO 26.78, CaO 0.64, Na_2 0.27, K_2O 0.06, H_2O 2.05			
d 3.102, α 1.616, β 1.628, γ 1.641	1.628	1.633	+0.005
92. Amphibole, $NaCa_2(Mg, Fe)_5(Al, Si)_7O_{22}(OH, F)_2$			
SiO_2 44.61, TiO_2 0.63, Al_2O_3 16.72, Fe_2O_3 0.72, FeO 8.20, MnO 0.11, CaO 10.36, MgO 15.26, Na_2O 1.72, K_2O 0.11, H_2O 1.51, F 0.08			
d 3.17, α 1.646, β 1.653, γ 1.668	1.656	1.656	0.000
93. Amphibole			
SiO_2 45.10, TiO_2 2.05, Al_2O_3 13.39, Fe_2O_3 1.58, FeO 9.60, MnO 0.09, MgO 13.69, CaO 11.15, Na_2O 1.55, K_2O 0.21, H_2O 1.49, F 0.18			
d 3.17, α 1.661, β 1.669, γ 1.678	1.669	1.668	−0.001
94. Amphibole			
SiO_2 48.07, TiO_2 0.57, Al_2O_3 11.16, Fe_2O_3 0.61, FeO 11.31, MnO 0.08, MgO 13.34, CaO 11.67, Na_2O 0.91, K_2O 0.14, H_2O 2.05, F 0.16			
d 3.15, α 1.648, β 1.664, γ 1.678	1.663	1.676	+0.013
95. Amphibole			
SiO_2 45.12, TiO_2 1.70, Al_2O_3 9.47, Fe_2O_3 3.45, FeO 14.48, MnO 0.07, MgO 10.46, CaO 11.50, Na_2O 1.45, K_2O 0.79, H_2O 1.37, F 0.23			
d 3.51, α 1.667, β 1.678, γ 1.685	1.677	1.741	+0.064

TABLE 3—(*continued*)

Mineral data	$(\alpha+\beta+\gamma)/3$ or $(2\omega+\epsilon)/3$	$dK+1$	Deviation
96. Amphibole			
SiO_2 39.51, TiO_2 1.46, Al_2O_3 12.16, Fe_2O_3 4.10, FeO 23.15, MnO 0.09, MgO 4.42, CaO 9.97, Na_2O 1.81, K_2O 1.38, H_2O 1.26, F 1.20			
d 3.42, α 1.690, β 1.702, γ 1.711	1.701	1.709	+0.008
97. Muscovite, $KAl_2Si_4O_{10}(OH, F)_2$			
SiO_2 46.75, Al_2O_3 34.73, Fe_2O_3 0.71, FeO 0.77, MgO 0.92, TiO_2 0.21, CaO 0.13, Na_2O 0.47, K_2O 10.61, BaO 0.13, F 0.16, H_2O 4.48			
d 2.82, α 1.555, β 1.589, γ 1.590	1.578	1.582	+0.004
98. Dalyite, $K_2ZrSi_6O_{15}$			
SiO_2 61.91, ZrO_2 21.72, K_2O 14.62, Na_2O 1.75			
d 2.84, α 1.575, β 1.590, γ 1.601	1.589	1.575	−0.014
99. Biotite, $K(Mg, Fe)_3(Si, Al)_4O_{10}(OH)_2$			
SiO_2 34.95, Al_2O_3 19.15, TiO_2 2.86, Fe_2O_3 0.88, FeO 20.81, MnO 0.10, MgO 8.42, CaO 0.26, Na_2O 0.24, K_2O 8.54, H_2O 3.79			
d 3.06, α 1.595, β 1.649, γ 1.649	1.631	1.640	+0.009
100. Kaersutite, $Ca_4(Na, K)_2(Mg, Fe)_7Al_6TiSi_{12}O_{46}(OH, F)_2$			
SiO_2 41.39, TiO_2 5.69, Al_2O_3 14.21, Fe_2O_3 3.32, FeO 5.69, MnO 0.08, MgO 13.64, CaO 11.60, Na_2O 2.29, K_2O 1.72, H_2O 0.12, F 0.42			
d 3.215, α 1.670, β 1.692, γ 1.701	1.688	1.698	+0.010
101. Searlesite, $Na_2B_2Si_4O_{12}\cdot 2H_2O$			
SiO_2 58.79, B_2O_3 16.92, Na_2O 15.29, H_2O 8.89, Al_2O_3 0.04, Fe_2O_3 0.04, MgO 0.03			
d 2.46, α 1.516, β 1.531, γ 1.535	1.527	1.534	+0.007
102. Hornblende, $W_{2-3}(XY)_5(Z_4O_{11})_2(OH, F, Cl)_2$			
SiO_2 39.80, Al_2O_3 11.39, Fe_2O_3 5.93, FeO 14.22, MgO 9.62, CaO 9.68, Na_2O 1.57, K_2O 1.60, H_2O+ 2.59, H_2O- 0.25, TiO_2 1.47, F 1.29, Cl 0.58, MnO 0.68			
d 3.211, α 1.666, β 1.689, γ 1.693	1.683	1.683	0.000
103. Hornblende			
SiO_2 38.38, Al_2O_3 11.01, Fe_2O_3 5.79, FeO 24.63, MgO 1.97, CaO 9.54, Na_2O 1.81, K_2O 1.72, H_2O 1.28, TiO_2 2.37, F 0.96, Cl 0.60, MnO 0.48			
d 3.445, α 1.694, β 1.717, γ 1.723	1.711	1.728	+0.017
104. Hornblende			
SiO_2 41.37, Al_2O_3 10.43, Fe_2O_3 3.86, FeO 16.33, MgO 8.05, CaO 10.29, Na_2O 1.59, K_2O 1.46, H_2O 1.80, TiO_2 2.91, F 1.17, Cl 0.60, MnO 0.76			
d 3.258, α 1.680, β 1.692, γ 1.696	1.689	1.693	+0.004

TABLE 3—(*continued*)

Mineral data	$(\alpha+\beta+\gamma)/3$ or $(2\omega+\epsilon)/3$	$dK+1$	Deviation
105. Pyroxene, $Ca(Mg, Fe)Si_2O_6$ SiO_2 52.49, Al_2O_3 2.72, Fe_2O_3 2.59, FeO 12.66, MgO 8.73, CaO 16.76, Na_2O 0.78, K_2O 0.28, H_2O 0.94, TiO_2 1.33, MnO 0.72 *d* 3.315, α 1.689, β 1.695, γ 1.716	1.700	1.700	0.000
106. Augite, $Ca(Mg, Fe)Si_2O_6$ SiO_2 50.13, Al_2O_3 4.31, Fe_2O_3 1.97, FeO 8.90, MgO 12.04, CaO 20.50, Na_2O 0.52, H_2O 0.74 *d* 3.315, α 1.689, β 1.695, γ 1.716	1.700	1.700	0.000
107. Ferrosalite, $CaFeSi_2O_6$ SiO_2 50.73, Al_2O_3 1.06, Fe_2O_3 0.53, FeO 18.57, MgO 5.70, CaO 22.86, Na_2O 0.16, K_2O 0.02, H_2O 0.12, TiO_2 0.07, MnO 0.18 *d* 3.413, α 1.708, β 1.714, γ 1.736	1.719	1.708	−0.011
108. Hedenbergite, $CaFeSi_2O_6$ SiO_2 48.41, Al_2O_3 0.30, Fe_2O_3 1.50, FeO 22.97, MgO 1.06, CaO 21.33, Na_2O 0.14, K_2O 0.03, H_2O 0.46, TiO_2 0.08, MnO 3.72 *d* 3.535, α 1.722, β 1.730, γ 1.750	1.734	1.734	0.000
109. Antigorite, $Mg_6Si_4O_{10}(OH)_8$ SiO_2 43.64, Al_2O_3 1.03, Cr_2O_3 0.02, Fe_2O_3 0.90, FeO 0.81, MnO 0.04, MgO 41.03, NiO 0.16, CaO 0.05, Na_2O 0.01, K_2O 0.03, H_2O 12.27 *d* 2.603, α 1.561, β 1.566, γ 1.567	1.565	1.575	+0.010
110. Kornerupine, $R_{40}(Si, B)_{18}O_{86}$ SiO_2, 30.28, B_2O_3 3.51, Al_2O_3 40.92, Fe_2O_3 0.42, FeO 8.53, MgO 14.89, CaO 0.06, Na_2O 0.08, H_2O 0.97, TiO_2 0.19, P_2O_5 0.09, Cr_2O_3 0.06 *d* 3.37, α 1.681, β 1.694, γ 1.695	1.690	1.677	−0.013
111. Kornerupine SiO_2 30.6, B_2O_3 2.8, Al_2O_3 37.7, Fe_2O_3 3.3, FeO 4.8, MgO 20.8 *d* 3.335, α 1.669, β 1.681, γ 1.682	1.677	1.675	−0.002
112. Chloritoid, $(Fe, Mg)_2(Al, Fe)_2(Al, Si)_4O_{10}(OH)_4$ SiO_2 25.12, Al_2O_3 40.25, Fe_2O_3 3.22, FeO 19.62, MnO 1.05, MgO 3.89, K_2O 0.09, H_2O 6.76 *d* 3.52, α 1.719, β 1.721, γ 1.725	1.722	1.734	+0.012
113. Ferrocarpholite, $H_4(Fe, Mg)Al_2Si_2O_{10}$ SiO_2 37.59, Al_2O_3 29.39, Fe_2O_3 2.07, TiO_2 0.22, MgO 2.52, MnO 0.14, FeO 17.98, H_2O 10.08 *d* 3.04, α 1.628, β 1.644, γ 1.647	1.640	1.652	+0.012

TABLE 3—(*continued*)

Mineral data	$(\alpha+\beta+\gamma)/3$ or $(2\omega+\epsilon)/3$	$dK+1$	Deviation
114. Allanite, $X_2Y_3Z_3O_{12}OH$			
SiO_2 28.66, Al_2O_3 9.95, Fe_2O_3 10.20, FeO 7.29, TiO_2 2.00, MgO 0.58, MnO 6.71, CaO 10.03, ThO_2 0.95, UO_2 0.01, $(Ce, La)_2O_3$ 22.30, H_2O 1.32			
d 3.95, α 1.791, β 1.815, γ 1.822	1.809	1.806	−0.003
115. Manganpyrosmalite, $(Mn, Fe)_8(Si_6O_{15})(OH, Cl)_{10}$			
MnO 39.25, FeO 12.48, MgO 0.74, ZnO 1.95, SiO_2 34.27, As_2O_5 0.13, Cl 3.82, H_2O 8.22			
d 3.13, ω 1.669, ϵ 1.631	1.656	1.663	+0.007
116. Wollastonite, $CaSiO_3$			
CaO 48.29, SiO_2 51.71			
d 2.915, α 1.616, β 1.629, γ 1.631	1.625	1.629	+0.004
117. Pseudowollastonite, $CaSiO_3$			
CaO 48.29, SiO_2 51.71			
d 2.905, α 1.610, β 1.610, γ 1.654	1.625	1.627	+0.002
118. Phenacite, Be_2SiO_4			
SiO_2 54.45, BeO 45.55			
d 3.00, ω 1.654, ϵ 1.668	1.659	1.663	+0.004
119. Fayalite, Fe_2SiO_4			
SiO_2 29.48, FeO 70.52			
d 4.34, α 1.835, β 1.877, γ 1.886	1.866	1.837	−0.029
120. Tremolite, $Ca_2Mg_5Si_8O_{22}(OH)_2$			
SiO_2 59.15, CaO 13.81, MgO 24.82, H_2O 2.22			
d 2.9, α 1.599, β 1.613, γ 1.625	1.612	1.611	−0.001
121. Acmite, $NaFeSi_2O_6$			
SiO_2 52.01, Fe_2O_3 34.57, Na_2O 13.42			
d 3.55, α 1.776, β 1.819, γ 1.836	1.810	1.824	+0.014

INDEX TO DATA OF TABLE 3

1. PALACHE, C., BERMAN, H., AND FRONDEL, C., (1944), Dana's System of Mineralogy: 7th Ed., Vol. I, John Wiley and Sons: N. Y., p. 499, anal. 1.
2. *Ibid.*, p. 507, anal. 1.
3. *Ibid.*, p. 691, anal. 11.
4. *Ibid.*, p. 505, anal. 1.
5. *Ibid.*, p. 662, data for pure compound.
6. *Ibid.*, p. 523, anal. 2.
7. *Ibid.*, p. 609, anal. 1.
8. LARSEN, E. S., JR., AND BERMAN, H., (1934), The microscopic determination of the nonopaque minerals: *U. S. Geol. Survey Bull.*, **848**, p. 69.
9. *Ibid.*, p. 96.
10. *Ibid.*, p. 49.
11. PALACHE, C., BERMAN, H., AND FRONDEL, C., *op. cit.*, pp. 556–557, average of best data for the pure compound.

12. *Ibid.*, pp. 583–588, density and indices of Binnental material.
13. *Ibid.*, pp. 589–593, average of best data for the pure compound.
14. *Ibid.*, pp. 641–642, data for the artificial compound.
15. Palache, C., Berman, H., and Frondel, C., (1951), Dana's System of Mineralogy: 7th Ed., vol. II, John Wiley and Sons: N. Y., pp. 150–152, data for the pure compound.
16. *Ibid.*, pp. 184–187, data for the pure compound.
17. *Ibid.*, pp. 162–163, data for the pure compound.
18. *Ibid.*, p. 168, data for the pure compound.
19. *Ibid.*, pp. 172–173, data for the pure compound.
20. *Ibid.*, pp. 177–178, data for the pure compound.
21. *Ibid.*, pp. 198–199, anal. 5.
22. *Ibid.*, pp. 218–219, anal. 2.
23. *Ibid.*, p. 221, data for the pure compound.
24. *Ibid.*, pp. 222–223, anal. 1.
25. *Ibid.*, pp. 224–225, data for the artificial compound.
26. *Ibid.*, pp. 225–226, anal. 7
27. *Ibid.*, p. 229, anal. 2.
28. *Ibid.*, pp. 230–231, data for the pure compound.
29. *Ibid.*, pp. 232–233, anal. 2.
30. *Ibid.*, pp. 234–235, anal. 2.
31. *Ibid.*, pp. 242–243, anal. 3.
32. *Ibid.*, p. 263, anal. 5.
33. *Ibid.*, p. 270, anal. 1.
34. *Ibid.*, p. 277, anal. 2.
35. *Ibid.*, p. 290, anal. 2.
36. *Ibid.*, p. 292, anal. 2.
37. *Ibid.*, pp. 294–295, data for artificial compound.
38. Donnay, G., and Donnay, J. D. H., (1953), The crystallography of bastnaesite, parisite, roentgenite, and synchisite: *Am. Mineral.*, **38,** 960, density is calculated from x-ray data, indices of refraction measured.
39. Jaffe, H. W., unpublished data for parisite, Mountain Pass, California, analysis by A. M. Sherwood, density and indices of refraction by H. W. Jaffe.
40. Jaffe, H. W., Meyrowitz, R., and Evans, H. T., (1953), Sahamalite, a new rare earth carbonate mineral: *Am. Mineral.*, **38,** pp. 746–748.
41. Axelrod, J. M., Grimaldi, F. S., Milton, C., and Murata, K. J., (1951), The uranium minerals from the Hillside Mine, Yavapai County, Arizona: *Am. Mineral.*, **36,** pp. 4–10.
42. *Ibid.*
43. *Ibid.*
44. Palache, C., Berman, H., and Frondel, C., (1951), *op. cit.*, p. 297, anal. 2.
45. *Ibid.*, pp. 309–310, anal. 2.
46. *Ibid.*, pp. 308–309, anal. 3.
47. *Ibid.*, p. 305, data for the artificial compound.
48. *Ibid.*, p. 303, data for the artificial compound.
49. *Ibid.*, p. 301, data for the artificial compound.
50. *Ibid.*, p. 306, data for the artificial compound.
51. *Ibid.*, p. 313, anal. 2.
52. *Ibid.*, pp. 336–337, anal. 3.
53. *Ibid.*, p. 344, anal. 2.
54. *Ibid.*, p. 352, anal. 3.

55. *Ibid.*, p. 338, anal. 6.
56. *Ibid.*, p. 340, data for the pure compound.
57. *Ibid.*, p. 359, anal. 2.
58. *Ibid.*, pp. 409–411, anal. 1.
59. *Ibid.*, pp. 416–417, anal. 1.
60. *Ibid.*, p. 426, anal. 1.
61. *Ibid.*, pp. 557–559, anal. 2.
62. *Ibid.*, p. 455, anal. 1.
63. *Ibid.*, p. 487, data for the artificial compound.
64. Lindberg, M. L., Pecora, W. T., and Fahey, J. J., (1938), Moraesite, a new hydrous beryllium phosphate: *Am. Mineral.*, **38,** p. 1130.
65. Palache, C., Berman, H., and Frondel, C., (1951), *op. cit.*, p. 1005, anal. 4.
66. Lindberg, M. L., (1950), Arrojadite, hüknerkobelite, and graftonite: *Am. Mineral.*, **35,** pp. 68–69.
67. *Ibid.*, pp. 59–75.
68. Pecora, W. T., and Fahey, J. J., (1950), The lazulite-scorzalite isomorphous series: *Am. Mineral.*, **35,** p. 5, anal. 1.
69. *Ibid.*, p. 5, anal. 8.
70. Lindberg, M. L., (1950), Zincian rockbridgite: *Am. Mineral.*, **35,** pp. 1028–1034.
71. Palache, C., Berman, H., and Frondel, C., (1951), *op. cit.*, p. 825, anal. 6.
72. Mrose, M. E., (1948), Adamite from Ojuela Mine, Mapimi, Mexico: *Am. Mineral.*, **33,** p. 454.
73. Frondel, C., and Lindberg, M. L., (1948), Second occurrence of brazilianite: *Am. Mineral.*, **33,** pp. 135–141.
74. Wolfe, C. W., (1949), Ludlamite from the Palermo Mine, North Groton, N. H.: *Am. Mineral.*, **34,** pp. 94–97.
75. Jaffe, H. W., (1955), Precambrian monazite and zircon from the Mountain Pass rare-earth district, San Bernardino County, California: *Geol. Soc. Am. Bull.*, **66,** No. 10, October, pp. 1247–1256.
76. Gordon, S., (1944), Mineralogy of the Cerro de Llallagua tin district, Bolivia: *Proc. Acad. Nat. Sci. Phila.*, **XCVI,** pp. 330–331.
77. Palache, C., Berman, H., and Frondel, C., (1951), *op. cit.*, p. 758, anal. 2.
78. *Ibid.*, p. 765, anal. 2.
79. *Ibid.*, p. 765, anal. 7.
80. Mrose, M. E., (1952), Hurlbutite, $CaBe_2(PO_4)_2$, a new mineral: *Am. Mineral.*, **37,** p. 936.
81. Palache, C., Berman, H., and Frondel, C., (1951), *op. cit.*, p. 881, data for the artificial compound.
82. *Ibid.*, p. 881, data for the artificial compound.
83. *Ibid.*, p. 1054, data for the artificial compound.
84. *Ibid.*, p. 1075, data for the artificial compound.
85. Rabbitt, J. C., (1948), A new study of the anthophyllite series: *Am. Mineral.*, **33,** pp. 270, 291, 299, anal. 1.
86. *Ibid.*, anal. 8.
87. *Ibid.*, anal. 9.
88. *Ibid.*, anal. 14.
89. *Ibid.*, anal. 17.
90. *Ibid.*, anal. 29.
91. *Ibid.*, anal. 30.
92. Larsen, E. S., Jr., and Draisin, W. M., (1948), Composition of the minerals in the rocks of the Southern California batholith: *International Geol. Cong. Rep't. of the18th Session, Great Britain,* Part II, p. 71, anal. 1.
93. *Ibid.*, anal. 3.

94. *Ibid.*, anal. 4.
95. *Ibid.*, anal. 9.
96. *Ibid.*, anal. 11.
97. Axelrod, J. M., and Grimaldi, F. S., (1949), Muscovite with a small optic axial angle: *Am. Mineral.*, **34,** p. 565.
98. Van Tassel, R., (1952), Dalyite, a new mineral from the Ascension Island: *Mineral. Mag.*, **XXIX,** No. 217, p. 856.
99. Mathias, M., (1952), An unusual cordierite rock from Upington, Cape Province: *Mineral. Mag.*, **XXIX,** No. 218, p. 939.
100. Campbell, I., and Schenck, E. T., (1950), Camptonite dikes near Boulder Dam, Arizona: *Am. Mineral.*, **35,** pp. 682–684.
101. Fahey, J. J., (1950), Searlesite from the Green River formation of Wyoming: *Am. Mineral.*, **35,** p. 1016.
102. Buddington, A. F., and Leonard, B. F., (1953), Chemical petrology and mineralogy of hornblendes in northwest Adirondack granitic rocks: *Am. Mineral.*, **38,** p. 894, anal. 1.
103. *Ibid.*, anal. 4.
104. *Ibid.*, anal. 5.
105. *Ibid.*, anal. 9.
106. Hess, H. H., (1949), Chemical composition and optical properties of common clinopyroxenes: *Am. Mineral.*, **34,** p. 655, anal. 21.
107. *Ibid.*, p. 652, anal. 16.
108. *Ibid.*, p. 653, anal. 18.
109. Hess, H. H., Dengo, G., and Smith, R. J., (1952), Antigorite from the vicinity of Caracas, Venezuela: *Am. Mineral.*, **37,** pp. 69–73.
110. Girault, J. P., (1952), Kornerupine from Lac Ste-Marie, Quebec, Canada: *Am. Mineral.*, **37,** p. 535, anal. 5*a*.
111. *Ibid.*, anal. 2.
112. Hietanen, Anna, (1951), Chloritoid from Rawlinsville, Lancaster County, Pennsylvania: *Am. Mineral.*, **36,** p. 867, anal. 2.
113. de Roever, W. P., (1951), Ferrocarpholite, the hitherto unknown ferrous iron analogue of carpholite proper: *Am. Mineral.*, **36,** p. 739, anal. 1.
114. Hutton, C. O., (1951), Allanite from Yosemite National Park, Tuolumne County, California: *Am. Mineral.*, **36,** pp. 238–242, anal. A.
115. Frondel, C., and Bauer, L. H., (1953), Manganpyrosmalite and its polymorphic relation to friedelite and schallerite: *Am. Mineral.*, **38,** pp. 755–757.
116. Winchell, A. N., (1931), The microscopic characters of artificial inorganic solid substances or artificial minerals: John Wiley and Sons, Inc., New York, pp. 297–299.
117. *Ibid.*, p. 298.
118. *Ibid.*, p. 286.
119. *Ibid.*, p. 292.
120. *Ibid.*, p. 301.
121. *Ibid.*, p. 315.

(*Continued from page 761*)

calculated and experimental n values for all but one entry, #95, where $dK+1$ deviates from $(\alpha+\beta+\gamma)/3$ by $+0.064$. The chemical composition of this amphibole, #95, suggests that the density of 3.51 is in error on the high side. Amphibole #96, for example, contains much more combined iron and titanium than amphibole #95 and has a lower density of 3.42.

The density of amphibole #95 calculated from $(n-1)/d=K$ is 3.21 and suggests that the measured value 3.51 is either a typographical or experimental error. On the other hand, the deviations of the calculated from the measured mean n values for rutile, anatase, and brookite (nos. 11, 12, 13, Table 3) are +0.029, +0.011, and +0.021 and must result from differences in bonding in the 3 different structures of the poly-

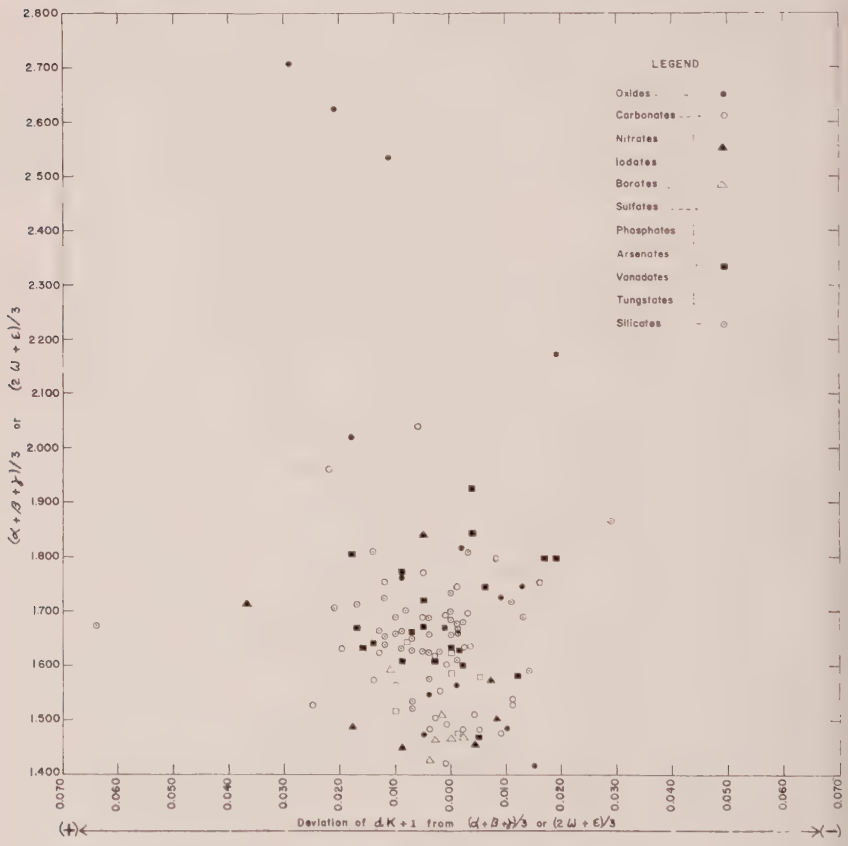


FIG. 1. ±Deviation of $dK+1$ from $(\alpha+\beta+\gamma/3)$ or $(2\omega+\epsilon)$ for 121 minerals.

morphs. Inasmuch as all 3 polymorphs show a positive deviation of $dk+1$, there is good possibility that Larsen's value, $k_{TiO_2}=.397$, is slightly on the high side.

The writer concludes that, on the basis of data for 121 minerals from the modern literature, the rule of Gladstone and Dale, $[(n-1)/d=K]$, holds surprisingly well for most minerals. Here is a rapid, workable method for (1) evaluating much of the old mineralogical data in the

literature, (2) checking new data before publication, (3) calculating a reasonably reliable approximation of the mean index of refraction or density where one or the other cannot be measured, and (4) locating an inaccurate chemical determination where the density, indices of refraction, and analytical determinations are otherwise accurate, e.g. use of the rule, $[(n-1)/d=K]$, revealed that an 88 per cent summation for a preliminary analysis of sahamalite, (Mg, Fe)(Ce, La)$_2$(CO$_3$)$_4$, resulted from an error in the CO_2 determination. This was accomplished by determining that the specific refractive energy (k) of the missing 12 per cent was approximately that of CO_2 (Jaffe, Meyrowitz, and Evans, 1953).

If this paper encourages more widespread use of the neglected rule of Gladstone and Dale, it will have served its purpose.

Acknowledgments

The author is indebted to E. S. Larsen, Jr., for suggesting the study and indicating where old data might be inaccurate for particular minerals. Thanks are due to J. D. H. Donnay and J. C. Rabbitt for suggesting methods of presenting the data and improving the manuscript.

References

Barth, T. F. W., (1930), Optical properties of mixed crystals: *Am. Jour. Sci., XIX*, 5th Ser. No. 110, 143–146.

Gladstone, J. H., and Dale, T. P., (1864), Researches on the refraction, dispersion, and sensitiveness of liquids; *Roy. Soc. London Philos. Trans.*, **153**, 337.

Jaffe, H. W., Meykowitz, R., and Evans, H. T., (1953), Sahamalite, a new rare earth carbonate mineral: *Am. Mineral.*, **38**, 749–750.

Larsen, E. S., Jr., (1921), The microscopic determination of the nonopaque minerals; *U. S. Geol. Survey, Bull.* **679**, 30–32.

——— and Berman, H., (1934), The microscopic determination of the nonopaque minerals; *U. S. Geol. Survey, Bull.* **848**, 2nd Ed., 30–32.

Palache, C., Berman, H., and Frondel, C., (1951), Dana's System of Mineralogy, 7th Ed., vol. II, John Wiley and Sons, New York, p. 286.

Rabbitt, J. C., (1948), A new study of the anthophyllite series: *Am. Mineral.* **33**, 270, 291, 299.

Manuscript received Jan 19, 1956.

TWINNING IN DIAMOND-TYPE STRUCTURES: HIGH-ORDER TWINNING IN SILICON*

J. A. Kohn, *Signal Corps Engineering Laboratories, Fort Monmouth, New Jersey.*

Abstract

Diamond-type structures are predisposed to twinning, owing to the relatively slight energy difference between the normal and twinned configurations. A non-parallel set of twinning operations produces high-order twinning. Previously known in diamond, this structural defect is extended to silicon. The method of analysis by x-ray means, applicable to the study of intergrowths in general, is given.

High-order twinning in diamond-type structures introduces substantial structure discontinuities. The geometrical aspects of such "high-order twin joins" are discussed.

Introduction

High-order twinning derives from a set of non-parallel twinning operations. In a diamond-type structure, for example, an initial twininng operation generates a twin, I, on (111) of a host crystal. A second operation generates a twin, II, on $(1\bar{1}1)$ of the same host crystal. The relationship between the host and each of twins I and II is that of simple, or first-order twinning; that between individuals I and II is high-order (in this case, second-order) twinning.

Twinning in diamond-type structures introduces deviations from normal bonding commencing with the tertiary coordinations. Since the primary and secondary coordinations remain unaffected by the twinning operation, there obviously exists only a very slight energy difference between the normal and twinned configurations. It is to be expected, then, that the frequency of twinning in such materials would be high. Also, since there are four structurally equivalent, potential twinning directions available, examination of these substances should reveal the type of multiple operations involved in high-order twinning.

A study of diamond crystals, even those of gem variety, almost invariably reveals the presence of at least microscopic twinning. High-order twinning in diamond has been described on the basis of both morphological (1) and x-ray (2) evidence. Nevertheless, owing to the limited availability of diamonds and to the fact that one cannot perform a simple synthesis and thus easily vary experimental conditions, the study of such structural defects is considerably handicapped. Fortunately, however, recent emphasis on solid state research in silicon and germanium has made available many excellent crystals for such studies. Since these materials are isomorphous with diamond, the information

* Presented at the Thirteenth Annual Pittsburgh Diffraction Conference, Pittsburgh, Pa., Nov. 3, 1955.

thus gleaned can easily be extrapolated to the latter. The present study demonstrates high-order twinning in silicon and discusses some general geometrical aspects of this phenomenon in diamond-type structures.

Procedure and Results

The particular crystal with which this paper is mostly concerned was grown by the Czochralski technique, i.e., by pulling an oriented seed from a melt. The seed, in this case, was oriented and pulled along [001]. A surface portion of the resultant silicon crystal showed a scallop-like structural outcrop, with cusps at 90°-intervals around the circumference of the crystal. One such cusp became the subject of detailed x-ray study. An enlargement of the area of interest is reproduced in Fig. 1, in

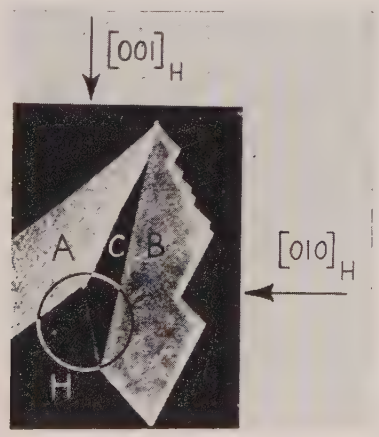


Fig. 1. Localized surface structure on silicon, viewed along [100] of the host (H) crystal. Circle shows position of incident x-ray beam (20×).

which the host crystal is viewed along [100]. In addition to the host (H), three other individuals, A, B, and C, are noted in the figure. Their mutual orientations were determined by the back-reflection Laue technique.

The area circled in Fig. 1 denotes that which was bathed by the x-ray beam. The resultant back-reflection Laue pattern, centered on (100) of the host crystal, is reproduced in Fig. 2a. The different profiles of the reflections on the pattern can be correlated with the shapes of the surface areas exposed to the beam by the different crystal orientations. Thus, it is easily possible to locate symmetry centers due to each of the individuals noted in Fig. 1. Three octahedral centers were located, which could be correlated with orientations A, B, and C. The schematic drawing in Fig. 2b shows clearly the threefold symmetry about $(11\bar{1})_A$ and

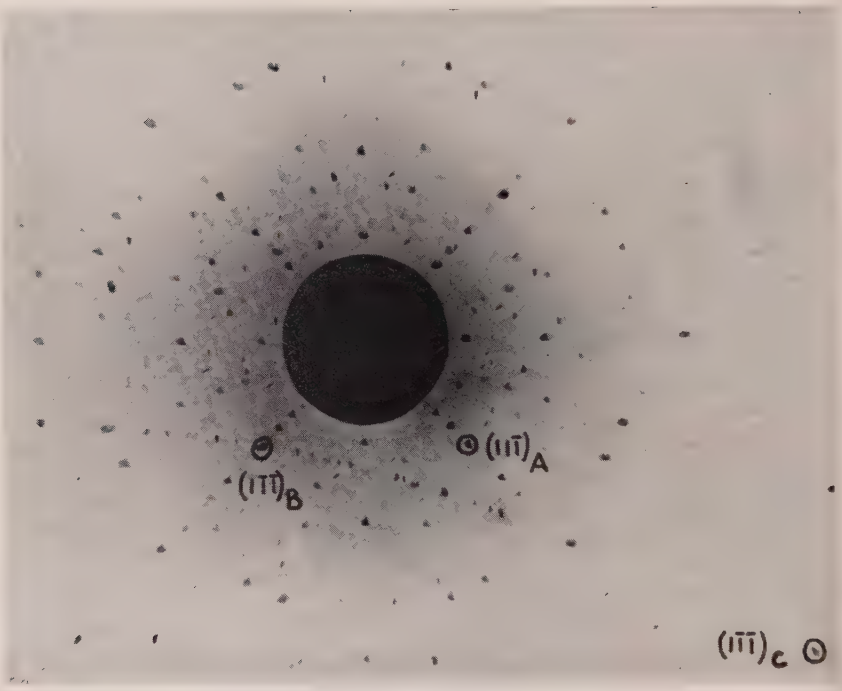


FIG. 2*a*. Back-reflection Laue pattern centered on (100) of the host crystal: CuK, 24 hrs., crystal to film = 2.78 cm. (1.1×).

$(1\bar{1}\bar{1})_B$. The threefold center due to individual *C* is not immediately evident, however the symmetrical distribution of reflections along the $(1\bar{1}\bar{1})_B$–$(1\bar{1}1)_C$ zone line bears out the positioning of $(1\bar{1}\bar{1})_C$. This symmetrical distribution can be traced in either direction from the $(11\bar{2})$ reflection (Fig. 2*b*), which is common to individuals *B* and *C*.

The model depicted in Fig. 3 demonstrates the mutual orientations of the four individuals, host, *A*, *B*, and *C*. The faces labelled on the model correspond with the symmetry centers noted in the Laue pattern. This postulated twin complex was confirmed by a comparison of calculated interfacial angles with those measured on the Laue pattern. The following table presents these data.

Angle between $[100]_H$ *and*	*Calculated*	*Observed*
$[11\bar{1}]_A$	15° 48′	15.8°
$[1\bar{1}\bar{1}]_B$	15° 48′	15.8°
$[1\bar{1}\bar{1}]_C$	33° 30′	33.4°

Thus, the localized silicon section under consideration is actually a twin complex in which the individuals are related as follows: *A* and *B*

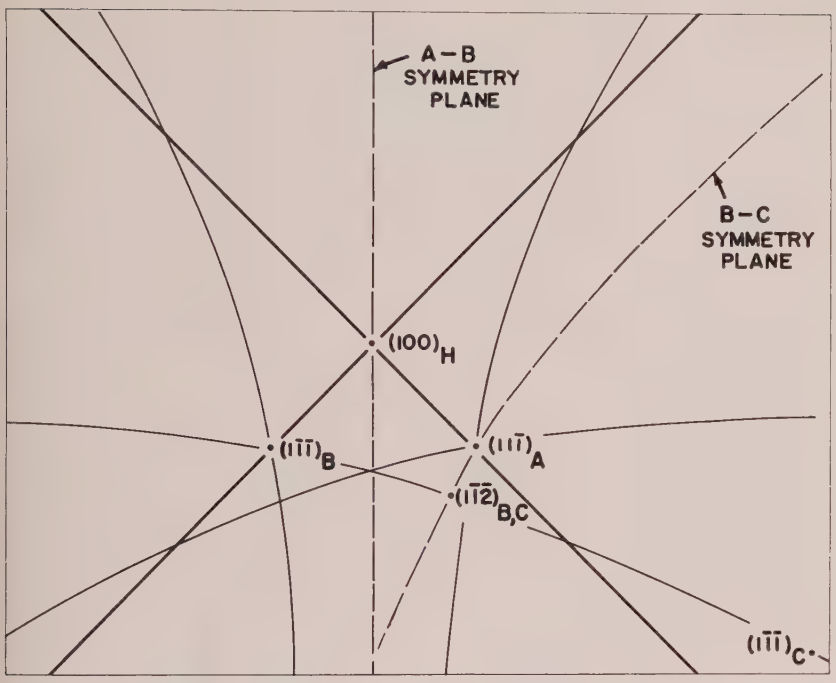


FIG. 2*b*. Schematic drawing of the symmetry relationships in Fig. 2*a*.

each bear a first-order twinning relationship with the host; *C* is a first-order twin with respect to *B*; *C* has a high-order (second-order) twin relationship with the host and a high-order relationship (third-order) with *A*.

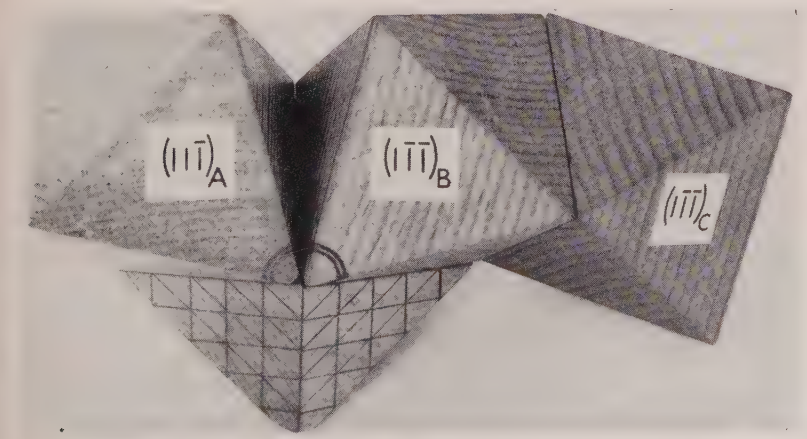


FIG. 3. Twinned complex, showing the orientations of the individuals noted in Fig. 1. View is along [100] (double arc) of the host crystal (ruled; only lower half visible).

In addition to the first-order twinning on (111) and ($1\bar{1}1$), as depicted in the model (Fig. 3), the host crystal also showed first-order twinning on the remaining two upper octahedral planes, i.e., ($\bar{1}11$) and ($\bar{1}\bar{1}1$). Upon sectioning for further investigation of the internal structure, it was disclosed that all twinning could be traced back to a common point within the crystal and that this point was coincident with a spherical cavity (gas bubble), approximately 0.7 mm. in diameter. Subsequent examination with an infrared image tube (3) revealed strong stress fields concentrated at the cavity. It seems probable that in this particular case the twinnings were simultaneously generated by the inclusion of a gas bubble within the structure.

Discussion

Twinning on all four upper (or, in some cases, lower) octahedral planes is limited to, and fairly common in, crystals grown by pulling along a cubic (fourfold) axis. The particular crystal described above is a special case for two reasons: (1) additional twinning has developed (individual *C*, Fig. 3) and (2) the twinning derived from a gas bubble inclusion. In other crystals examined, the twinnings were simultaneously generated by a sudden change in either the pulling rate or temperature gradient. The restriction of this twinning pattern to crystals pulled along a fourfold axis is explained by the fact that only in such a case do all four octahedral planes make the same angle with the direction of the temperature gradient (pulling direction).

Figure 4 presents a view along the gradient direction of a crystal pulled along [001] and twinned on all four upper octahedral planes. Such a drawing need not be considered idealized, since crystals have been observed in which the boundary traces have actually attained the pictured geometrical perfection. The dashed lines in the pattern are first-order twin boundaries. The vertical dashed line to the right, for example is the trace of the boundary between the host crystal and an individual developed by twinning on ($\bar{1}11$) of the host. Such boundaries represent minor structure discontinuities, since the initial deviation from normal bonding lies in the tertiary coordinations. The cross-hatched lines are traces of boundaries between high-order (second-order) twins and represent substantial structure discontinuities, since even the primary coordinations are disturbed. These are common in diamond crystals and are usually the loci of inclusions. From a geometrical point of view, boundaries of this type could be termed "high-order twin boundaries." Such terminology, however, implies that the discontinuity is a composition plane across which there has been a twinning operation, and this is not the case. It is merely the plane (or planes) along which two individ-

uals related by high-order twin geometry are joined. In this respect, it might more properly be termed a "high-order twin *join*." Considerations such as these emphasize the importance of regarding twinning as a physical rather than a geometrical phenomenon.

Owing to the sensitive structural dependence of electrical properties in the diamond-type semiconductors silicon and germanium (4), the presence of substantial structure discontinuities in these materials is

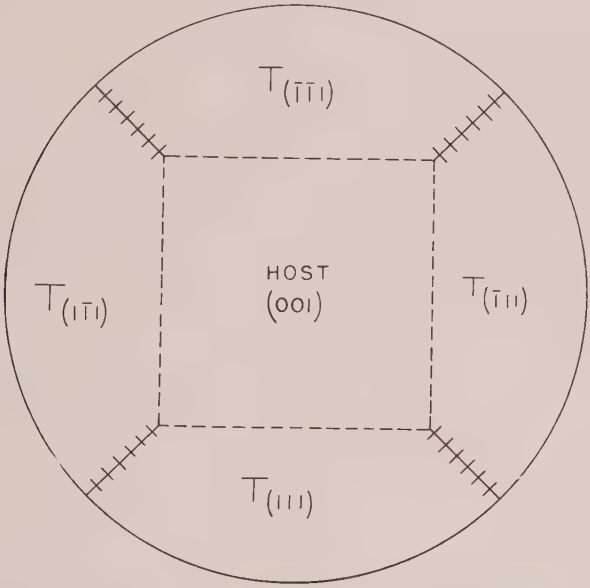


FIG. 4. Schematic drawing of the twinning pattern on (001) of a silicon crystal pulled along [001].

significant. Knowing that such discontinuities can be introduced by high-order twinning of a diamond-type material, it remains to describe their nature and variety.

A general grain boundary has five degrees of freedom, three deriving from the mutual orientation of the two individuals, and two introduced by the orientation of the join itself (5). The twinning operations establish the first three degrees of freedom. The join, however, will seek a minimum energy position, which in turn is influenced by environmental factors. Geometrical analysis of second- and third-order twinning has revealed a surprisingly small number of possible grain boundaries, as regards the first three degrees of freedom, i.e., the mutual orientation of the two individuals. Second-order twinning, as typified in Fig. 4, can develop but *one* such grain boundary. Specifically, this is a pure tilt boundary (6),

having a tilt angle of 38°57′ about [110]. Third-order twinning (cf. *A–C* relationship, Fig. 1) can introduce only *two* additional grain boundaries. One is a pure tilt operation of 31°35′ around [110]. This is the case with the *A–C* relationship in Figs. 1 and 3. The other third-order twin join is of the more general tilt-twist variety (7). The mutual orientation of the two individuals is defined as follows: $[111]_1 \wedge [111]_2 = 77°53'$; $[111]_1 \wedge [1\bar{1}1]_2 = 22°11'$. It must be remembered, however, that the orientation of the join itself is not uniquely established by the twinning operations.

Summary

A unique, localized, structural outcrop on a silicon crystal pulled from a melt is actually a four-individual twin complex. This is a special case of a more general twinning pattern, typical of crystals pulled along a four-fold axis, wherein twinning develops on all four upper (or lower) octahedral planes. Such non-parallel, multiple twinning in diamond-type materials results in high-order twin joins, which represent substantial structure discontinuities.

Acknowledgments

The writer is indebted to Dr. W. Kaiser, of this laboratory, for the infrared observations and for periodic helpful discussions, to Mr. W. Pharo, Evans Signal Laboratory, who grew the crystal and kindly donated it for study, and to Dr. H. Kedesdy, also of this laboratory, for his critical review of the manuscript.

References

(1) Slawson, C. B., *Am. Mineral.*, **35,** 193 (1950).
(2) Kohn, J. A., *Ind. Diamond Rev.*, **13,** 56 (1953).
(3) Bailly, René, *Bull. Geol. Soc. Am.*, **60,** 1871 (1949).
(4) Taylor, W. E., Odell, N. H., and Fan, H. Y., *Phys. Rev.*, **88,** 867 (1952).
(5) Read, W. T., Jr., Dislocations in Crystals, McGraw-Hill, New York, 173, 183 (1953).
(6) *Ibid.*, 156, 178.
(7) *Ibid.*, 182.

Manuscript received Jan 18, 1956.

NOTES AND NEWS

NIOCALITE—A NEW CALCIUM NIOBIUM SILICATE MINERAL[1]

E. H. Nickel, *Mines Branch, Department of Mines and Technical Surveys, Ottawa, Canada.*

A new mineral species, for which the name "niocalite" is here proposed, has been identified in rock from the Oka district, 20 miles west of Montreal, Quebec. It has a vitreous luster, is light yellow in color, and occurs as prismatic crystals up to 10 mm. in length and 1 mm. in width in coarse white crystalline calcite. Other associated minerals are apatite, diopside, biotite, pyrochlore, and niobian perovskite. The lithology of the area has been described by R. B. Rowe (1955).[2]

A preliminary partial chemical analysis reveals that it is essentially a calcium niobium silicate with a formula approximating $Ca_4Nb\ Si_2O_{10}(O, F)$. The analysis, performed by Dr. J. A. Maxwell[3] is as follows:

CaO	46.8%
Na_2O	0.7
Nb_2O_5	16.8
R_2O_3	2.0
SiO_2	26.8
H_2O	0.2
F	1.7
	95.0%

The R_2O_3 includes rare earths and alumina. In addition, a semi-quantitative spectrographic analysis indicates appreciable amounts of manganese, iron, and strontium. The proposed name, niocalite (nio-cal'-ite, was chosen to indicate two of the principal components—niobium and calcium.

Debye-Scherrer *x*-ray patterns, taken with iron-filtered cobalt radiation, have the following strongest lines:

	d(Å)	*I*(meas.)
1.	3.01	10
2.	2.89	6
3.	2.85	6
4.	3.24	5
5.	1.84	4

[1] Published by permission of the Deputy Minister, Department of Mines and Technical Surveys, Ottawa, Canada.

[2] Rowe, R. B. (1955), Notes on columbium mineralization, Oka District, Two Mountains County, Quebec: *Geological Survey of Canada*, paper 54–22.

[3] *Geological Survey, Department of Mines and Technical Surveys.*

A characteristic feature of niocalite appears to be its twinning and in the search for a crystal suitable for single crystal x-ray determinations, no untwinned crystal has so far been found. The twinning takes place about a twinning axis which coincides with the acute bisectrix X which is presumably also a crystallographic direction. If the mineral is monoclinic, as it appears to be, this would be the b-axis. Other properties of niocalite are:

Optical Properties:
Biaxial negative
$-2V = 56°$
$\alpha = 1.700$; $\beta = 1.721$; $\gamma = 1.730$
Birefringence $\gamma - \alpha = 0.030$
Specific gravity: 3.32
Hardness: approximately 6 (Mohs scale).

There is a distinct similarity between the optical and physical properties of niocalite and wöhlerite. The latter, however, has a much higher sodium and zirconium content than niocalite.

A NEW TECHNIQUE FOR MICROMETRIC ANALYSIS OF THIN-SECTIONS*

Joseph A. Mandarino, *University of Michigan, Ann Arbor, Michigan.*

The method of thin-section analysis described in this note is based on the fact that, if a microscope objective is uncentered, a circular succession of grain images will pass through the intersection of the crosshairs when the stage is rotated. In effect, the rotation axis of the thin-section has been shifted from a point at the center of the field to a point near or beyond the edge of the field. The method may be used for either Rosiwal or point count analyses.

Comparison with Linear Rosiwal Method

To compare the results obtained from a circular analysis with those obtained from a conventional Rosiwal analysis, a large "synthetic thin-section" was constructed on paper. This "thin-section" consisted of seven constituents. The position of each grain was determined by using a random number table. These numbers corresponded to grid points on the thin-section. Shapes and sizes of grains were varied to approximate those of minerals actually seen in thin-sections of rocks possessing hypautomorphic-granular texture. After the thin-section was completed, the planimetric percentages of the constituents were determined by measuring the areas of all the grains with a planimeter.

* Contribution No. 198 from the Department of Mineralogy, University of Michigan.

A conventional Rosiwal analysis was performed by running five linear traverses along the length and five along the width of the "section." Next, twelve circular traverses were run. Table 1 shows the results of the two Rosiwal analyses compared with the planimetric percentages. The twelve circular traverses, because of the radius chosen, correspond to 75.36 linear units. The ten linear traverses correspond to 160.15 linear units.

In order to be sure that the personal factor did not exert too great an influence on the construction of the synthetic thin-section with respect to grain orientation, a similar pair of analyses was run on a thin-section of granodiorite from St. Cloud, Minnesota. The objective was uncentered about one millimeter for the circular traverses. The amount of

TABLE 1. SYNTHETIC THIN-SECTION

Constituent	Planimetric %	Rosiwal		Point Count	
		Linear	Circular	Grid	Circular
A	18.2	17.6	17.5	18.6	17.7
B	15.1	15.7	15.0	15.2	15.2
C	1.4	1.0	1.3	1.4	1.9
D	1.0	1.3	1.1	0.6	0.3
E	0.9	0.5	0.7	1.6	0.5
F	0.5	0.6	0.6	0.8	0.6
G	62.9	63.4	63.8	61.8	63.8
Total	100.0	100.1	100.0	100.0	100.0

uncentering was measured with a stage micrometer. The point of rotation was shifted just beyond the edge of the field. Twelve circular traverses, corresponding to approximately 38 mm. of linear transverse, were run on the thin-section. The centers of adjacent traverses were approximately three millimeters apart. The conventional linear traverses (five along the length and five along the width) corresponded to approximately 121 mm. The results of the two analyses are given in Table 2.

Twenty other linear Rosiwal analyses were run on the synthetic thin-section to determine the standard deviation from the mean for Constituent "A." The analyses were performed with each set of traverses parallel to each other, but displaced a short distance from the preceding set. The values obtained from the twenty analyses formed a Gaussian distribution. The standard deviation for Constituent "A" was 3.0%. This means that about 68% of the linear Rosiwal analyses would yield values ranging from 15.2% to 21.2% for "A," and the full range of values

TABLE 2. THIN-SECTION OF GRANODIORITE, ST. CLOUD, MINNESOTA

Constituent	Rosiwal		Point Count
	Linear	Circular	Circular
Quartz	15.5	15.3	16.6
Microcline	33.3	33.4	33.9
Plagioclase	35.2	36.6	33.6
Hornblende, Biotite	14.3	13.2	14.1
Magnetite, Sphene, Apatite	1.7	1.5	1.8
Total	100.0	100.0	100.0

would be from about 9.2% to about 27.2%. Thus, the results obtained by the two methods from the true thin-section (Table 2) are compatible.

The primary objection to the use of the circular Rosiwal method lies in the fact that the angle through which the stage rotates in traversing across a grain must be recorded by noting the angular positions before and after the traverse. This difficulty is about the same as that encountered when using an ordinary non-integrating mechanical stage for linear Rosiwal analysis where the linear positions must be recorded before and after traversing each grain.

In using the circular Rosiwal method it is convenient to work to the nearest degree. For this reason, the amount that the objective is uncentered should be selected such that the smallest grain desired subtends an angle of at least one degree.

Comparison with Linear Point Count Method

The circular technique also seems to be applicable to the point counting method. The objective is uncentered as before, and the stage is rotated in angular increments to fix the points to be counted. This method together with a grid-type point count was used on the synthetic thin-section. The points for the circular method were fixed by rotating the stage in five degree increments. The results are shown in Table 1. The grid point count used 897 points; the circular used 864 points. The results of a circular point count on the previously mentioned granodiorite are given in Table 2. The points were spaced five degrees apart on the same twelve circles used for the circular Rosiwal analysis.

An inexpensive circular point counter was constructed by cutting a

disc out of 1/16 inch metal and cutting notches in the periphery. The notches were spaced five degrees apart by use of a protractor. The disc was fastened to the stage and a small piece of spring brass was fastened to the stationary part of the stage in such a manner that it engaged the notches as the stage was rotated. The stage is rotated until a click is heard which indicates the point to be counted. Before a circular point count is begun, the position of the stage with respect to the vernier should be noted in order that no more than one complete revolution be made in the same spot. It is convenient to paint a reference mark on the disc to indicate the starting point.

The circular point counter was constructed in about two hours, and only common hand tools such as files, drills, and a hack saw were used.

The methods as outlined here should be of value to those petrographers who do not do enough thin-section analyses to warrant the purchase of an integrating stage, a mechanical stage, or a point counter. For circular Rosiwal analyses, no apparatus is required other than a petrographic microscope. For circular point counts, an easily constructed notched disc may be used. The method should also be useful in petrography classes where the ratio of students to integrating stages and/or point counters is high.

ANOMALOUS FLUORESCENCE IN TORBERNITE FROM RUM JUNGLE, N.T. AUSTRALIA

R. J. P. Lyon, *Research Officer, Mineragraphic Section, C.S.I.R.O., Melbourne, Australia.*

Although most, if not all, torbernite is non-fluorescent, reports of torbernite showing anomalous fluorescence appear from time to time. Where such torbernite has been subjected to microscopic examination it has been found to consist of intergrowths of one or more fluorescing minerals, notably autunite, with the torbernite (Meixner, 1939, p. 438), whereas the torbernite in the intergrowths did not fluoresce.

A striking example of torbernite showing such anomalous fluorescence was found recently at Rum Jungle, N.T., in Northern Australia (*C.S.I.R.O. Mineragraphic Report No. 619*). This specimen, which is about 9 in. × 6 in., is covered with protuberances 1 to 2 mm. high consisting of stacks and clusters of a platy emerald green mineral, apparently torbernite, but the surface fluoresces a vivid greenish-yellow, except in a single band across the center. This band consists of non-fluorescent, slightly darker green crystals.

These darker green non-fluorescent crystals consist of meta-torbernite.

They have $\beta = 1.618$ and are optically negative with a low 2V. They dissolve readily in acid and the solution yields positive microchemical tests for copper, uranium and phosphorus.

The slightly lighter green fluoresecent crystals when examined microscopically under a Mineralight, where found to be composite, consisting of interlayered plates of a mineral with a strong yellow-green fluorescence, and of a non-fluorescent mineral in parallel orientation (Fig. 1). The non-fluorescent green plates, forming about two-thirds of the composite

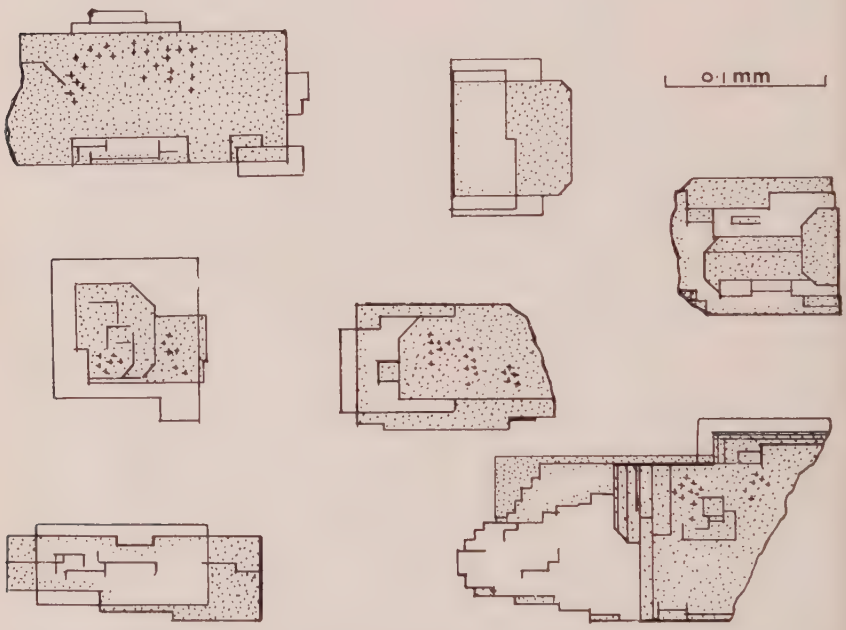


FIG. 1. Cleavage flakes from composite crystals showing torbernite (clear) and autunite (stippled). Weak stippling indicates autunite covered by torbernite. Crosses are fine brown crystallites of an unknown secondary mineral ($\beta = 1.730$). Scale as shown. Individual plates 0.005–0.015 mm. thick.

crystals, are square or rectangular in outline, whereas the yellow fluorescent plates (shown stippled) have, in addition, octagonal facets. The composites range from 0.05 to 0.5 mm. in area, from 0.005 to 0.015 mm. thick, and both minerals have two good cleavages at right angles.

The fluorescent plates vary from pale yellow in color, with a weak birefringence and $\beta = 1.594$, $(-)2V = 30\ 40°$, to slightly more green with $\beta = 1.598$, $(-)2V = 38°$. They consist of meta-autunite presumably in slightly varied states of hydration. They are readily soluble in acid and the solutions yield positive microchemical tests for uranium and phos-

phorus, and weakly positive tests for copper. The non-fluorescent plates were identified as meta-torbernite, with properties similar to the non-fluorescent plates of the darker green band.

The parallel interlayering of autunite and torbernite plates is well known (Dana, 1951, p. 985), and Pelloux (1934, p. 163) has remarked upon the octagonal habit of autunite interlayered with rectangular plates of torbernite. He also noted that the composite crystals are a brilliant green color.

A strong fluorescence for intergrown autunite and torbernite is recorded by Meixner (1939, p. 439), who reports that the bright fluorescence came from a wafer-thin *coating* of autunite on the surface of the non-fluorescent torbernite. The Rum Jungle material consists of interlayered plates on the two minerals, often stacked ten to twenty plates high.

When a thin plate of the torbernite is placed so that it completely covers a strongly fluorescing plate of the autunite, the flourescence is completely extinguished. Such effects may be observed under the microscope, with ultra-violet illumination, using a low power ($\times 10$) objective. However if a corner of the autunite projects from beneath the covering torbernite, then that corner will fluoresce strongly, while the remainder exhibits a weak fluorescence through the torbernite plate. Similar weak fluorescence appears if the overlying torbernite has strongly developed cleavage cracks, these cracks being accentuated by the yellow green fluorescence from the underlying autunite. Again, if a plate showing fluorescent areas is rotated on the point of a needle it can be seen that the fluorescence is confined to exposed plates of autunite, or the edges of interlayered plates.

Autunites are susceptible to base-exchange and Fairchild (1929, p. 265) was able to produce calcium-, sodium, potassium,- barium-, manganese-, magnesian-"autunites" by soaking an artificial soda-autunite in the respective metal-chloride brine for several days. To test this a natural autunite was immersed in copper chloride solution at 80° C. for seven days. The strongly fluorescent sulphur yellow autunite from Mt. Painter in South Australia, with $\beta = 1.575$, $\gamma = 1.577$ $(-)2V = 40°$, was converted to a pale green, non-fluorescing meta-torbernite with $\beta = 1.600$ by this method. This agrees well with Fairchild's "copper-autunite" with $\beta = 1.608$ and containing 5.61% Cu, 0.73 Na_2O, 15.62% H_2O by analysis, after similar treatment, using artificial soda-autunite.

In view of the ease with which copper can be substituted for calcium in autunites it is concluded that the interlayering of the copper-rich and copper-free secondary uranium minerals at Rum Jungle and elsewhere must reflect a delicate chemical balance during their deposition. Later

copper bearing solutions percolating through the specimen would have reacted to produce a more homogeneous torbernite.

References

Dana, J. D., and Dana, E. S. (1951), System of Mineralogy, 11, ed. 7, by C. Palache, H. Berman and C. Frondel, New York.

Fairchild, J. G. (1929), Base exchange in artificial autunite: *Am. Mineral.*, **14,** 265–275.

Lyon, R. J. P. (1955), Intergrown autunite and torbernite from Rum Jungle, Northern Territory: *Minergraphic Report 619, C.S.I.R.O., Melbourne.*

Meixner, H. (1939), Fluoreszenanalytische, optische und chemische Beobachtungen an Uranmineralen: *Chemie der Erde,* **12,** 433–450; also (1940) *Mineral. Abst.*, **7,** 529.

Pelloux, A. (1934), I minerali uraniferi e le sorgenti di acque radioactive della miniera di Lurisia presso Roccaforte di Mondovi: *Atti Soc. Ligustica Sci. Lett.* Genova, **13,** 137–170; also (1937); *Mineral. Abst.*, **6,** 518–519.

NOTE ON TWINNING AND PSEUDO-TWINNING IN DETRITAL QUARTZ GRAINS

Iris Borg, *Princeton, University, Princeton, New Jersey.*

Detailed studies of etch figures and morphology have shown that with few exceptions single crystals of quartz are made up of more than one individual intimately grown together. The most common intergrowths are described by the Dauphiné, Brazil and combined Dauphiné-Brazil twin laws (Gordon, 1945; Gault, 1949). These types of twinning cannot be detected optically in thin sections of customary thickness. The purpose of the present note is to point out that a second group of intergrowths composed of sub-individuals whose *c* axes do not coincide are not uncommon, though hitherto they have seldom been recognized as such. A twin relationship can be demonstrated between members of some intergrowths of this second group, while in others the relation closely approximates one of the thirteen twin laws designated by Zyndel (1914). Because of the small but consistent departures from the laws of Zyndel, this type of intergrowth has been called pseudo-twinning by Hintze (1915, p. 1270).

Intergrowths of the second group are most conspicuous in individual grains of sandstones. They were repeatedly encountered by the writer in the course of a petrographic examination connected with the artificial deformation of the Asbury Park beach sand (Maxwell and Verrall, 1954; Borg and Maxwell, 1956). Although the crystallographic orientation of a twinned grain can be determined only on deformed material in which recognizable cleavage fractures have formed, twins and pseudo-twins are not themselves products of experimental deformation. They are equally common in the sand prior to deformation. Approximately $1\frac{1}{2}\%$ of the grains in the Asbury Park sand are intergrowths recognizable in

thin section. Those that survive experimental deformation also contain minor fracturing controlled in large part by $r\{10\bar{1}1\}$, $z\{01\bar{1}1\}$, and $m\{10\bar{1}0\}$. Thus it is possible in favorable instances to describe the crystallographic relations between participating members of the intergrowths by measuring experimentally induced fractures, c axes and composition planes, if present, with a universal stage and by plotting the results on a stereographic projection.

Intergrowths cannot be seen in plane polarized light (Fig. 1*A*) unless foreign material has lodged along discontinuities bounding members of the intergrowth (Figs. 1*C* and 1*E*). Under crossed nicols the rounded grains appear to be made up of many sub-individuals of different orientation (Fig. 1*B*); however usually two and no more than three orientations may be recognized by measuring the exact position of the c axes in the various sub-individuals. The apparently large number of sub-individuals seen stems from overlap of portions of one individual on another resulting in areas of slightly different birefringence. The grain shown in Fig. 1*D* contains a nearly planar surface separating two members of the intergrowth in the manner of a composition plane. If this irregular surface were sub-parallel to the plane of the thin section, a grain of mottled extinction would be seen.

Twenty carefully measured intergrowths were found to be true twins on the Japanese law or pseudo-twins approximating the Esterel, Breithaupt, or Sardinian laws. The following is a résumé of the theoretical relations stipulated by these laws.

Table 1. Penetration Twins of Quartz

	Twin plane	$c/\backslash c'$ angle*
1. Japanese law	ξ $\{11\bar{2}2\}$	84° 33′
2. Breithaupt law	s $\{11\bar{2}1\}$	48° 54′
3. Esterel law	r $\{10\bar{1}1\}$	76° 26′
4. Sardinian law	d $\{10\bar{1}2\}$	64° 50′

* The angle between the respective c axes of the two twinned sub-individuals.

Figure 2*A* is a stereographic projection of the c axes, fractures and approximate composition plane in a grain twinned by the Japanese law. Figure 2*B* is a similar projection of a grain whose sub-individuals nearly but not exactly conform to the Breithaupt law. The observed value of the angle $c/\backslash c'$ in grains twinned on the Japanese law in no case depart from the ideal value by more than 2°, whereas deviations of 3°–6° were consistently recorded for pseudo-twins approximating the other three laws. In addition several grains were observed in which the c axes of the

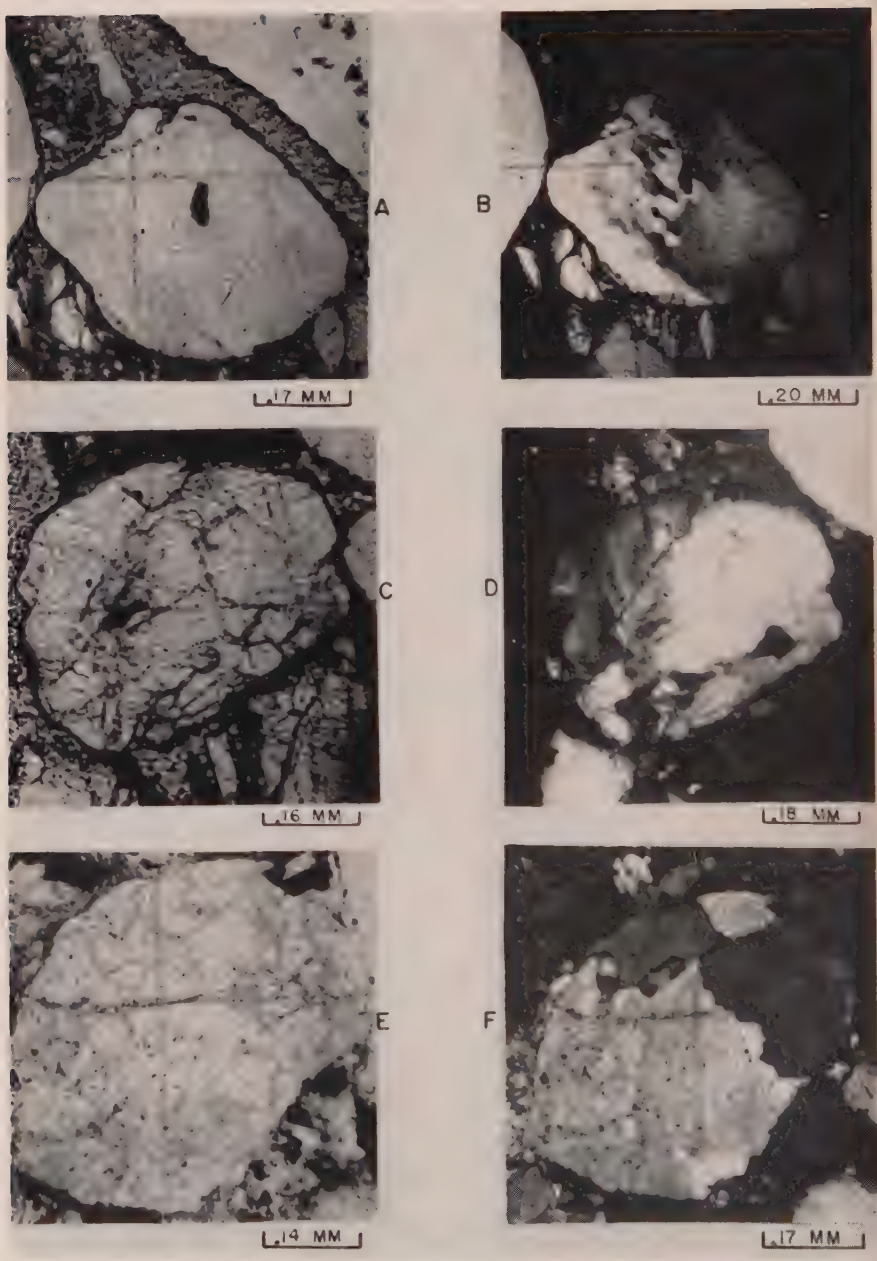


FIG. 1. Photomicrographs of intergrowths and twins. *A* and *B* are of a grain twinned by the Japanese law, the pairs *C* and *D*, and *E* and *F* are grains nearly conforming to the Esterel and Sardinian laws respectively. *A*, *C*, and *E* were taken with plane polarized light, *B*, *D*, and *F* under crossed nicols.

participating sub-individuals intersect at acute angles. Unfortunately fractures were not well enough developed in these grains to ascertain whether or not they conform to other "twin laws" or to intergrowths described by Zyndel and others.

An interesting feature of the intergrowths is the constant appearance of well developed undulatory extinction or "strain shadows" (Fig. 1*D*). Boehm or deformation lamellae are commonly developed also. The appearance of these features does not depend on experimental deforma-

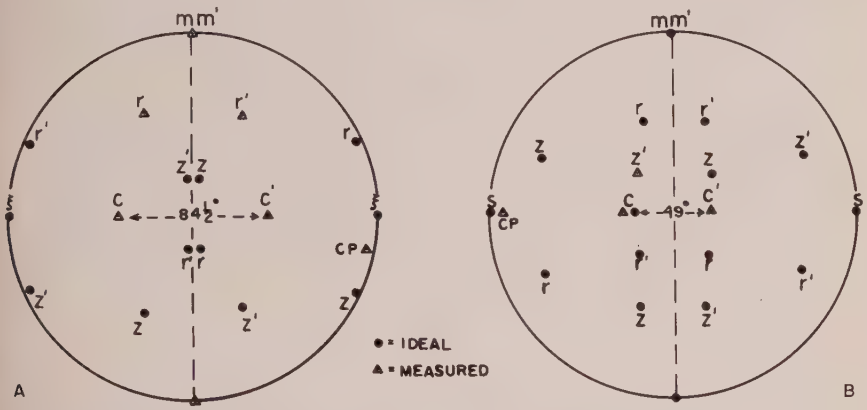


FIG. 2. Stereographic projection of intergrowths. *A*. Twinning according to the Japanese law, $\xi\{11\bar{2}2\}$. *B*. Pseudo-twinning approximating the Breithaupt law, $s\{11\bar{2}1\}$. Approximate position of the pole of the composition plane is indicated by *C.P.* Dotted line is twin plane.

tion, for they are seen in grains (intergrowths) in the loose sand subsequently used by Maxwell for his experiments. Most likely they reflect anisotropic contraction of the structure after formation of the intergrowths in response to falling temperature. It is also possible that some of the pseudo-twinning observed has been inherited in modified form from a higher temperature form of quartz, e.g. β quartz which twins by similar laws. Another explanation may be that the intergrowths are inversion twins subject to contraction upon further cooling, although to date only the Dauphiné law has been recognized to develop upon inversion of β to α quartz.

ACKNOWLEDGMENTS

The petrographic analysis of the deformed Asbury Park sand was made possible by a grant from the National Science Foundation to J. C. Maxwell. The writer is indebted to J.C. Maxwell, A. Buddington and F. J. Turner for reading the manuscript and to the Department of Geology, Princeton University for providing research facilities.

References

Borg, I., and Maxwell, J. C. (1956), Interpretation of fabrics of experimentally deformed sands: *Am. Jour. Sci.*, **254,** 71–81.

Gault, H. R. (1949), The frequency of twin types in quartz crystals: *Am. Mineral.*, **34,** 142–162.

Gordon, S. G. (1945), Inspection and grading of quartz: *Am. Mineral.*, **30,** 269–290.

Hintze, Carl (1915), Handbuch der Mineralogie: Band 1, Leipzig, Veit and Comp.

Maxwell, J. C., and Verall, P. (1954), Low porosity may limit oil in deep sands, Parts I and II: *World Oil,* **138,** n. 5 and 6, pp. 106–113, pp. 102–104.

Zyndel, F. (1914), Über Quartzzwillinge mit nichtparallelen Hauptaxen: *Zeits. Krist.*, Band **53,** Heft 1, 15–52.

NOTE ON LARGE CORDIERITE PORPHYROBLASTS, FREMONT COUNTY, COLORADO

Russell B. Travis,* *Colorado School of Mines, Golden, Colorado.*

Cordierite occurs abundantly and, in places, conspicuously in metamorphic rocks of the Front Range, Colorado. It is most readily detected as porphyroblasts, although it is undoubtedly abundant as a more subtle constituent in granoblastic hornfelses; for example, cordierite-anthophyllite rocks, a few miles north of Salida, Colorado.

The purpose of this note is to draw attention to some unusually large porphyroblasts (four to five inches in greatest dimension) in a readily accessible exposure. This occurrence is 2.8 miles east of Texas Creek, on U. S. Highway 50 in Fremont County. At this point, a contact between Precambrian granitic rock and Precambrian metamorphic rock strikes across the highway and the Arkansas River (Fig. 1). Although the contact is generally well defined, it is complicated by abundant pegmatite dikes which thoroughly invade the metamorphic rocks giving them a sporadic distribution along the contact. Also, in some places, large masses of metamorphic rocks are included within the granitic rock at dozens, and even hundreds, of feet from the contact. Most of the metamorphic rock along the contact and within the granitic rock is cordierite-bearing schist.

Because of the pronounced, nearly vertical, foliation, the steep slopes on the highway side of the river are littered with large slabs of gray cordierite schist. The cordierite, in large black or dark gray porphyroblasts, stands out conspicuously against the gray or silvery gray groundmass (Figs. 2–4). The porphyroblasts range from $\frac{1}{8}$ inch to 5 inches in greatest dimension but commonly occur in two, and in some places, three sets of different sizes (Fig. 3). Most of them are blocky or prismatic but some are spheroidal, and in all, the greater dimensions are more or less

* Present address: International Petroleum Company, Ltd., Talara, Peru.



FIG. 1. Cordierite-bearing schists, lower right, in contact with granitic rock, upper left. (Photo by L. W. LeRoy.)



FIG. 2. Dark gray cordierite porphyroblasts in slab of silvery gray quartz-muscovite schist.



FIG. 3. Slab of silvery gray schist exhibiting two sets of dark gray cordierite porphyroblasts. Those in the smaller set do not exeeed $\frac{1}{2}$ inch.



FIG. 4. Cross sectional view of schist showing relation of porphyroblasts to foliation. Most of these are spheroidal.

aligned in the foliation plane (Figs. 2–4). The groundmass is composed chiefly of quartz and muscovite, with subordinate iron ore and minor sillimanite, plagioclase, biotite, cordierite, and green tourmaline. The total proportion of porphyroblasts in the schist ranges from about 10 to 50 per cent. However, as is rather characteristic of cordierite, these porphyroblasts are crowded with inclusions of quartz and iron ore so that cordierite does not constitute more than 60 or 70 per cent of the porphyroblasts. Small quantities of muscovite, biotite and green tourmaline also are included. Professor N. Cyril Schieltz kindly prepared an x-ray powder pattern, and pointed out that it is identical with one of a cordierite-quartz mixture which he had included in a paper on x-ray analysis techniques in 1950 (Schieltz,[1] Plate 7).

The inclusions form conspicuous trains coinciding with the foliation of the schist and, in places, delineate relic microfolds. It seems reasonable to conclude, even on such cursory examination, that the cordierite was formed by contact metamorphism of quartz-mica schist. The tourmaline is probably a relic constituent, as it conforms closely to the foliation.

Although these porphyroblasts are small compared to the classic 30 cm. ones in Finland described by P. Eskola, and although larger ones can probably be found in the Front Range, their size and easy accessibility make them worth noting.

[1] Schieltz, N. C. (1950), *X*-ray Analysis, pp. 211–239 in subsurface geologic methods, L. W. LeRoy, editor, *Colorado School of Mines, Golden, Colorado.*

HYDROTHERMAL ALTERATION OF MUSCOVITE IN STEAM GAGE-GLASSES[1]

William T. Holser,[2] *Battelle Memorial Institute, Columbus, Ohio.*

Sheet muscovite is used to protect sight glasses in the water-level gages of steam power stations (Ptacek, 1952), but under certain conditions the mica becomes clouded and must be replaced after as little as two weeks use. Examination of several such replaced glasses from various power stations reveals an interesting mode of hydrothermal alteration that has not been described previously for this mineral.

Mica for a gage glass consists of a sheaf of 4 or 5 splits of clear muscovite, about 3×12 in., trimmed to shape. The mica is assembled with a thick glass plate and clamped around the edge, using asbestos gaskets. All the gage-glass samples examined were muscovite, either clear or very

[1] Publication No. 61, Institute of Geophysics, University of California, Los Angeles 24, California.

[2] Present address: Institute of Geophysics, University of California, Los Angeles 24, California.

pale red or green. One surface of the mica assembly is in contact with the water or steam of the gage. In the gages examined, the 2-phase water-steam system is at about 315° C., the resulting pressure being about 100 bars. The pH as measured at room temperature is in the range 11.0–11.5.

The cloudy portions of the mica surface were examined by microscopy and x-ray diffraction. The principal phase was diaspore in 0.001 by 0.01 mm. colorless needles, similar to those described by Ervin and Osborn (1951). Other important phases were 0.01 mm. colorless euhedral plates of boehmite, 0.005 mm. dark reddish brown euhedral plates of hematite, and 0.01 mm. crystals of a nonmagnetic opaque spinel-type mineral with $a_0 = 8.42$.

The textures of these products, in relation to the surface of the mica and to each other, are best described in terms of suggested stages in their origin. These stages apparently overlap in time and space.

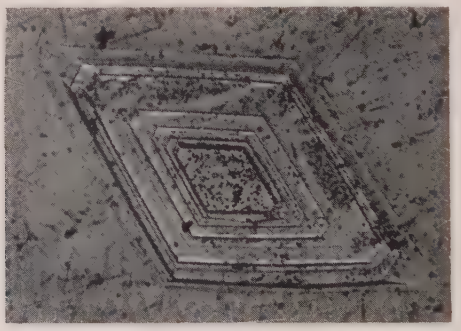


FIG. 1. Pit etched on muscovite cleavage by water, in plane-polarized light, ×120. Long edges are parallel to (110), short edges to (010). Note multiple levels of the pit, and their uniform width.

Stage 1: Etching of shallow pits in the surface of the mica by steam or water. The largest pits may be seen with the unaided eye as diamond-shaped markings a millimeter or more in length. As seen under the microscope (Fig. 1), the principal edges of the etch pits are of the form (110), cut off by minor (010) surfaces. The pit illustrated in Fig. 1 is composed of at least 10 parallel steps, but most pits have fewer steps, as illustrated in Fig. 2. The latter figure also illustrated the random distribution of the pits on the cleavage surface.

If etch pits are generated at the intersection of screw dislocations with the surface, as suggested by Gevers (1953), these dislocations must be much more numerous on a mica cleavage surface than found by interferometry (Amelinckx, 1952*a*). Some of the pits resemble the shallow "*B*" type described by Gevers for SiC and topaz (1953, p. 323), but they are not arranged along regular linear or helical patterns. On the other



FIG. 2. Array of pits etched on muscovite, plane-polarized light, ×60. Pits have only one or a few levels, and seem to be distributed randomly on the cleavage surface.

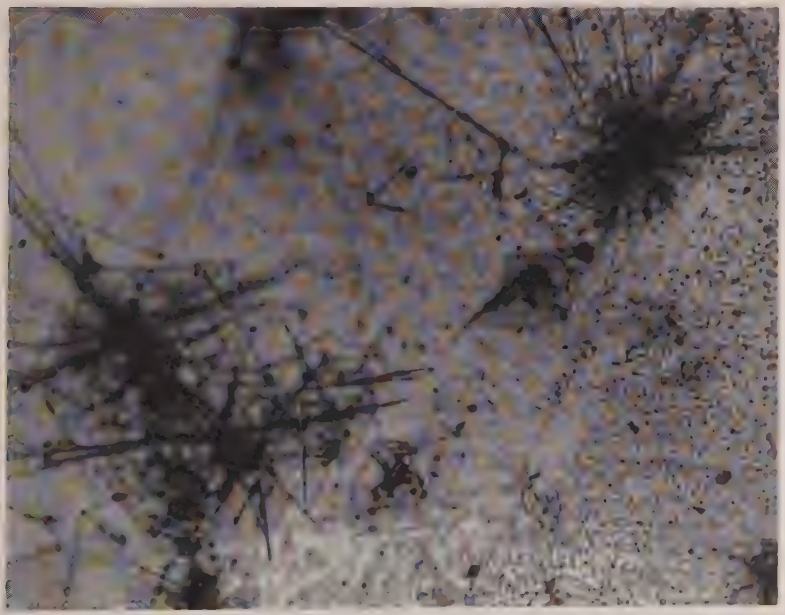


FIG. 3. Needles of diaspore altering mica around etch pits, plane-polarized light, ×55. Needles show a preferred orientation along prismatic directions in the muscovite. In most cases the needles enter between layers of the mica from the edges of the pits.



FIG. 4. Needles of diaspore radiating into the muscovite from a scratch in the surface. Smaller equant crystals are boehmite. In plane-polarized light, ×107.



FIG. 5. Intense alteration of muscovite to diaspore and boehmite around an etch pit (upper left) and a shear plane (lower right). In the lower half of the photograph much of the muscovite surface is covered by a dark deposit of boehmite, diaspore, hematite, and the spinel-group mineral. In plane-polarized light, ×53.

hand, the pits do not resemble the growth spirals found on biotite (Amelinckx, 1952*b*), as the latter show a continuous spiral with a more equal development of the six straight edges. Although the pits may be seen easily on the dry mica, they do not contribute significantly to the cloudiness of the mica sheet when it is in contact with water, which has a higher refractive index than air.

Stage 2: Chemical alteration of mica at the edges of pits, scratches and bent or sheared regions. In the latter case, the shear produced where the mica is bent along the inner edge of the gasket seemed particularly vulnerable. The alteration consists principally of the growth of fibrous diaspore edgewise into the mica layers, beginning with a few fibers aligned along the (110) directions of the mica crystal. As the amount of diaspore increases, it becomes a mat of fibers in random orientation (Fig. 3). Some boehmite may be crystallized along with the diaspore (Fig. 4).

Stage 3: Deposition on the mica surface of an aggregate of boehmite, hematite, and diaspore (Fig. 5). A black crust of the spinel-group mineral is found in a few places. Most of this material appears to have been deposited from solution rather than by direct alteration of the mica, but the aluminum for the boehmite and diaspore was certainly furnished by the mica. The hematite and spinel-mineral probably represent material in solution from slight metallic corrosion elsewhere in the steam system.

According to the published data (Ervin and Osborn, 1951), boehmite is the stable phase in contact with a saturated solution in the system Al_2O_3-H_2O under these conditions of temperature and pressure, with diaspore stable only above 300 C. and 140 bars. However, more recent work (Kennedy, 1956) proves that the diaspore field extends down to at least 220 C., and the observations made here suggest that it extends down to the vapor line. The other components of the mica, potassium and silicon, have apparently been removed in solution. At this temperature and pressure, SiO_2 attains the appreciable solubility of 0.07 weight per cent, according to Kennedy (1950), which would account for the removal of the silica from the mica. No comparable data are available for the solubility of AlOOH, but an analogous leaching of potassium and silicon from microcline has been demonstrated at somewhat higher temperatures by Morey and Hesselgesser (1951).

The clouding of gage-glass was investigated for the Diamond Power Speciality Corporation of Lancaster, Ohio.

References

Amelinckx, Severin (1952*a*), Screw dislocations in mica: *Nature*, **169**, 580.

———, ——— (1952*b*), La croissance helicoidale de cristaux de biotite: *Acad. Sci. Paris Comple Rendus*, **234**, 971–973.

Ervin, Guy, and Osborn, E. F. (1951), The system $Al_2O_3-H_2O$: *Jour. Geology*, **59**, 381–394.

Gevers, R. (1953), Observations microscopiques et interferometriques de figures de corrosion et leur interpretation a l'aide des dislocations: *Jour. Chim. Physique*, **50**, 321–328.

Kennedy, George (1950), A portion of the system silica-water: *Econ. Geology*, **45**, 629-653.

———, ——— (1956), The system Al_2O_3-H_2O (to be published).

Morey, G. W., and Hesselgesser, J. M. (1951), The solubility of some minerals in superheated steam at high pressures: *Econ. Geology*, **46**, 821–835.

Ptacek, F. (1952), Development of improvements in boiler water level gages: *Combustion*, **24**, No. 4, 56–59.

CONFIRMATION OF THE CRYSTAL STRUCTURE OF PENTLANDITE

A. David Pearson and M. J. Buerger,
Massachusetts Institute of Technology.

Because of the comparative weakness of the powder method to give symmetry information, and because of its absolute inability to provide adequate intensity data for structures having many of the merohedral symmetries, there is always doubt as to the validity of a complicated structure based upon data derived by the powder method. The structure of pentlandite was proposed by Lindqvist, Lundqvist, and Westgren[1] (herein referred to as LLW) on the basis of powder diffraction data. For this reason it was thought desirable to check it by a single-crystal method.

Professor Clifford Frondel of Harvard University kindly furnished us with a sample of pentlandite from the Creighton Mine, Sudbury, Ontario. While the material consisted of fragments, one of the smaller pieces had the form of a plate with two parallel plane surfaces, and appeared to be a possible single crystal. Assuming this to be the case, it was mounted for the precession camera so that the normal to the plane surface was the precessing axis. The resulting precession photographs had the appearance of being based upon a single crystal, and showed plane symmetry $6mm$ for the zero level and $3m$ for the upper levels.

A cone axis photograph taken with the same fragment showed a period along the precessing axis of 17.56 Å. Because of the trigonal symmetry of the axis it was a candidate for the direction [111] of an isometric crystal. If so, the period along [100] is $17.56/\sqrt{3} = 10.14$ Å. Since this value is close to the value for a given by LLW, namely 10.02 Å, this correlation of the precessing axis with [111] was tentatively accepted as correct.

[1] Lindqvist, Märta, Lundqvist, Dick, and Westgren, A., The crystal structure of Co_9S_8 and of pentlandite $(Ni, Fe)_9S_8$: *Svensk. Kemisk. Tidskrift*, **48**, 156–160 (1936).

Accordingly the crystal was remounted so that [100] became the precessing axis, and a series of precession photographs was taken for the levels 0, 1, 2, 3, and 4. The cell edge, computed from measurements on the zero level, was found to be $a = 10.03$ Å, as compared with 10.02 Å of LLW.

The plane symmetry of each of the levels proved to be $4mm$. This information combined with the symmetry $3m$ of the [111] axis, shows that the diffraction effects of the crystal have symmetry $4/m\ \bar{3}\ 2/m$, which is consistent with any of the three crystal classes $4/m\ \bar{3}\ 2/m$, $\bar{4}3m$, or 432. The lattice proved to be face-centered, and there were no extinctions other than those required by the face-centered lattice. This fixes the space group as one of the three $F4/m\ \bar{3}\ 2/m$, $F\bar{4}3m$, or $F432$. The symmetry adopted by LLW was the first of these.

The cell and symmetry of the structure proposed by LLW are therefore consistent with our findings by single crystal methods. It remained to check the particular structure proposed by LLW. This is in space group $F4/m\ \bar{3}\ 2/m$, with the 36 Fe and Ni atoms distributed at random over equipoints $4b$ and $32f$, with $x = \frac{1}{8}$, and the 32 S atoms distributed over equipoints $8c$ and $24e$, with $y = \frac{1}{4}$. We computed the amplitudes to be expected from such a structure, squared them, and multiplied by the Lorentz-polarization factor appropriate to the various levels of the precession photographs. These computed intensities were then compared with the degrees of blackness of the various corresponding spots on the precession photographs. All-around satisfactory agreement was found. From this it was concluded that the structure proposed by LLW for pentlandite is essentially correct.

A NOTE ON THE CALCITE-WOLLASTONITE EQUILIBRIUM

A. J. Ellis and W. S. Fyfe, *Chemistry Department, University of Otago, Dunedin, New Zealand.*

The equilibrium pressure and temperature conditions of the reaction:

$$\text{Calcite} + \text{Quartz} = \text{Wollastonite} + \text{Carbon Dioxide}$$
$$CaCO_3 + SiO_2 = CaSiO_3 + CO_2$$

are important in limiting the conditions of formation of some broad groups of metamorphic rocks. Goldschmidt's original calculations have recently been improved by Danielsson (1) by the application of more recent thermodynamic data. At the time of Danielsson's calculations P-V-T data for carbon dioxide were not available for much of the region of interest. Kennedy (2) has recently published such data up to 1400 bars and 1000° C. and these data have been used to check the calculations further.

Free energies of carbon dioxide from 50 bars to 1400 bars were obtained for each temperature from Kennedy's data by graphical integration using the relation:—

$$G_{(T,\ P)} = G_{(T,\ 50\ \text{bars})} + \int_{50\ \text{bars}}^{P} V_T dP$$

Free energies from 1-50 bars were obtained from the data of Sweigert, Weber and Allen (3).

The equations for ΔG_0 given by Danielson are correct and were used in the present calculation. The equilibrium pressures were then calculated from the relation:—

$$\Delta G_{(T,\ P)} = \Delta G_T^0 + \int_1^P V_g dP + \int_1^P \Delta V_s dP$$

Where ΔG_T^0 is the standard free energy change at temperature T, ΔV_s is the difference in molar volumes of the solid phases and V_g the molar volume of carbon dioxide. At equilibrium $\Delta G_{(T,P)} = 0$, and using the calculated free energies of carbon dioxide the equilibrium pressure was calculated by successive approximation. Thermal expansion and compressibility of the solid phases were neglected.

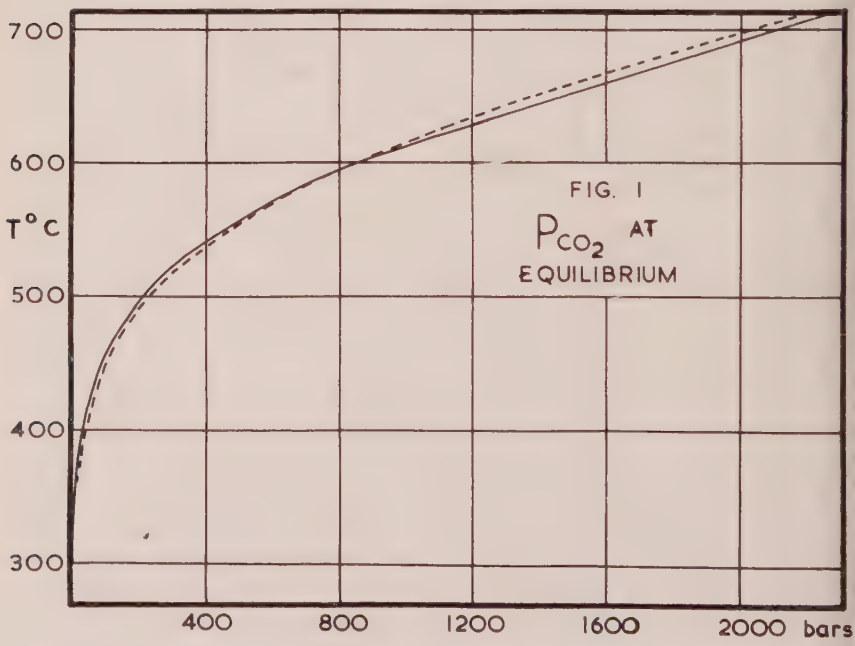


FIG. 1. Pressure-temperature curve for the reaction $CaCO_3 + SiO_2 = CaSiO_3 + CO_2$. Full curve, present calculation, dashed curve after Danielsson. The area under the curve is the field of calcite and quartz.

The results obtained with the improved *P-V-T* data are compared with those of Danielsson in Fig. 1. It is apparent that there are only small differences between the two curves. All points beyond 1400 bars necessitated extrapolation of Kennedy's data. The pressure of carbon dioxide is taken as the total pressure.

Little need be added to the many discussions of the geological significance of the reaction. The field of stability of the wollastonite bearing rocks of the hornfels and amphibolite facies may be very broad, especially when it is remembered that the partial pressure of carbon dioxide in a fluid phase may not be great compared with the partial pressure of water and that fluid and rock pressure may differ. At the same time the assemblage calcite-quartz could be stable into the region of partial melting in deep seated metamorphism.

References

(1) Danielsson, Allan (1950), Das Calcit-Wollastonitgleichgewicht: *Geochimica et Cosmochimica Acta*, **1,** 55–69.

(2) Kennedy, G. C. (1954), *P-V-T* relations in CO_2 at elevated temperatures and pressures: *Am. Jour. Sci.*, **252,** 225–241.

(3) Sweigert, R. L., Weber, Paul, and Allen, R. L. (1946), Thermodynamic properties of gases, carbon dioxide: *Ind. Eng. Chem.*, **38,** 186–200.

George Frederick Kunz Memorial Prize

At the March Meeting of the New York Mineralogical Club the George Frederick Kunz Memorial Prize was awarded to Mr. Davis Lapham, a graduate student in geology at Columbia University, for his paper entitled "Epidote from Hawleyville, Connecticut." This paper has been submitted for publication in *The American Mineralogist*. Mr. Lapham was the first recipient of this prize, established by the New York Mineralogical Club in 1955.

The Prize is made possible by a bequest of the late Dr. George Frederick Kunz, founder and first President of the New York Mineralogical Club. The prize is awarded annually for the most acceptable paper dealing with the study of a mineral locality or minerals from a deposit located within a 50 mile radius of New York City. The award is made by a Committee of three recognized mineralogists selected by the Board of Trustees of The New York Mineralogical Club. All papers for the next award must be submitted by February 15, 1957 for consideration. The rules governing the submission of papers or other information concerning the award can be obtained from Dr. Ralph J. Holmes, Chairman of the George Frederick Kunz Memorial Prize Committee of the New York Mineralogical Club, Department of Geology, Columbia University, New York 27, N. Y.

BOOK REVIEWS

INTRODUCTION TO THE SPACE GROUPS, by P. TERPSTRA. 160 pages. J. B. Wolters, Uitgevers Maatschappij, Oude Boteringestraat 24, Groningen, Netherlands. (1955). Price (unbound) $4.00.

The title of this fascinating book is a bit misleading. Indeed, it would scarcely be comprehensible to one having no previous acquaintance with space groups. The purpose of the book may be suggested by quoting its opening lines:

"THERE ALREADY EXIST A GREAT NUMBER OF WRITTEN RECORDS about space groups. And then one book would still be lacking?

"Such is indeed the case since the year 1950, when Niggli's articles about his matrix method were published."

The reference is to Paul Niggli's *Die vollständige und eindeutige Kennzeichnung der Raumsysteme durch Charaktertafeln*, I, *Acta Cryst.*, **2**, 263–270 (1949); and II, *Acta Cryst.*, **3**, 429–433, (1950), extended by Alfred Niggli and Paul Niggli in *Raumgruppensymmetrie und Berechnungsmethoden der Kristallstrukturlehre, Zeits. für angew. Math. & Physik, (ZAMP)* **2**, 217–232; 311–327 (1951). The opening sentence of the English abstract of the first of these articles reads: "Space groups can be given a novel representation by means of tables of characters having the form of square matrices." In the first article the application of such a scheme to space groups of primitive lattice in the trimetric systems only is set forth and in the second extended "to space groups with face- or body-centered translation groups and to those of the tetragonal, hexagonal and cubic systems." Professor Ewald (*Acta Cryst.*, 1953, **6**, 226) referred to these papers in the following words: "Niggli's urge for unifying, condensing and classifying knowledge so as to make it applicable to ever wider fields stands out in his papers on 'Charaktertafeln' (1950–51) in which a method is developed for symbolizing each space group so as to make any further reference to tables unnecessary." Niggli (1950, p. 433) planned to present his tables in a separate work which he did not live to finish.

In the ensuing five years Niggli's scheme has found little application but Professor Terpstra is convinced of its usefulness. He states (p. 44) "The application of these matrices may be compared with the procedures of an experienced calculator who, for example, uses logarithms without reference to the theory of logarithms." And on page 75 he says "The value of these matrices for this kind of space problem is, at the very least, as great as that of the advantages which are offered by the stereographic projection method in elementary geometrical crystallometry. Perhaps one is inclined to put the method of the matrices as superior in this comparison, because the geometry of the space groups is much more difficult than that of the geometrical crystallography, although the matrices are much more easily handled than stereographic projections."

Professor Terpstra's book lacks a table of contents and the nine chapters have no titles. It begins with a two page "Apology" the opening lines of which have been quoted above and ends with a two page "Summary" in which the gist of each chapter is set forth in a few sentences. The first three chapters review certain aspects of crystal symmetry, space lattices and Hermann-Mauguin symbols needed for the following development. Some previous familiarity with these matters will be required of the reader. In the fourth chapter a few necessary theorems and conventions are explained. The term "*form of points*" is introduced and a usage recommended by Niggli & Niggli (1951, p. 218–22) explained as follows: "Thus the form comprising all points equivalent to the point x, y, z, is represented by the symbol $<xyz>$. In the same way the symbol $<[uvw]>$ represents the assemblage of edges equivalent to the edge $[uvw]$ and the symbol $<(hkl)>$ has the corresponding function for the face (hkl)."

In chapter V Niggli's "tables of characters" are introduced. They depend on choice of origin in a symmetry center or "potential" symmetry center and are best adapted to the characterization of space groups D_{2h}^{1-16} and their subgroups. From these tables or matrices it is possible to determine directly the character and position of the symmetry elements and coordinates of points in a "general" position as well as information on subgroups, special positions, change in *H-M* symbol with orientation, extinctions and so on. By means of some simple auxiliary devices the same can be done with a single matrix for space groups with a primitive lattice in the classes C_{2v}, D_2, C_{2h}, etc. The matrices are very compact and can be set up for each space group from the *H-M* symbol. Many examples were pictured by Niggli (1949). The information to which they provide the key is usually given in tables requiring a page or more for each space group.

In chapter VI the extension of the scheme to orthorhombic space groups with centered lattices is explained. This requires the use of "matrix" and "by-matrix." Though somewhat cumbersome these devices yield the same information as the single matrix for the simple space groups and in addition give a clue to the alternative *H-M* symbols which may be applied to such groups. Terpstra does not take up the extension to space groups of the tetragonal, hexagonal and cubic systems, very briefly set forth by Niggli (1950).

The last three chapters give the application of Niggli's approach to structure factors, to Fourier summations for electron density and to vector sets. With the aid of an "algorithm" (p. 76) and a scheme for its application (p. 82) taken from Niggli and Niggli (1951, 313–314) the structure factor and electron density equations can be derived from the matrix for each space group in the form most convenient for computation. In the application to vector sets the author introduces the "Harker-matrix" (p. 131) from which the array of Harker sections (M. J. Buerger, *Acta Cryst.*, **3**, 465, 1950) may be seen.

Every application of the matrices is illustrated with specific examples which are worked out with great care. There are innumerable references to the *International Tables for X-ray Crystallography* and many illuminating comments thereon as well as on Donnay and Nowacki's *Crystal Data*. There is an abundance of excellent drawings, and repetition, even of figures, is not shunned where it may help understanding. The author shows his concern by such statements as "The reader is now asked to finish the incomplete scheme above" (p. 132) and "Does the reader understand this clearly?" (p. 98). The book is best read with a copy of the *International Tables* and pencil and paper at hand.

There is a general index of less than two pages and an incomplete list of references to space groups. The typography is excellent and there are very few misprints.

Professor Terpstra is one of the few masters of classical crystallography with a keen understanding of some of the latest developments, even to the vector sets of Buerger and the statistical material in Donnay and Nowacki's *Crystal Data*. Possibly this leads him to the statement (p. 14) that "the examination of a crystal usually starts with crystallometric determinations and afterwards comes the study by means of x-rays, from which can be obtained data concerning the crystal structure." Unfortunately there are few American crystallographers who proceed in this way. Had they been indoctrinated by Professor Terpstra it might be otherwise. Though his latest book will hardly serve as a textbook on space groups it can be recommended to all students and teachers of geometrical crystallography as valuable collateral reading.

A. Pabst,
University of California, Berkeley 4, Calif.

MICROSCOPIC PETROGRAPHY, by E. Wm. Heinrich. Pages xiii+296, 1956. McGraw-Hill Book Co., Inc., New York. Price $6.50.

This book is intended as a beginning to intermediate text for microscopic rock study; however, it will serve as a fine reference for workers in most geological and related fields.

The author attempts to bring our older petrographic descriptions up-to-date in 257 pages allotted as follows; igneous 84, sedimentary 71, and metamorphic 102. The treatment of each of these three rock types is equally well executed. The classification is simple and suitable for both field and laboratory work. The author has succeeded in presenting a vast amount of information, and the book is in general accurate, authoritative, well organized, and practical.

A short chapter on methods of microscopic study offers very useful material, much relatively new, on thin section preparation and micrometric analysis. It is pointed out that few petrologists today prepare their own thin sections, the work "being carried out by trained preparators." The student, however, should not be led to believe that a thin section professionally prepared is necessarily a section properly prepared. All too frequently preparations are accepted without question, and no check made for possible errors in labelling or orientation. A brief explanation of how to check thin sections should be included in our modern texts.

This book is illustrated by 132 photomicrographs in which the general rock fabric is clear, but higher magnifications are needed to bring out details, especially for the beginner. Most illustrations should have had their magnifications doubled. Some should have sacrificed larger scale features to secure magnifications of 50 or 100 times. Many will be of little value to the beginner. The student wants to see more clearly what is meant by trachytic texture, quartz overgrowth, and hornfelsic texture; but, unfortunately, the illustrations offered are of little help.

Only about 20 pen-and-ink sketches have been used; many more should have been included. For the beginner they are superior in most respects to photomicrographs. Furthermore, they are more economical.

The weakest sections of the book are those on textures and structures of rocks. This material needs further development, reorganization, and expansion. Loosely and vaguely defined terms are numerous and help to promote nothing but improper usage and corruption. Petrographic terminology certainly needs no assistance along these lines. From page 23 the student is likely to conclude that an overgrowth is the same as a reaction rim, or that radial clusters are also spherulitic. Relict texture is an example of a very poorly defined term. On page 24 the author implies that aplitic and saccharoidal textures are to be distinguished from mosaic texture. The manner of distinction, however, is not stated, and it is very doubtful if the beginner will readily discover it from the illustrations cited. The terms poikilitic and poikiloblastic seem adequately defined, but they are used very inconsistently in the chapter on metamorphic rocks.

The difficulty lies in the brevity of definitions. Further qualification and finer distinction are necessary. In many instances one must refer to several places in the book before he can obtain a complete picture. Zoning in minerals is mentioned in many parts of the book, but there is not a single striking illustration of this important structure. A totally inadequate description of zoning is given on page 22, and the beginner will be at a loss to understand the differences between various types of zoning. The chemical significance and petrological importance of this seemingly simple feature merit considerable attention.

There has been surprisingly little change in our petrography books over the half century since Rosenbusch. Although these works enable the student to describe and classify rocks, they fail completely to demonstrate the reason for obtaining such information.

Heinrich and other writers point out that petrography is a geological research tool, not an end in itself. If we are to succeed in getting this idea across to the student, we must catch him from the beginning. He must understand that rock study embraces two complementary operations; one is data-gathering and the other is interpretation. With the first the student has little trouble, and here our books on petrography are most useful. But the first operation, which can never be truly divorced from the second, is of little value without the second; and to bring this point home to the student, we must require him to make these

two operations right from the start. Special emphasis must be placed upon interpretation to counteract the natural tendency to drift toward the notably easier, passive act of description.

Such a statement as "A xenocryst is an included foreign grain or crystal" is not adequate. The student wants to know how to recognize a xenocryst and how to distinguish it from a phenocryst. To say that certain features are autoclastic and others cataclastic is useless unless the criteria for such distinction are given.

It is true that much on the interpretive side can be handled by the instructor, but it is also true that much valuable class time can be saved if the textbook covers general principles of interpretation.

A new textbook, an "interpretive petrography," would be an extremely worthwhile contribution. Several chapters of Harker's *Metamorphism* are suggestive. Preparing such a text would be complicated due mainly to differences in interpretation of rock features. Though no simple task, the various ideas should be presented, with supporting evidence where possible, enabling the student to become acquainted with these differences of opinion from the beginning. The problems should be disclosed, not suppressed.

The need for integrating microscopic work with field relations is paramount, and the student must learn how futile is an attempt to solve geologic problems with thin sections alone. Obviously it is impossible to include all relevant field material in such a text, but a sufficient number of examples could be given to illustrate the type of information needed in a variety of problems.

A few statements as to the importance of textural and structural features and the need for working out mineral sequences is inadequate and does not durably impress the student. If the main value of petrography lies in an understanding of the mineral associations, textures, and structures of rocks, then our texts must be revamped and built around these features with interpretation as a main objective. If the scope of petrography has changed in the past few few decades, then there is great need for a new type of textbook in this field.

CARLETON A. CHAPMAN,
University of Illinois, Urbana, Illinois

GEOCHEMIE, by A. A. SAUKOV. 311 pp. 40 tables, 21 figures. VEB Verlag Technik, Berlin (East Zone), Germany. 1953.

This is a German translation from the Russian by R. Sallum and Tatjana von Schenk and edited by Professor F. Leutwein of Freiburg. The preface indicates that the original is intended as a short introduction to the study of geochemistry in Soviet colleges and universities. However, there will doubtless be many who will take issue with the evaluation that "the work not only exceeds such a framework but also the presently known international literature in this field."

The introduction defines geochemistry, its scope and techniques. In chapter 1 is presented a short history of the development of geochemical ideas, emphasizing the role of Russian scientists. Chapter 2 is an elementary discussion of the periodic table of elements, of atomic structure, and of the geochemical classification of elements. The structure of earth is dealt with in the long chapter 3, under such topics as chemical composition of the crust, genesis and composition of meteorites, hypotheses of origin of interior shells, the atmosphere, and the hydrosphere. The next chapters deal successively with the relation of mineral structure and composition, the migration of elements, and the association of elements in the crust. Chapters 7 to 9 are concerned with magmatic, hydrothermal, and supergene processes respectively. In the last chapter the geochemistry of single elements is described, with but three examples, H, Fe, and Hg.

The book is a disappointment in scope and in detail. One might overlook the abject, self-depreciatory preface that the German publishers use as a *raison d'etre* for the appear-

ance of this translation; after all, they may well be in a position resembling that of Tennyson's immortal brigade. But it is difficult to forgive their superiors, who, having in their resources the classic efforts of Fersman and Vernadsky, have palmed off a substitute. The book cannot hold a candle to Geochemistry by Rankama and Sahama as a reference work, or to Principles of Geochemistry by Brian Mason as a textbook, neither of which is listed in the references.

E. Wm. Heinrich,
University of Michigan,
Ann Arbor, Michigan

AN INDEX OF MINERAL SPECIES AND VARIETIES ARRANGED CHEMICALLY, by Max H. Hey. British Museum (Natural History), Cromwell Road, London, S. W. 7, England. Second, revised edition. 728+xxiv pages, 1955, £3.

The first edition of this work, which was reviewed in the *American Mineralogist,* **36,** 634 (1951) has been exhausted for some time, owing to the great demand for the book and the limited impression. It is gratifying, therefore, to see that Dr. Hey and his assistants, who cheerfully again undertook the painstaking drudgery of compilation, checking, and cross checking, have once more successfully concluded their lucubration. Although not of immediate scientific fruit to them, the results are so highly useful to all mineralogists that the entire profession is in their debt. *Dios se los pagará!*

In the new edition has been incorporated all material coming to the notice of the author up to March 1955. This has led to a considerable expansion of the book, which, however, retains its original format—a first index by chemical groups in which each entry is assigned a decimal number, and a second alphabetical list.

In this edition a pronouncing index of accepted mineral names covering 65 pages has been added, a courageous attempt to reduce chaos to mere disorder. For some individuals pronunciation of mineral tongue twisters is usually based on "Whom did you hear it from the loudest the first time?" There is little room for dogma in pronunciation of mineral names, for, after all, orthoëpy is an art.

Doubtless this edition too will head the mineralogical "best seller" list. It is an indispensable reference tool and the first edition, now well thumbed, has saved this reviewer many hours of tedious checking. It is still deplorable, however, that the book makes not the slightest effort to reduce the number of varietal and trivial names, by indicating the proper substitute of a chemical adjectival modifier (Schaller system), a usage now widely practiced. Weeds grow more abundantly than flowers; "Off with their heads."

E. Wm. Heinrich,
University of Michigan,
Ann Arbor, Michigan

LA PROSPECTION DE L'URANIUM. Presidency of the Council, Commissariat for Atomic Energy. With a preface by Marcel Roubault. 62 pp., 13 figures, 1 black and white plate, 2 colored plates. In French. Masson et Cie, Editeurs, 120 Boulevard Saint-Germain, Paris—6e, France. Paper bound. 1955. 450 fr.

This is an attractive and well organized example of a manual designed to acquaint laymen with basic information prerequisite to prospecting for uranium. And it ranks high in quality for brochures of this type, which have been issued by several countries (e.g., U. S. A., Canada, Brazil, England, Australia and New Zealand) and by several states in the United States (e.g., Georgia, Virginia, Texas, Colorado, Utah, Washington, Oregon, and California).

The slim volume has four chapters: I. General prospecting methods, including a summary of fundamental geological data and general principles common to all types of pros-

pecting. II. Details of prospecting for uranium. III. Summary description of the principal minerals containing uranium, including primary and secondary minerals and a table of the principal uranium and thorium-bearing minerals. IV. Detection of uranium minerals with the aid of the Geiger-Müller counter—description and utilization of apparatus, interpretation of radioactive measurements, preparation of a radioactive-count map, and other physical and chemical detection methods. V. Essential characteristics of uranium deposits.

The two colored plates (II and III) of six figures each, depicting well crystallized autunite, torbernite, renardite, curite, billietite, beta-uranophane, uranophane, kasolite, and parsonite, are the finest colored reproductions of secondary uranium minerals seen by the reviewer, and alone are worth the cost of the booklet.

E. Wm. Heinrich,
University of Michigan,
Ann Arbor, Michigan

GEOLOGY OF SOUTHERN CALIFORNIA. Bulletin **170,** California Division of Mines. With 103 contributors, edited by R. H. Jahns. 878 pp., 441 text figures, 95 maps. Boxed, measuring 13×9½×4 inches, weighing 10 lbs. 1954. $12.00.

This gigantic symposium rapidly became a best seller; in fact it is already out of print and can no longer be purchased. It consists of ten chapters, bound separately, five geologic guides for selected field trips, also separately bound, and 34 map sheets. The chapters are:

I. General features, 3 sections.
II. Geology of the natural provinces, 10 sections.
III. Historical geology, 8 sections.
IV. Structural features, 7 sections.
V. Geomorphology, 9 sections.
VI. Hydrology, 3 sections.
VII. Mineralogy and Petrology, 8 sections.
VIII. Mineral deposits and mineral industry, 7 sections.
IX. Oil and gas, 4 sections.
X. Engineering aspects of Geology, 3 sections.

Of particular interest to members and fellows of the Mineralogical Society are Chapters VII and VIII. The various sections in Chapter VII include: 1. Minerals in southern California by Joseph Murdoch and Robert W. Webb. 2. Problems of the metamorphic and igneous rocks of the Mojave desert by Thane H. McCulloh. 3. The batholith of southern California by Esper S. Larsen, Jr. 4. Miocene volcanism in coastal southern California by John S. Shelton. 5. Pegmatites of southern California by Richard H. Jahns. 6. Contact metamorphism in southern California by Ian Campbell. 7. Contact metamorphism at Crestmore, California by C. Wayne Burnham. 8. Anorthosite complex of the western San Gabriel Mountains, southern California by Donald V. Higgs. Chapter VIII deals with salines, the Mountain Pass rare-earth deposits, tungsten, base metal and iron deposits, gold and silver mining districts, and nonmetallic substances.

The work represents the enormous combined effort of many people, efficiently organized by Jahns. It is one of the most valuable and complete regional geological studies to appear in many years, and in many ways sets an enviable standard of excellence for such studies, which will be difficult to exceed or even match. Possessors of copies may count themselves fortunate.

E. Wm. Heinrich,
University of Michigan,
Ann Arbor, Michigan

NEW MINERAL NAMES

Bismuth jamesonite

M. S. Sakharova, Bismuth sulfosalts of the Ustarasaisk deposits. *Trudy Mineralog. Muzeya Aka. Nauk S.S.S.R., No.* **7,** 112–116 (1955) (in Russian).

Bismuth jamesonite was found as radiating aggregates of fine capillary crystals in cavities with quartz crystals in carbonate veinlets cutting arsenopyrite ore in the Ustarasaisk deposits, western Tyan-Shan. The crystals are usually some mm. long, at times up to 1 cm. long, a fraction of a mm. in cross-section. They contain inclusions of native antimony, visible only under high magnification. A little realgar and cinnabar are associated minerals.

The mineral is lead-gray, luster metallic, with one perfect cleavage. Hardness low. Under the microscope it is white, birefringent, strongly anisotropic with reddish reflections apparent only with immersion. Reflectivity 35%.

Analysis by V. M. Senderova gave Bi 30.50, Sb 16.50, Pb 32.25, Fe 1.39, Cu 0.30, S. 17.62, insol. 1.59; sum 100.15%, corresponding to $PbS \cdot (Bi, Sb)_2S_3$.

X-ray powder data are given. (The 26 lines given correspond very closely with those given for normal jamesonite by Berry, *Mineralog. Mag.*, **25,** 597–608 (1940), except that strong lines given by Berry at 4.03 and 3.76 are not listed. M.F.)

Discussion: The mineral is considered to be a variety of jamesonite. However, the ratio Bi:Sb = 1.07:1, so that this is not a bismuthian jamesonite. The formula is given as $PbS \cdot (Bi, Sb)_2S_3$; the iron content given in the analysis is low for the formula generally accepted for normal jamesonite, $4\,PbS \cdot FeS \cdot 3\,Sb_2S_3$.

Michael Fleischer

Ustarasite

M. S. Sakharova, Bismuth sulfosalts of the Ustarasaisk deposits. *Trudy Mineralog. Muzeya Akad. Nauk S.S.S.R., No.* **7,** 112–126 (1955) (in Russian).

Ustarasite was found in quartz-bismuthinite veins in the deposits of Ustarasaisk, western Tyan-Shan. It occurs as prismatic crystals, some of which are bent or twisted. It is silvery-gray to gray, luster metallic. There is one perfect cleavage; a second appears on long etching. Hardness $2\frac{1}{2}$.

Under the microscope, ustarasite is pure white, strongly anisotropic, without inner reflections. Reflectivity 42%. It is etched rapidly by HNO_3, slowly by HCl and turns brown, by concentrated KOH, turning brown, blackened by aqua regia. No reaction with KCN, $FeCl_3$, $HgCl_2$, or $KMnO_4$.

Analyses of two different samples by V. M. Senderova and Yu S. Nesterova gave Bi 65.33, 64.90; Sb 2.96, 1.87; Pb 10.51, 11.35; Cu 0.30, 0.74; Fe 0.60, 1.40; As none, 0.15; S 17.25, 17.25; insol. 0.34, 0.54; sum 97.29, 98.20%. A little pyrite, chalcopyrite, and native Bi were present. The analyses give the formula $PbS \cdot 3\,(Bi, Sb)_2S_3$. Spectrographic analysis by N. V. Lizunov showed also the presence of traces of Ag, Si, Ca, Te, Sn, Mg, Mn, Al, Cr, Sr, and Cd. *X*-ray spectral determinatinons on several samples confirmed the constancy of the ratio Pb:Bi.

X-ray powder data were obtained by N. N. Sludsko; 52 lines are given. The strongest are 3.527 vs. broad, 3.080 S, 2.508 S, 1.915 S, broad, 1.732 S., 1.483 vs, 1.140 S, 1.057 vs.

Other minerals described include bismuthinite, kobellite, a rezbanyite-like mineral, and bismuth jamesonite.

M. F.

Pseudolaueite

H. STRUNZ, Pseudolaueit, ein neues Mineral. *Naturwissenschaften*, **6**, 128 (1956).

The name pseudolaueite is given to an orange-yellow phosphate, which, from microchemical and spectroscopic determinations, appears to be a dimorph of laueite, $MnFe_2(OH)(PO_4)_2 \cdot 8H_2O$ (see *Am. Mineral.*, **39**, 1038 (1954). It is monoclinic-prismatic; the unit cell has a_0 9.57, b_0 7.45, c_0 10.16 Å., β 104°40′, $Z=2$. The crystals are prismatic to thick tabular with forms a {100}, c {001}, m {110} and rare {011} and {$\bar{2}$01}. $G.=2.463$. $H.=3$. Optically biaxial, positive, optic axis perpendicular to (010), $2V_\gamma=80°$ (calcd.), *ns* α 1.626, β 1.650, γ 1.686, $X:c$ 2° pale yellow, $Y:a$ 12° pale yellow, $Z=b$ yellow. *X*-ray powder data are given. The strongest lines of pseudolaueite are 9.926 10, 5.869 7, 3.472 4; of laueite 9.926 10, 3.276 6, 4.922 5, 6.515 4. Pseudolaueite occurs in the Hagendorf, Bavaria, pegmatite as incrustations and as the core of stewartite crystals associated with oxides of Mn and Fe.

M. F.

Calciborite

E. S. PETROVA, Sbornik "Geol. gorno-khim. Syr'e," *Trudy gosudarst nauch.-issled. inst. gorno-khim. syr'e, fasc.* **2**, 218–223; from an abstract by E. M. Bonshtedt-Kupletskaya in *Zapiski vses. mineralog. obshch.*, **85**, 76–77 (1956).

The mineral occurs as white radial aggregates. Analyses by T. A. Zvereva, (1) material picked under binoculars, (2) the fraction with sp. gr. 2.9–2.95, gave: B_2O_3 47.42, 47.15; CaO 49.25, 48.30; MgO 0.81, 0.90; MnO 0.03, 0.07; alkalies—, none; Al_2O_3 0.02, 0.24; Fe_2O_3 0.30, 0.16; SiO_2 0.82, 0.65; P_2O_3—, none; CO_2 1.22, 0.71; As 0.03, 0.45; H_2O^- 0.12, 0.10; sum 100.02, 98.73%. This corresponds to $Ca_5B_8O_{17}$. The analyzed material contained a little dolomite, garnet, and pyroxene.

Insoluble in water, readily soluble in acids on heating. Fuses at 1002°, giving a bright green flame, to a greenish enamel-like bead.

The mineral is monoclinic (?). No cleavage, fracture uneven, on aggregates conchoidal. Hardness about $3\frac{1}{2}$. $G.=2.878$. Optically biaxial, neg., with *ns* α 1.595, β 1.654, α 1.670, $\gamma-\alpha$ 0.070–0.072, $2V=54°$. Extinction angle 22°. Luminesces bright green in cathodic light. The strongest *x*-ray lines are at 3.419, 3.774, 2.300, 1.787, and 2.629 Å.

Calciborite was found in deep drill cores at the contact of Middle Devonian limestone with quartz diorite in a copper deposit of the skarn type in the Urals. It is associated with calcite and dolomite, with minor amounts of garnet, magnetite, and pyroxene. It also fills fissures in limestone and was observed to replace calcite.

The name is for the composition.

DISCUSSION: No compound of this composition was stable at the melting point in the system $CaO-B_2O_3$. Melts of this composition gave CaB_2O_4 with optical properties and *x*-ray powder pattern different from those for calciborite.

M. F.

Smythite

R. C. ERD, AND H. T. EVANS, JR., The compound Fe_3S_4 (smythite) found in nature. *Jour. Am. Chem. Soc.*, **78**, 2017 (1956).

Minute, plate-like inclusions in calcite crystals from Bloomington, Ind., are opaque, strongly ferromagnetic, and of a dark bronze color, but gave an *x*-ray pattern distinct from that of pyrrhotite. *X*-ray fluorescence and microchemical tests showed Fe and S present, with a little Ni. Buerger precession photographs show the crystals to be rhombohedral, probable space group $R\,\bar{3}m-D_{3d}^5$, with hexagonal unit cell dmensions a_0 3.47, c_0 34.5 Å.,

containing Fe_9S_{12}. G. calcd 4.09, measured by flotation 4.06±.03. The structure is related to that of pyrrhotite. The composition was derived from the structural analysis.

The name (pronounced smĭth-ite) is for Professor C. H. Smyth, Jr. of Princeton University.

DISCUSSION: Not to be confused with smĭth-ite.

M. F.

Secondary Uranium Minerals

JEAN CHERVET AND GEORGES BRANCHE, Contribution a l'étude des mineraux secondaires d'uranium français. *Sciences de la Terre, Ann. École Natl. Supérieure Géol. Appl. et Prospection Minière Univ. Nancy*, **3**, No. 1–2, 1–188 (1955).

On p. 178 of this monograph are listed a number of new names taken from samples exhibited by the U.R.S.S. delegation to the Geneva Conference on Peaceful Uses of Atomic Energy, August, 1955.

Orlite. $3\,PbO \cdot 3\,UO_3 \cdot 4\,SiO_2 \cdot 6\,H_2O$.

Nenadkevite. $U^{+6}(U^{+4}, Th)(Mg, Ca, Pb)_3(SiO_4)_2(OH)_8 \cdot nH_2O$. Named for K. Nenadkevich, Russian geologist. Not to be confused with Nenadkevichite, see *Am. Mineral.*, **40**, 1154 (1955).

Prjevalskite. $PbO \cdot 2UO_3 \cdot P_2O_5 \cdot 4H_2O$. Named for N. Prjevalsky, Russian explorer of Central Asia.

Lermontovite. $(U, Ca, R.E.)_3(PO_4)_4 \cdot 6H_2O$. In nodular and botryoidal green aggregates.

Sodium Autunite. $Na_2(UO_2)_2(PO_4)_2 \cdot H_2O$.

Hydrogen Uranospinite. $H_2(UO_2)_2(AsO_4)_2 \cdot 8H_2O$.

Priguinite. $UO_3 \cdot 2MoO_3 \cdot 4H_2O$. Yellow.

Moluranite. $UO_2 \cdot 2UO_3 \cdot 5MoO_3 \cdot 12H_2O$. Black.

M. F.

DISCREDITED MINERALS

Mikheevite = Görgeyite

E. I. NEFEDOV, Neue Minerale. *Geologie* **4**, No. 5, 526–528 (1955).

HEINZ MEIXNER, Zur Identität von Mikheewit (Micheewit) mit Görgeyit. *Geologie* **4**, No. 6, 576–578 (1955).

Nefedov corrects some of the data previously given (see *Am. Mineral.*, **40**, 551 (1955)), thus removing most of the discrepancies between mikheevite and görgeyite. Meixner shows that the properties are now so close that the minerals must be identical.

M. F.

Canbyite (=Hisingerite)

S. H. U. BOWIE, Thucolite and hisingerite-pitchblende complexes from Nicholson Mine, Saskatchewan, Canada. *Bull. Geol. Survey Great Britain, No.* **10**, 45–57 (1955).

Canbyite was described in 1924 as a crystalline mineral with a composition identical with that of the amorphous mineral hisingerite. A new analysis and optical data are given for hisingerite. X-ray powder photographs of canbyite and of 5 samples of hisingerite, including one of type material from Riddarhytten, Sweden, all show five broad bands, strong ones at 4.39–4.45 Å, 3.53–3.58 Å, 2.56–2.58 Å, and 1.53–1.54 Å, and a weak one at 1.70–1.71 Å. Hisingerite is therefore cryptocrystalline and the name canbyite should be dropped. The relation of hisingerite to nontronite is not clear; nontronite gives a strong basal reflection at 14–15 Å that is absent from the powder patterns of hisingerite.

M. F.